SAPIENZA
UNIVERSITÀ DI ROMA

PhD in Biochemistry

XXXVI Cycle (2020/2023)

Insights into the mechanism(s) of action of the membrane-active host-defence Esc peptides on model and living systems

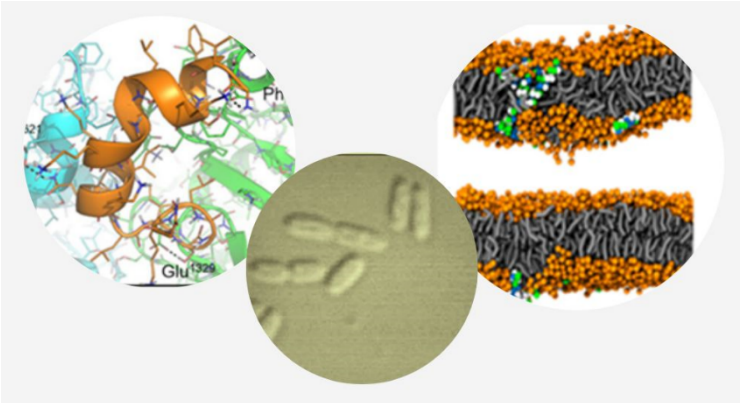

PhD student

Elena Puglisi

Tutor: Prof. Maria Luisa Mangoni

Coordinator: Prof. Maria Luisa Mangoni

Index

“La mente scientifica non fornisce tanto le risposte giuste quanto le giuste domande”.

Claude Levi-Strauss

List of papers relevant for this thesis

- Canè C., Casciaro B., Di Somma A., Loffredo M.R.**, Puglisi E.,** Battaglia G., Mellini M., Cappiello F., Rampioni G., Leoni L., Amoresano A., Duilio A. and Mangoni M.L., **'**The antimicrobial peptide Esc(1-21)-1c increases susceptibility of Pseudomonas aeruginosa to conventional antibiotics by decreasing the expression of the MexAB-OprM efflux pump': *Front. Chem. - Chemical Biology: Volume 11 - 2023 | doi: 10.3389/fchem.2023.1271153.*

- Ferrera L., Cappiello F., Loffredo M.R., **Puglisi E.***,* Casciaro B. ,Botta B., Galietta L.J.V., Mori, M., Mangoni M.L., 'Esc Peptides as Novel Potentiators of Defective Cystic Fibrosis Transmembrane Conductance Regulator: An Unprecedented Property of Antimicrobial Peptides', *Cellular and Molecular Life Sciences: CMLS* 79, no. 1 (31 December 2021): 67, https://doi.org/10.1007/s00018-021-04030-2.

List of other papers

- Casciaro B., Ghirga F., Cappiello F., Vergine V., Loffredo M.R., Cammarone S., **Puglisi E.**, Tortora C., Quaglio D., Botta B. and Mangoni M.L., 'The Triprenylated Anthranoid Ferruginin A, a Promising Scaffold for the Development of Novel Antibiotics against Gram-Positive Bacteria', *Antibiotics (Basel, Switzerland)* 11, no. 1 (11 January 2022): 84, https://doi.org/10.3390/antibiotics11010084.

- Cappiello F., Casciaro B., Loffredo M.R., **Puglisi E.** and Mangoni M.L., 'Pulmonary Safety Profile of Esc Peptides and Esc-Peptide-Loaded Poly(Lactide-Co-Glycolide) Nanoparticles: A Promising Therapeutic Approach for Local Treatment of Lung Infectious Diseases', *Pharmaceutics* 14, no. 11 (26 October 2022): 2297, https://doi.org/10.3390/pharmaceutics14112297.

Abbreviations

AMP Antimicrobial peptide

ABR Antibiotic resistance

AFM Atomic Force Microscopy

CFBE Bronchial epithelial cells

CF Cystic Fibrosis

CFTR Cystic Fibrosis Transmembrane Conductance Regulator

CFU Colony-forming units

DPC Dodecylphosphocholine

EGFR Epidermal Growth Factor Receptor FBS Fetal Bovine Serum

ESKAPEE Enterococcus faecium , Staphylococcus aureus, Klebsiella pneumoniae, Acinetobacter baumannii, P. aeruginosa, Enterobacter spp. and Escherichia coli

FBS Fetal Bovine Serum

FRT Fischer rat thyroid (FRT)

LB Luria-Bertani broth

LC-MS/MS Liquid Chromatography/Tandem Mass Spectrometry

LFD Lipid film dissolution

LPS Lipopolysaccharide

MD Molecular siumulation

MEMg Minimum Essential Medium supplemented with 2 mM glutamine

MIC Minimal inhibitory concentration

MTT 3(4,5-Dimethylthiazol-2yl)2,5-diphenyltetrazolium bromide

NMR Nuclear Magnetic Resonance

PBPs Penicillin-binding proteins

PBS Phosphate buffered saline

POPC 1-palmitoyl-2-oleoyl-sn-glycero-3-phosphocholine

POPG 1-palmitoyl-2-oleoyl-sn-glycero-3-phosphoglycerol

RP-HPLC Reversed-Phase High-Performance Liquid Chromatography

SDS Sodium-dodecylsulfate

SLB Supported lipid bilayer

SUVs Small unilamellar vesicles

TEER The transepithelial electrical resistance

1.Introduction

1.1 Antibiotic resistance and ESKAPEE pathogens

The discovery of penicillin by Alexander Fleming in 1928 marked the beginning of the era of antibiotics. Penicillin was the first true antibiotic, meaning it was the first substance that could selectively kill or inhibit the growth of bacteria without harming the host. This breakthrough had a significant impact on the treatment of bacterial infections (Lobanovska et al.,2017). The excessive and inappropriate use of antibiotics in both human and veterinary medicine has indeed contributed to the emergence and spread of antibiotic-resistant bacteria, leading to what is commonly referred to as antibiotic resistance (ABR) (Fig.1).

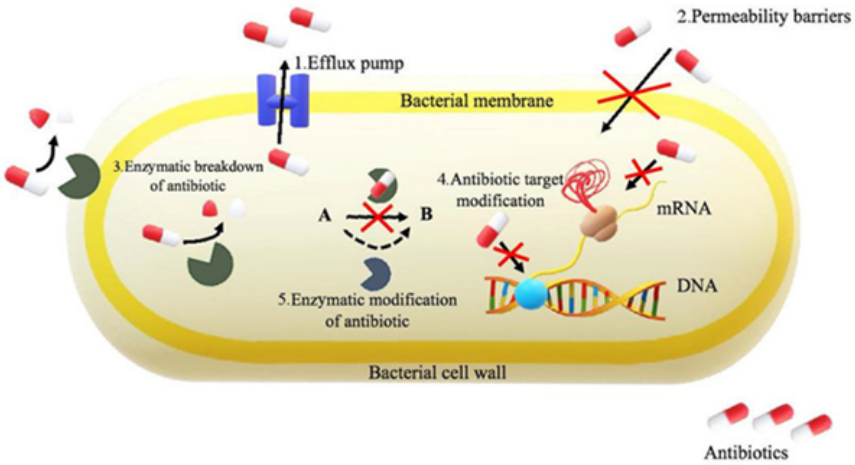

Fig. 1 Molecular mechanisms of antibiotic resistance developed by bacterial cells (Pauter et. al 2020).

ABR occurs when bacteria evolve and develop mechanisms to withstand the effects of antibiotics, included the classes of ß-lactam antibiotics, aminoglycosides, fluoroquinolones.

In general, Antibiotic resistance (ABR) is referred to resistance to drugs used to treat infections caused by bacteria and other microbes including parasites, such as malaria, viruses such as HIV, and fungi such as *Candida spp.*

(Wall et al., 2019).

Addressing this challenge requires the adoption of new strategies and the development of alternative treatments to combat AMR effectively (Akram et al., 2022).

Antibiotic resistance can be classified into natural (intrinsic) and acquired resistance: the first one refers to the natural or inherent non-responsiveness of an organism to an antibiotic due to characteristics or features that are part of its genetic background, while in the second case the bacterium changes to protect itself from the antibiotic.

Understanding the mechanisms of resistance in different bacterial species is crucial in selecting the appropriate antibiotic for effective treatment.

For example, Gram-positive bacteria, such as *Staphylococcus aureus* and *Streptococcus pneumoniae*, can exhibit resistance to β-lactam antibiotics (e.g., cephalosporins and penicillins) (Chen et al., 2011). This resistance is often due to the production of β-lactamase enzymes or to the alteration of penicillin-binding proteins (PBPs) (Chen et al., 2011).

It has been argued that this phenomenon is likely due to major differences in the cell envelope between Gam-negatives and Gram-positives bacteria.

In the former, the presence of an outer membrane permits to "control" the entry of molecules to the periplasmic space. Indeed, most β-lactams require specific porins to reach the PBPs, which are in the inner membrane.

A comprehensive classification of antibiotic resistance mechanisms is provided, according to the biochemical route involved in the resistance.

- **Proteolytic cleavage (drug inactivation);** is the enzymatic hydrolysis of a peptide bond in a peptide or protein substrate by proteases (Klein et al., 2018).

- **Modifications of the antimicrobial molecule**; it consists in the production of enzymes that inactivate the drug by adding specific chemical moieties to the compound or that destroy the molecule itself, rendering the antibiotic unable to interact with its target. Many types of modifying enzymes have been described, and the most frequent biochemical reactions they catalyze include i) acetylation (aminoglycosides, chloramphenicol, streptogramins), ii) phosphorylation (aminoglycosides, chloramphenicol), and iii) adenylation (aminoglycosides, lincosamides) (Klein et al., 2018).

- **Prevention to reach the antibiotic target** (by decreasing penetration or actively extruding the antimicrobial compound); bacteria have developed mechanisms to prevent the antibiotic from reaching its intracellular or periplasmic target by decreasing the uptake of the antimicrobial molecule.

This mechanism is particularly important in Gram-negative bacteria, limiting the influx of substances from the external milieu. In fact, the outer membrane acts as the first-line of defense against the penetration of multiple toxic compounds, including several antimicrobial agents (Klein et al., 2018).

- **Changes of target sites;** a common strategy for bacteria to develop antimicrobial resistance is to avoid the action of the antibiotic by interfering with their target site. To achieve this, bacteria have evolved different strategies, including protection of the target and modifications of the target site, resulting in decreased affinity for the antibiotic molecule. This last choice is the most common mechanism of antibiotic resistance in bacterial pathogens affecting almost all families of antimicrobial compounds. These target changes may consist of point mutations in the genes encoding the target site; enzymatic alterations of the binding site (e.g. addition of methyl groups); and/or replacement or bypass of the original target (Klein et al., 2018).
- **Resistance due to global cell adaptive processes**; it is a development of resistance to daptomycin (DAP) and vancomycin (low-level in *S.aureus*), the most clinically relevant examples of resistance phenotypes that are the result of a global cell adaptive response to the antibacterial attack (Klein et al., 2018).

Resistance in bacteria can be acquired through two main mechanisms: vertical evolution and horizontal gene transfer:

- **vertical evolution** refers to the development of resistance through genetic mutations in existing genes within the bacterial population (Schmieder et al., 2012):

- **horizontal gene transfer**, on the other hand, involves the acquisition of new genes or genetic elements from other bacteria or microbial species (Schmieder et al., 2012).

These mechanisms lead bacteria to survive to the use of the specific antibiotic and to develop a resistance that can be passed to other bacteria as they multiply. Bacteria also can become resistant through mutation of their genetic material (Habboush et al., 2022).

The categorization of pathogens into critical, high, and medium priority pathogens by the World Health Organization (WHO) helps to highlight the severity of the antibiotic resistance problem and guides research and development efforts towards addressing the most urgent needs.

In the critical priority list, carbapenem-resistant *Acinetobacter baumannii* and *Pseudomonas aeruginosa*, as well as extended-spectrum β-lactamase (ESBL) or carbapenem-resistant *Klebsiella pneumoniae* and Enterobacter species, are identified.

These pathogens pose significant challenges due to their resistance to multiple classes of antibiotics, including last-resort options like carbapenems.

In the high priority group, vancomycin-resistant *Enterococcus faecium* (VRE) and methicillin- and vancomycin-resistant *Staphylococcus aureus* (MRSA and VRSA) are listed. These pathogens are associated with difficult-to-treat infections, and their resistance to multiple antibiotics, including those commonly used as a first-line treatment, necessitates the development of alternative treatment options (Santajit et. al., 2016). A systematic review of clinical and economic impact of antibiotic resistance reveals that ESKAPEE pathogens are associated with the highest risk of mortality thereby resulting in increased health care costs (Ruekit et al., 2022; Founou et al., 2017).

The term "ESKAPEE" is an acronym derived from the first letter of the following bacterial species: *Enterococcus faecium, Staphylococcus aureus, Klebsiella pneumoniae, Acinetobacter baumannii, P. aeruginosa, Enterobacter spp. and Escherichia coli* (Ruekit et al., 2022; Mulani et al., 2019; Ruekit et al.,2022), a group of micro-organims that have been identified as the major causes of healthcare-associated infections and are associated with high levels of resistance to traditional antibiotics, “escaping” the biocidal action of antimicrobial agents and the host’s immune response. These bacteria can form sessile communities, named biofilms that physically prevent the attack of host immune cells. Biofilm cells enter into dormient (metabolically-inactive) state which protect them from the action of traditional antibiotics that usually inhibit biological processes, like DNA, protein and cell wall synthesis.

It is, therefore, imperative to find alternative ways to treat infections especially those caused by ESKAPEE pathogens.

1.2 *Pseudomonas aeruginosa*, a relevant pathogen in cystic fibrosis

P. aeruginosa is a Gram-negative bacterium that is widely distributed in the environment.

It is an opportunistic widespread pathogen (commonly found in soil and water environments, including rivers, lakes, and sewage) with the ability to cause infections in diverse settings.

P. aeruginosa can cause a wide range of infections in humans, and many of these infections can be severe and life-threatening, especially in individuals who are immunocompromised or hospitalized. Some of the infections associated with *P. aeruginosa* include: pneumonia, skin and soft tissue infections, urinary tract infections, otitis externa, eye infections (Gellatly et al., 2013; Wu et al., 2011).

P. aeruginosa exists in two main forms: planktonic (free-floating) (Fig. 2A) and sessile cells organized in biofilms (Fig. 2B): this latter definition corresponds to bacterial community of cells which adheres to surfaces and are embedded in a self-produced matrix of extracellular polymeric substances (EPS).

The presence of *P. aeruginosa* in biofilms contributes to their ability to cause persistent and recurrent infections (Flemming et al., 2016).

A **B**

Fig. 2 Electron microscopy images of P. aeruginosa free-living cells (A) and biofilm (B). The micrographs are from https://www.repubblica.it/salute/medicina-e-ricerca and https://www.laboratuvar.com

This bacterium has adapted to survive in moist environments and harsh conditions and can persist in these habitats, forming biofilms that provide protection (Klockgether et al., 2017).

It can cause a wide range of infections in humans, and many of these infections can be severe and life-threatening, especially in individuals who are immunocompromised or hospitalized. Some of the infections associated with this bacterium include: pneumonia, skin and soft tissue infections, urinary tract infections, otitis externa, eye infections (Gellatly et. al., 2013; Wu et al., 2011).

P. aeruginosa has an intrinsic resistance to a broad range of antimicrobial agents, including β-lactams, aminoglycosides, and fluoroquinolones (Smith et al., 2017).

This resistance is primarily attributed to unique characteristics of this bacterium such as low membrane permeability and the presence of multidrug efflux pumps (Smith et al., 2017).

The outer membrane of *P. aeruginosa* acts as a barrier, limiting the entry of many antimicrobial agents into the bacterial cell.

This reduced permeability makes it more difficult for antibiotics to penetrate and exert their antibacterial effects (Gellatly et al.,2013). The multidrug efflux pumps of the bacterium are membrane proteins that expel them, before they reach their targets, and exert their antimicrobial activity. The development of resistance in this bacterium can occur through the selection of mutations in chromosomal genes or through the acquisition of resistant determinants via horizontal gene transfer. (Morita et al., 2014; Ruiz-Garbajosa et.al., 2017; Klockgether et al., 2017; Rodrigo-Troyano et al., 2017).

One of the environments commonly colonized by *P. aeruginosa* is the respiratory tract of cystic fibrosis (CF) patients (Gaspar et al., 2013; Dalemans et al., 1991, Odolczyk et al., 2013). The chronic lung infections caused *by P. aeruginosa* are associated with alteration of pulmonary functions and general health of CF patients. The difficulty of eradicating this pathogen comes from its ability to evolve towards high-persistence phenotypes through genetic adaptation (Camus et. al., 2021) and to formation of biofilm communities.

1.3 Cystic Fibrosis

Cystic Fibrosis (CF) is a genetic disease that affects a wide range of populations (approximately 75,000 individuals worldwide) and involves several organs, including pancreas, liver, gastrointestinal tract, reproductive system, sweat glands and, particularly, the respiratory system. CF is caused by mutations in the CFTR gene, which encodes the CF transmembrane conductance regulator protein (CFTR). This protein is responsible for controlling the transport of chloride and bicarbonate ions across the epithelial cells membrane, primarily in the airways. (Elborn et al., 2016, Davies et. al.; 2018). The mutations in the *cftr* gene are grouped into 5 classes (Fig. 3) (Welsh et al., 1993) as follows:

- **First class**: Mutations able to generate a premature stop codon (e.g. G542X, W1282X, R1162X). Such mutations determine the production of a truncated, non-functional protein (Hamosh et al., 1991) or even the total absence of the CFTR protein itself.

- **Second class**: Mutations that affect the maturation of the CFTR protein, resulting in its trafficking defect (Cheng et al., 1990) and degradation. The most representative mutation is the F508del, determined by deletion of phenylalanine at position 508, which is also the mutation more frequent in CF patients.

- **Third class**: Gating mutations which alter the opening and closing mechanism of the channel (gating defect). In this case, the CFTR protein remains for a much longer time in the closed state. These mutations are G551D and G1349D that affect NBD domains.

- **The fourth class**: They alter the conductance of the channel, resulting in a partial reduction of the transport of Cl-. These mutations affect the amino acids involved in the pore formation.
- **The fifth class:** Mutations capable to impair maturation (splicing) of CFTR mRNA, reducing levels of normal protein (eg. 3849 + 10Kb C→T)

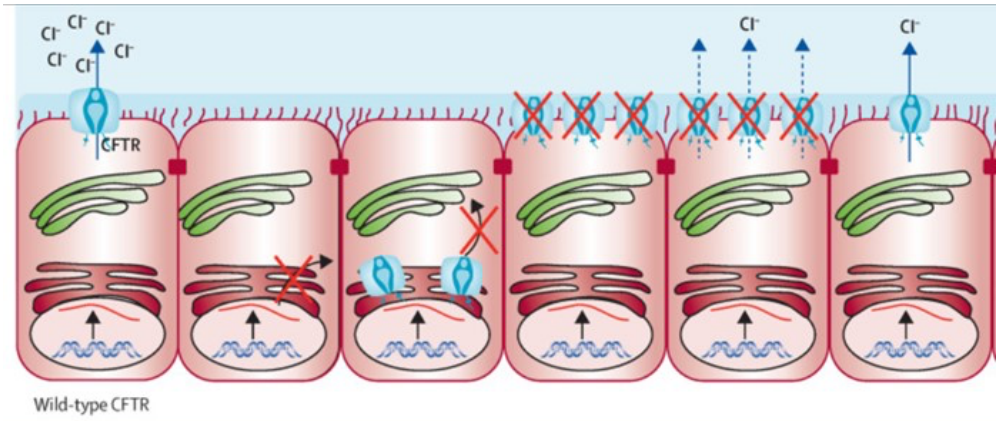

	Class I	Class II	Class III	Class IV	Class V
CFTR defect	No protein	No traffic	Impaired gating	Decreased conductance	Less protein
Mutation examples	Gly542X, Trp1282X	Phe508del, Asn1303Lys, Ala561Glu	Gly551Asp, Ser549Arg, Gly1349Asp	Arg117His, Arg334Trp, Ala455Glu	Ala455Glu, 3272-26A→G, 3849+10 kg C→T
Corrective therapy	Rescue synthesis	Rescue traffic	Restore channel activity	Restore channel activity	Correct splicing

Fig. 3 Classes of mutation in Cystic Fibrosis
(https://www.fibrosicisticaricerca.it/commento/nei-giorni-della-pandemia-e-della-paura-la-ricerca-in-fibrosi-cistica-dimostra-di-poter-cambiare-il-destino-delle-persone/)

As stated above, the most common mutation in the CFTR gene found in individuals with CF is the deletion of phenylalanine 508 (F508del-CFTR).

This mutation leads to the production of a misfolded CFTR protein that is rapidly degraded within the cells (Keating et al., 2018).

As a result, only a small fraction of the protein reaches the plasma membrane (Almughem et al., 2020) and exhibits a defect in channel gating (the opening and closing of the CFTR channel, which regulates the flow of chloride ions and water across the epithelial cells).

This reduced amount of functional CFTR protein at the cell surface contributes to the impaired chloride and bicarbonate transport across the epithelial cells, particularly in the airways. This leads to increased water absorption by the epithelial cells. The imbalance in ion transport and increased water absorption by the epithelial cells gives rise to the formation of a thick and sticky mucus in the airways. This mucus provides an ideal environment for the accumulation of inhaled microbes, including *P. aeruginosa*, leading to the onset of chronic pulmonary infections with serious respiratory dysfunctions.

1.3.1 CFTR and current potentiators and correctors

The CFTR protein is a large transmembrane protein with a molecular weight of approximately 165 kDa. This human protein consists of 1,480 amino acids and is organized into several functional domains. It spans the cell membrane and acts as an ion channel that facilitates the movement of ions across the cell membrane.

As a member of the ABC family (Gadsby et al., 2006), CFTR exhibits a structure characteristic of these proteins.

It consists of two transmembrane domains (MSDs) and two cytoplasmic nucleotide-binding domains (NBDs).

These domains are connected by the regulatory domain (R domain), which sets CFTR apart from other ABC transporters (Fig. 4).

The MSD1 and MSD2 domains are responsible for spanning the cell membrane and forming the ion channel pore and they are made of six α-helical segments that traverse the lipid bilayer.

The NBD1 and NBD2 domains, are involved in ATP binding and hydrolysis.

The R domain, located between NBD1 and MSD2, is unique to CFTR and distinguishes it from other ABC transporters: it contains multiple phosphorylation sites, and it serves as a regulatory region that influences CFTR channel activity and gating.

The phosphorylation of the R domain by protein kinases, such as protein kinase A (PKA), plays a crucial role in modulating CFTR function and its response to cellular signalling pathways.

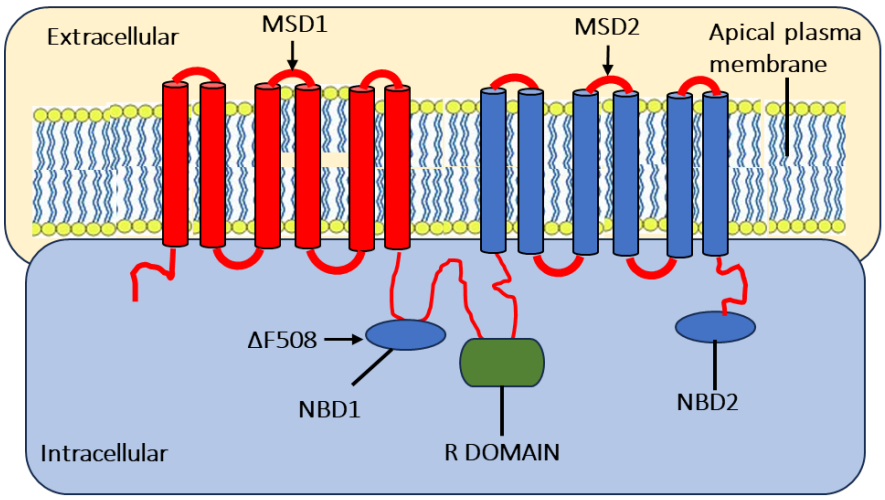

Fig.4 Structure of CFTR protein: the carboxy terminal (TRL) is anchored with the cytoskeleton; Membrane-spanning domain 1(MSD1), Membrane-spanning domain 2 (MSD2), Nucleotide-binding domain 1 (NBD1), Nucleotide-binding domain 2 (NBD2), Regulatory domain (R) (phosphorylation site)

Image modified from http://www.cusmibio.unimi.it/scaricare/walking/fibrosinew.pdf

The CFTR protein is primarily found on the apical plasma membrane of epithelial cells in various tissues throughout the body: airways, intestines, pancreas, glandular ducts, moles sweat gland tubules, pancreatic acini, bile ducts, moles testicles, in which it contributes to the regulation of chloride and bicarbonate transport (Sheppard et al., 1999; Jacquot et al.,1993).

The phosphorylation of R domain is mediated by protein kinases such as PKA, which is activated by the cyclic adenosine monophosphate (cAMP).

The opening and closing of the CFTR ion channel pore involve the binding and hydrolysis of ATP molecules, respectively. ATP binding occurs at the interface between NBD1 and NBD2 of CFTR (Gadsby et al., 2006, Vergani et. al., 2005). The F508del mutation, being the most common mutation associated with cystic fibrosis, has been a focus of research efforts to develop therapies that can correct the trafficking defect and gating defect of the mutated CFTR protein. The gating defect of the mutated CFTR channel can be treated with small synthetic molecules called **potentiators** (Fig .5).

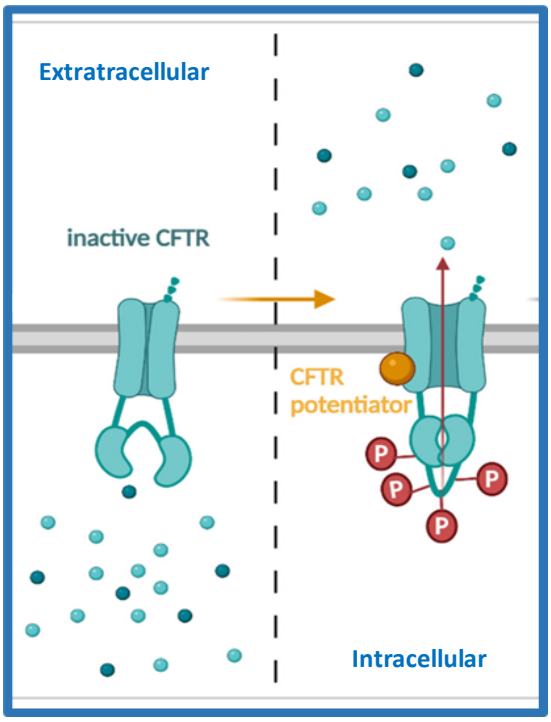

Fig. 5 Mechanism of action of Potentiators. (Image modified from Marjolein et. al., 2022). https://www.mdpi.com/2073-4409/11/12/1868. Left: inactive CFTR. Right: CFTR potentiators (orange) interact directly with CFTR to promote function, in a phosphorylation-dependent manner.

They are chemical compounds belonging to the classes of flavonoids, of xanthines and benzimidazolones.

At micromolar concentrations, such compounds can increase the activity of the mutated CFTR channel by favouring NBD dimerization and therefore ions permeation through the channel.

In the last few years, the list of potentiators has been significantly expanded through the screening of a large scale of chemical compounds (Verkman et al., 2004).

In this way, phenylglycines, sulfonamides and 1,4-dihydropyridines were discovered as potentiators at nanomolar concentrations (Pedemonte et al., 2005a; Pedemonte et al., 2005b; Pedemonte et al., 2007). Potentiators are not only useful for mutation F508del but particularly effective on the class 3 mutations, for example G551D, in which only gating defect is observed (Moran et. al.,2005). Ivacaftor (VX-770) developed by Vertex Pharmaceuticals is one of the most successful and well-known potentiators used for treatment of cystic fibrosis. Clinical studies have shown significant improvements in respiratory function, body weight, and sweat chloride concentration in patients with mutation G551D-CFTR (Ramsey et al., 2011).

The trafficking defect associated with the F508del-CFTR mutation, can be partially corrected *in vitro* using chemical chaperones, such as glycerol and dimethyl sulfoxide (DMSO). These chaperones act by stabilizing protein folding and aiding the proper trafficking of misfolded CFTR proteins (Denning et al., 1992; Sato et al., 1996).

These molecules known as **correctors**, have the potential to improve the trafficking defect associated with the F508del-CFTR mutation (Pedemonte et al., 2005c), preventing the degradation of the protein by proteasome.

Other compounds can interact with other proteins facilitating the release of F508del-CFTR from endoplasmic reticulum and its transport to plasma membrane.

Finally, a third type of correctors could act by slowing the internalization of the mutated protein from cell surface and degradation by the lysosome.

Among the correctors that have shown promise in preclinical and clinical studies, lumacaftor (VX-809), developed by Vertex Pharmaceuticals, has gained significant attention. However, the mechanism of action of the correctors is still not completely clear.

In vitro studies have shown that the complete activation of CFTR channels with gating mutations can be achieved by the addition of specific compounds. One approach involves the use of forskolin (FSK), which acts as an activator of adenylate cyclase. By stimulating adenylate cyclase, FSK promotes the production of cAMP, while genistein, an isoflavone acting as potentiator, enhances the open channel probability of defective CFTR by stabilizing the dimerization of NBDs domains of CFTR (Ferrera et al., 2022).

Pulmonary infections in CF still present significant challenges because bacteria can develop resistance to commonly used antibiotics, forming biofilm that are difficult to eradicate. Therefore, the search for new anti-infectious drugs is highly demanded and antimicrobial peptides hold promise to address this issue.

1.4 Natural antimicrobial peptides and innate immunity

The development of new antimicrobial strategies is crucial, due to the emergence and spread of multidrug-resistant (MDR) bacterial strains. Antibiotics that were effective against these bacteria are becoming less effective, leading to limited treatment options and increased morbidity and mortality rates. Antimicrobial peptides (AMPs) represent a promising avenue for the development of new antimicrobial therapies.

They offer a potential solution to combat multidrug-resistant bacteria and provide alternative options for treatment of infectious diseases (Mangoni et al., 2011; Alba et al., 2012; Fjell et al., 2011). AMPs, also known as host defense peptides (HDPs), are evolutionarily conserved molecules found in various organisms including bacteria, fungi, insects, plants, amphibians, and mammals, among others (Ageitos et al., 2016/2017). The discoveries of insect cecropins by Hans Boman (Boman et al., 1995), human α-defensins by Robert Lehrer (Turner et al.,, 1998), and magainins by Michael Zasloff (Zasloff et al., 1987) in the 1980s significantly contributed to the growth of AMPs research (Wang et al., 2016a). AMPs serve as an essential component of the innate immune system, acting as a first line of defense against a wide range of infectious agents.

They exhibit antimicrobial activity against various types of microorganisms, including Gram-positive and Gram-negative bacteria, viruses, fungi, and certain parasites.

The innate immune system, present in all organisms, is rapid and does not change during repeated infections, while the adaptive immune system, which evolved most recently in vertebrates, is highly specific for pathogens.

AMPs are primarily secreted by tissues that form a barrier against the external environment, such as the skin and mucous membranes to prevent colonization of host tissues by pathogens.

AMPs from higher eukaryotes, in addition to their antimicrobial activity, have been found to possess various immunomodulatory properties.

These properties enable them to influence the host immune response and contribute to various physiological processes: stimulation of chemotaxis (Mookherjee et al., 2007), suppression of pro inflammatory cytokine release (Afacan et al., 2012), immune cell differentiation (Davidson et al., 2004), promotion of angiogenesis and wound-healing (Wu et al., 2010) to prevent colonization of host tissues by pathogens (Fig. 6).

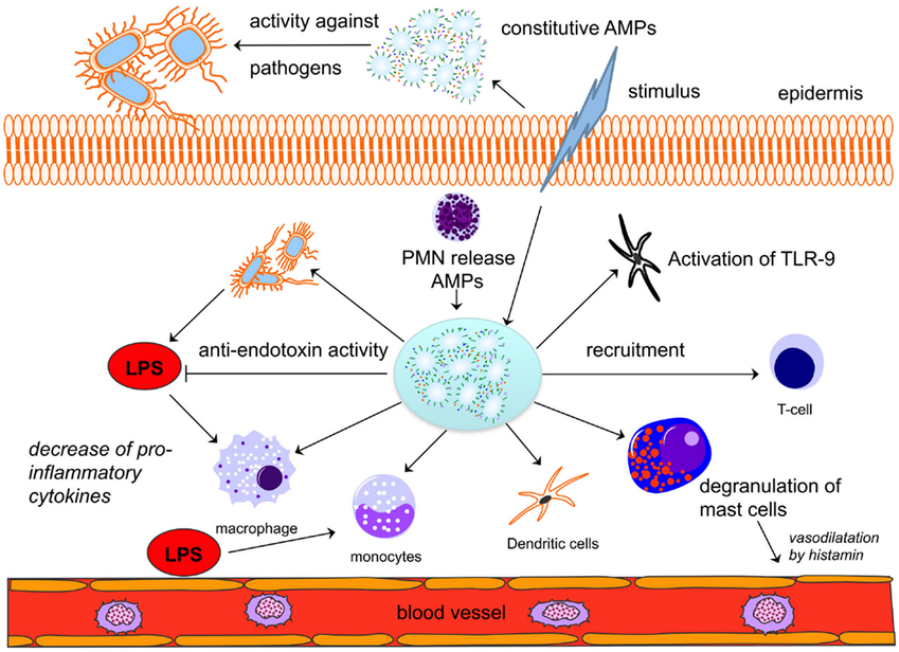

Fig. 6 Multiple functions of antimicrobial peptides in host defense.

Abbreviations: AMPs, antimicrobial peptides; LPS, lipopolysaccharide; PMNs, neutrophils.

Image from https://www.researchgate.net/figure/Antimicrobial-peptides-play-a-central-role-in-innate-and-adaptive-immunity-A-given_fig4_281622331

1.5 Structural properties and general features

AMPs generally contain less than 100 amino acids (Ganz et al., 2003).

The synthesis of AMPs differs from conventional antibiotics in terms of their origin and production process. While conventional antibiotics are typically synthesized by microorganisms through complex biosynthetic pathways involving multiple enzymes, AMPs are encoded by genes and synthesized by the host organism's ribosomes (Boman et al.,1995).

Besides humans, natural AMPs have been found in different kingdoms (animals, plants, bacteria, fungi but also archaea and protists) (Vanzolini et al., 2022).

They are initially synthesized as pre-propeptides, which are larger precursor molecules ranging from 60 to 170 amino acids in length.

The pre-propeptide structure consists of distinct regions, including an N-terminal signal peptide for endoplasmic reticulum recognition, an anionic portion, which has the function of neutralize the positive charges of the peptide making it inactive and the C-terminal cationic peptide which acquires its antimicrobial activity after cleavage from the rest of the molecule by different kind of proteases (Bals et al., 2000). Another common feature is represented by the hydrophobicity conferred by hydrophobic amino acids that often overcome 50% of the total amino acid sequence. The high lipophilicity is useful especially for the penetration in the biological membranes (Vanzolini et al., 2022).

Many natural AMPs show host toxicity, rapid degradation by proteases, instability due to pH changes, loss of activity in presence of serum and high salt concentrations, lack of suitable delivery systems, and high costs of production (Sarkar et al., 2021; Nordström et al., 2017). Therefore synthetic peptides have been developed to overcome the difficulties linked to the natural peptides while mimicking their pharmacological qualities (Lei et al., 2019). The approaches commonly used for the development of non-natural AMPs are the following:

- site-directed mutations characterized by the addition, deletion or substitution of amino acids;

- de novo design without using any template sequence;
- template-based design that uses fragments of the parental compound as starting point for the construction of new AMPs;
- self-assembly-based design that exploits the formation of simple nanostructures like dimers, vesicles and nanotubes (Huan et al., 2020).

Naturally-occurring AMPs generally undergo post-translational modifications encompassing glycosylation, C-terminal amidation (a very common modification in linear AMPs from frog skin) (Mangoni et al., 2006; Nicolas et al., 2009), amino acid isomerization, halogenation, cyclization, N-terminal acetylation and hydroxylation, that modify their activity (Zasloff et al., 2002; Wang et al., 2012).

They play an important role in modulating the activity and properties of AMPs. These modifications can occur during or after the synthesis of the pre-propeptides and contribute to the functional diversity observed among AMPs.

AMPs often exhibit a positive charge due to the presence of amino acid residues such as lysine (Lys) and arginine (Arg), and also they possess a substantial portion (usually ≥30%) of hydrophobic residues conferring the AMPs an amphipathic character (Zasloff et al., 2002; Rinaldi et al., 2002; Hancock et al., 2006). Note that when the AMPs interact with hydrophobic environments such as biological or artificial membranes, they tend to adopt amphipathic conformations.

These conformations involve the arrangement of the peptide sequence in a way that separates hydrophobic and hydrophilic regions (Powers et al., 2003).

AMPs can be classified into different families based on their secondary structure: α-helices, β-sheets, non-α- or β-structures (extended) and with a hairpin-loop structure (Fig. 7) (Mojsoska et. al., 2015) as follows:

- **α-helical peptides (Fig. 7A)**: the peptide backbone forms a coiled structure with a helical shape. Peptides belonging to this group are well known: the human cathelicidin LL-37, the frog skin magainins and the insects cecropins (Boman et al., 1995; Zanetti et al., 2002; Mahlapuu et al., 2016; Huang et al., 2010).
- **β-sheets peptides (Fig. 7B):** these AMPs form β-sheet structures, where the peptide backbone forms extended strands that are stabilized by hydrogen bonding between adjacent strands. The hydrophobic and hydrophilic residues are typically distributed on different sides of the β-sheet, creating an amphipathic structure. Some examples are the defensins which are produced by neutrophils, macrophages and epithelial cells (Lai et al., 2009) and protegrins, discovered in porcine leukocytes (Taylor et al., 2008). The β-sheet peptides are more ordered in aqueous solution because of their rigid structure (Yeaman et. al., 2003).

- **Extended/random-coil linear peptides (Fig. 7C):** these AMPs do not adopt a well-defined α-helix or β-sheet structure. They often contain a high content of arginine, proline, tryptophan, and/or histidine residues and they fold into amphipathic structures after contact with a membrane (Takahashi et al.,2010; Nguyen et al., 2011).

- **Peptides exhibiting a hairpin-loop structure (Fig. 7D):** the peptide chain folds back on itself to form a loop or turn. This structure often brings together hydrophobic and hydrophilic residues on different sides of the hairpin, creating an amphipathic arrangement. (Ma et al., 2016).

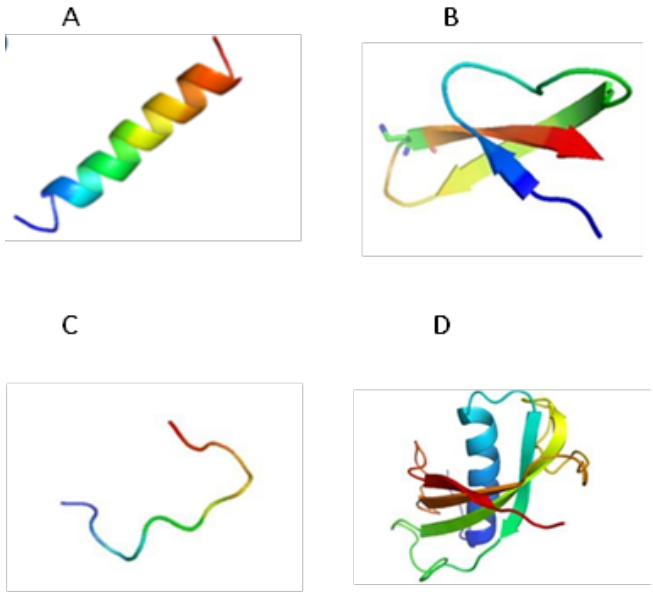

Fig. 7 Structure of Antimicrobial peptides (AMP) (B.S. Lopes et. al 2022)

1.6 AMPs: mechanism of antibacterial activity

AMPs can be categorized into two main classes based on their mechanism of microbicidal activity:

- **Membranolytic peptides**: These AMPs exert their antimicrobial activity by directly targeting and disrupting the microbial cell membrane. They interact with the negatively charged microbial membranes, often rich in phospholipids, through electrostatic interactions between their cationic residues and the negatively charged membrane components (Zhang et al., 2021).
- **Non-membrane active peptides**: They have antimicrobial activity that is not primarily dependent on direct membrane disruption. Instead, they target intracellular components or biological processes of microorganisms, such as DNA, RNA, proteins, enzymes, or cell wall synthesis (Zhang et al., 2021).

The initial step in the interaction of AMPs with microbial cells is the electrostatic attraction between the positively charged AMPs and the negatively charged components on the microbial cell surface such as the lipopolysaccharides (LPS), in the outer membrane of Gram-negative bacteria, or acidic polysaccharides (teichoic and teichuronic acids), in the peptidoglycan layer of Gram-positive bacteria (Brogden et al., 2005) (Fig. 8).

The presence of bivalent ions, particularly Ca^{2+} and Mg^{2+}, helps to stabilize the LPS structure and maintain the integrity of the outer membrane of Gram-negative bacteria. By displacing these ions, cationic peptides can cause destabilization and disruption of the outer membrane.

This disruption allows the peptides to gain access to the periplasmic space, which is located between the outer and inner membranes of Gram-negative bacteria. (Hancock et al., 1997; Zasloff et al., 2002). Microbial membranes, especially those of Gram-negative bacteria, contain a higher proportion of anionic phospholipids, such as phosphatidylglycerol and cardiolipin, compared to mammalian cell membranes, which are predominantly composed of zwitterionic lipids like phosphatidylcholine, sphingomyelin, and cholesterol (Lohner et al., 2009).

The difference in lipid composition between microbial and mammalian membranes plays a significant role in the selectivity of AMPs. Since mammalian cell membranes contain a higher proportion of zwitterionic lipids, they have a reduced affinity for cationic AMPs compared to microbial membranes.

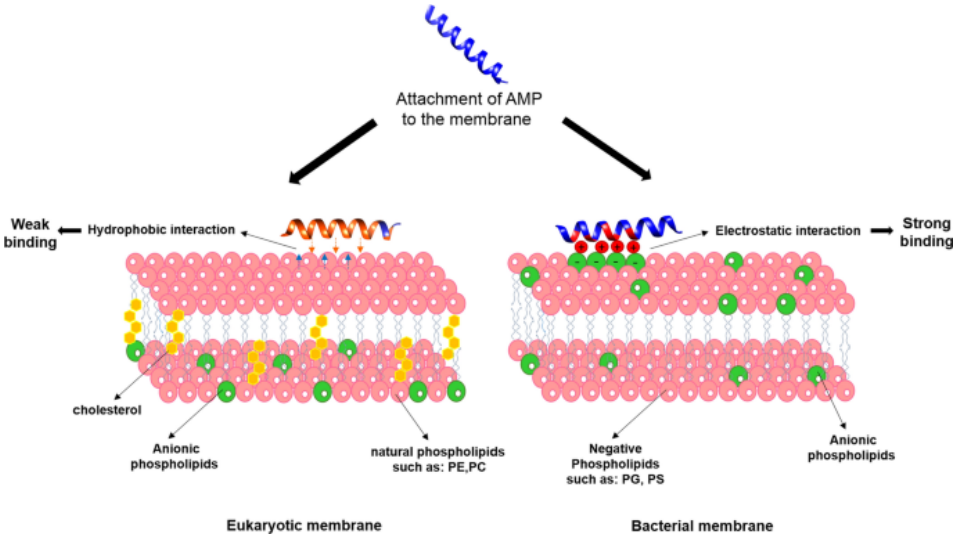

Fig. 8 Molecular basis of cell selectivity of AMPs. AMPs form amphipathic structures with a positively charged face (red) and a hydrophobic face (orange). (Image taken from Parchebafi et al., 2022)

The permeabilization of the microbial membrane is a crucial step in the microbicidal activity of AMPs. After initial interaction with the microbial membrane, AMPs can disrupt the membrane integrity, leading to membrane permeabilization.

Several models that explain membrane disruption by AMPs have been proposed:

- **Barrel-stave model** (Ehrenstein et al., 1977): AMPs form transmembrane channels or pores by inserting into the lipid bilayer in a "barrel-stave" arrangement. They are inserted perpendicularly to the plane of the membrane bilayer forming a pore like a stave (Fig. 9).
  The hydrophobic regions of the AMPs align themselves with the hydrophobic core of the lipid bilayer, while the cationic regions face the aqueous environment.

- **Toroidal pore model** (Ludtke et al.,1996; Matsuzaki et al.,1996): in this model, the formation of transmembrane pores involves a dynamic interaction between the peptides and the lipid bilayer, leading to a toroidal structure. The peptides intercalate into the lipid bilayer, with their polar faces in contact with the polar head groups of the membrane phospholipids (Brogden et al., 2005) (Fig. 9).

- **Carpet-like model** (Shai et al., 1999; Pouny et. al., 1992) (Fig. 9): AMPs do not insert into the hydrophobic core of the lipid bilayer but instead align parallel to the membrane surface. The peptide molecules cover the membrane surface in a carpet-like manner, forming a continuous layer without penetrating into the hydrophobic region of the lipid bilayer. Initially, the peptides may orient themselves with their hydrophilic face toward the phospholipid headgroups and their hydrophobic face toward the lipids (Shai et al., 2002).

- **Disordered toroidal pore model**: the pore formation is more stochastic and involves fewer peptides (Sengupta et al., 2008). AMPs form toroidal pores in the lipid bilayer, but unlike the toroidal pore model described earlier, the peptide-lipid interactions are not well-organized and structured (Fig. 9).

- **Membrane thinning/thickening affection model:** the ability of AMPs modulate the thickness of the lipid bilayer (Grage et al., 2016).

Depending on the specific properties of the AMP and the lipid composition of the membrane, AMPs can induce either thinning or thickening of the membrane. (Grage et al., 2016) (Fig. 9).

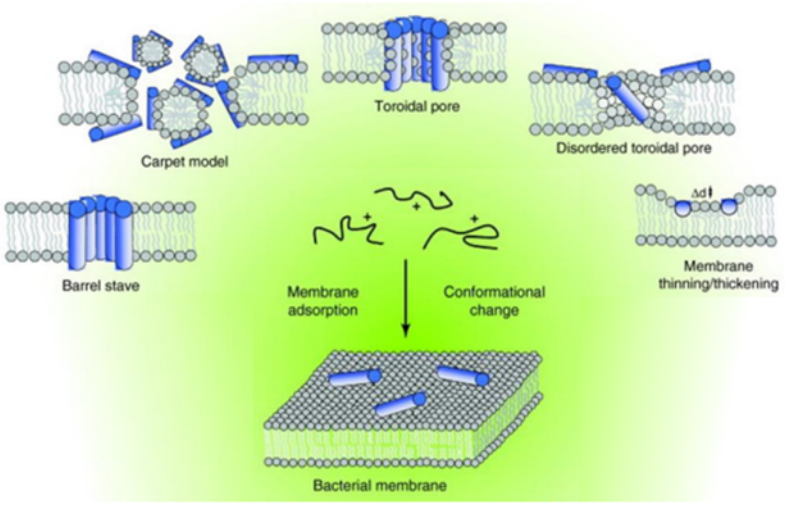

Fig. 9 Schematic representation of some mechanisms of action of membrane-active AMPs (modified by Nguyen et al., 2011).

Unlike conventional antibiotics that often target specific cellular components or processes, AMPs exert their antimicrobial activity through a non-specific mechanism of action. They do not require stereospecific interaction with chiral targets such as receptors.

The limited emergence of resistance to AMPs is attributed to the highly disrupting membranolytic mechanism in association with other intracellular targets (Zasloff et al., 2002; Kraus et al., 2006).

Non-membrane active mechanism

Besides membrane disruption, recent studies have shown how peptides can act on other targets.

Some AMPs can bind some components and receptors on the extracellular side of the membrane and cell wall, thus activating intracellular signalling pathways that have, as a response, the inhibition or activation of several biological processes (Vanzolini et al., 2022).

An important clue of a non-lytic mode of action is the temporal dissociation between cell death, measured as inhibition of colony formation, and changes in membrane permeability.

Other AMPs manage to enter the cytosol through direct penetration, endocytosis (both micropinocytosis and receptor-mediated) (Madani et al., 2011), where they can affect different enzymes and intermediates involved in vital processes.

Usually, AMPs that act on the protein biosynthesis target the ribosome subunits (Polikanov et al., 2018) but some others can interfere with the incorporation of histidine, uridine and thymidine (Friedrich et al., 2001, Patrzykat et al., 2002), the amino acid synthesis pathways (Ho et al., 2016; Florin et al., 2017), the regulation of sigma factors (El-Mowafi et al., 2015), the nucleotide and coenzyme transport (Ho et. al.; 2016) and the degradation of DNA-replication-associated proteins (van Eijk et al., 2017).

AMPs display an indirect antimicrobial activity by affecting the immunomodulatory response of the host reducing endotoxin-induced inflammatory response or the secretion of cytokines and macrophages recruitment, inhibiting proteins' synthesis by targeting ribosomes, inhibiting DNA/RNA synthesis (Casciaro et al., 2020).

There are also inhibitors of cell division that block DNA replication or the mechanisms essential for the repair of DNA damages, then resulting in the block of the cell cycle, the failure of septation, in substantial change in the cell morphology with clearly visible blebbing and elongation towards a filamentous shape (Chileveru et al., 2015; Salomón et al., 1992).

Mechanism underlying the immunomodulatory properties of AMPs

Regarding the mechanism of action of to explain how AMPs activate mammalian cells, three models have been proposed (Lai et al., 2009) (Fig. 10):

- **Trans-activation model**: AMPs can induce the release of membrane-bound growth factors, such as HB-EGF (heparin binding epidermal growth factor), which then bind to its high-affinity receptor EGFR (epidermal growth factor receptor) and activates downstream signalling pathways.

- **Alternate ligand model**: AMPs, such as defensins and cathelicidins, can directly bind to specific receptors, initiating signaling pathways and eliciting cellular responses. This mode of action is different from the traditional receptor-ligand interaction, where ligands are typically small molecules or proteins.

  Two examples of such receptors are chemokine receptor 6 (CCR6) and formyl peptide receptor 1 (FPRL-1).

- **Membrane disruption model**: AMPs can interact with the membrane and alter its properties, leading to changes in the localization and function of membrane-bound receptors. One example of this phenomenon involves the epidermal growth factor receptor (EGFR) and the disruption of lipid rafts, where these receptors are located (Pike et al., 2005) and the consequent inhibition of ligands binding to EGFR and its activation.

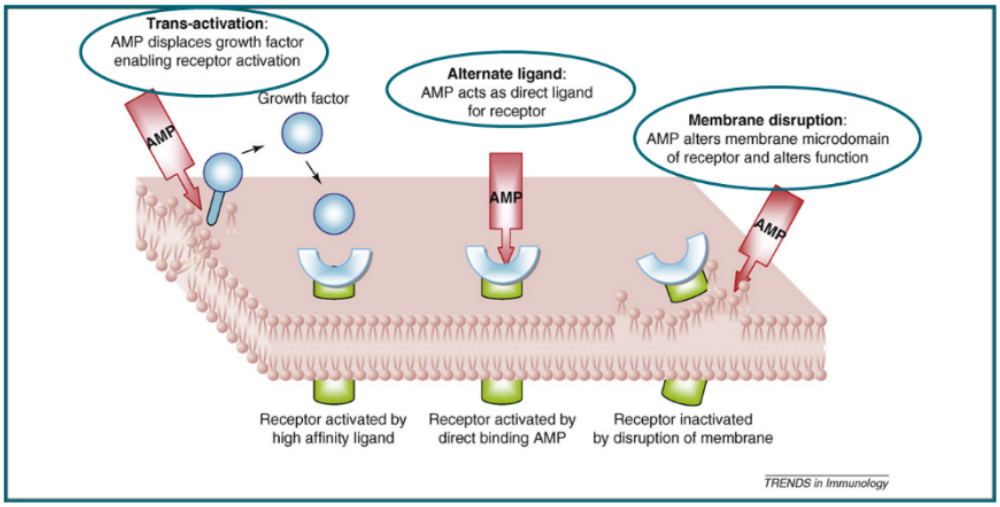

Fig. 10 Image modified of alternative models for host activation by antimicrobial peptides (from Lai et al., 2009).

1.7 Frog-Skin AMPs

The skin of amphibians is indeed one of the richest sources of biologically active compounds. Amphibians, such as frogs and toads, have evolved a diverse array of chemical compounds in their skin, which serves for physiological regulation and defense mechanisms.

AMPs in amphibians are often stored in dermal serous glands, which are primarily located in the skin's dorsal region. These glands are surrounded by myocytes (muscle cells) and innervated by sympathetic fibres (Fig. 11).

Under certain conditions, such as stress or physical injury, adrenergic stimulation occurs in the myocytes.

This stimulation leads to the compression of the serous glands, resulting in the discharge of their contents. This process is often described as a holocrine-like mechanism (Simmaco et al., 1998; Conlon et al., 2004).

Fig. 11 Histological preparation of Pelophylax lessonae/ridibundus frog skin (previously named Rana Esculenta) (from Mangoni et al., 2006)

Amphibian AMPs are grouped into different families, e.g. magainins, temporins, brevinines -1 and -2, ranalexins, ranacyclins, bombinins and esculentins-1 and -2 (Conlon 2004; Conlon et al. 2009; Mangoni et al. 2003; Morikawa et al. 1992) (**Table 1**).

Table 1 Primary structure of some frog-skin AMPs (Conlon 2004; Conlon et al. 2009; Mangoni et al. 2003; Morikawa et al. 1992)

Genus	Peptide	Sequence
Xenopus	Magainin-1	GIGKFLHSAGKFGKAFVGEIMKS
	Magainin-2	GIGKFLHSAKKFGKAFVGEIMNS
Bombina	Bombinin	GIGALLSAAKVGLKGLAKGLAEHFAN-NH2
	Bombinin H1	IIGPVLGMVGSALGGLLKKI-NH2
Rana	Temporin A	FLPLIGRVLSGIL-NH2
	Brevinin-1	FLPVLAGIAAKVVPALFCKITKKC
	Brevinin-1	GLLDSLKGFAATAGKCVLQSLISTASCKLAKTC
	Ranalexin	FLCCLIKIVPAMICAVTKKC
	Ranaciclin-T	GALRGCWTKSYPPKPCK-NH2
	Esculentin-1	GIFSKLGRKKIKNLLISGLKNVGKEVGMDVVRTGIDIAGCKIKGEC
	Esculentin-2	GILSLVKGVAKLAGKGLAKEGGKFGLELIACKIAKQC

Since the isolation of magainins by Zasloff in the 1980s, numerous AMPs have been isolated and identified from various amphibian species.

Some of the species encompass *Xenopus laevis, Bombina variegata, Bombina orientalis, Phyllomedusa sauvagei*, and different species of the genus Rana (commonly known as frogs) (Ladram et al., 2016).

1.7.1 Esculentin-1 family

The esculentin-1 family of peptides was first isolated and purified from the skin secretion of European frogs belonging to the species *Pelophylax lessonae/ridibundus* (previously known as *Rana esculenta*) (Conlon et al., 2008) (Fig. 12), after electrical stimulation of animals. The collected secretion was then analyzed by reverse phase-liquid chromatography and the single peaks containing peptides identified and characterized for their primary structure (Simmaco et al., 1993).

Fig. 12 A specimen of Pelophylax lessonae/ridibundus.

All members of this frog AMP family have a highly conserved amino acid sequence consisting of 46 residues and characterized by a C-terminal loop stabilized by a disulphide bridge forming an hepta peptide ring (Simmaco et al., 1994).

They have a net charge of +5 at neutral pH and an amphipathic α-helical structure in membrane mimetic environments (Mangoni et al., 2015; Wang et al., 2016b).

Esculentins-1, belonging to esculentin family of peptides, have been found to possess a broad spectrum of antimicrobial activity. They are effective against both Gram-positive and Gram-negative bacteria, including challenging pathogens like *P. aeruginosa*. Additionally, they exhibit antifungal activity against species such as *C. albicans*.

The lethal concentrations of esculentin-1 against these microorganisms typically range from 0.1 to 1.5 μM, indicating potent antimicrobial properties. One notable advantage of esculentin-1 peptides is their relatively low cytotoxicity towards mammalian cells (Simmaco et al., 1993; Ponti et al., 1999; Mangoni et al., 2015). In addition to the full-length esculentin-1 peptides, a fragment corresponding to the 19-46 portion of esculentins-1, called Esculentin-1a(19-46), was isolated from the skin secretions. However, this fragment was found to be devoid of antimicrobial activity. The lack of antimicrobial activity in esculentin-1a(19-46) was attributed to its low net positive charge at neutral pH (Simmaco et al., 1994). Compared to the full-length esculentins-1, which typically have a net positive charge of +5, this fragment only has a net positive charge of +1.

The net positive charge is important for the interaction of antimicrobial peptides with negatively charged microbial membranes.

To investigate the potential antimicrobial activity of the N-terminal 1-18 portion of esculentins, which was not found in the HPLC profile of the secretion, likely due to proteolytic degradation, it was chemically synthesized. To maintain a net charge of +5 at neutral pH and to enhance its stability, the C-terminus of Esc(1-18) was amidated (Mangoni et al., 2003).

The synthetic Esc(1-18) was then analyzed for its antimicrobial activity. It was observed that it adopted an α-helical structure in lipid vesicles mimicking the anionic character of microbial membranes.

This structural characteristic suggested that Esc(1-18) could interact with and disrupt the membranes of microorganisms, leading to antimicrobial effects. Further studies showed that the antimicrobial activity of the synthetic Esc(1-18) was comparable to that of the full-length esculentin-1 (Mangoni et al., 2003).

This finding suggested that the antimicrobial activity of esculentins primarily reside in its N-terminal portion.

To investigate the importance of the N-terminal region for antimicrobial properties, a longer analog named esculentin-1a(1-21)NH2, or Esc(1-21) (**Table 2**), was synthesized and characterized.

This longer analog was designed to have 21 amino acids to ensure that it met the minimum length requirement for an α-helical peptide to span a phospholipid bilayer, which is approximately 30 Å thick (Gamberi et al., 2007).

Esc(1-21) was then evaluated for its biological properties, including antimicrobial activity.

Table 2 Primary structure of some derivatives of esculentins-1 (Mangoni et al., 2003; Mangoni et al., 2015; Gamberi et al., 20007)

Peptide designation and sequence	**Net charge***
Esc(1-21) **GIFSKLAGKKIKNLLISGLKG-NH₂**	**+6**
Esc(1-21)-1c **GIFSKLAGKKIKNL$_{(D\ Leucin\ 14)}$ LIS$_{(D\ Serin\ 17)}$ GLKG-NH₂**	**+6**
Esculentina-1a **GIFSKLAGKKIKNLLISGLKNVGKEVGMDVVRTGIDIAGCKIKGEC**	**+5**
Esc(1-18) **GIFSKLAGKKLKNLLISG-NH₂**	**+5**
Esculentina-1b **GIFSKLAGKKLKNLLISGLKNVGKEVGMDVVRTGIDIAGCKIKGEC**	**+5**

*Basic and acid amino acids are indicated by red and blues letters, respectively. Net charge, at physiological pH

1.8 Esc peptides: Esc(1-21) and Esc(1-21)-1c structural features and biological properties

The Fig. 13 represents the l-amino acid sequence of the peptide Esc(1-21).

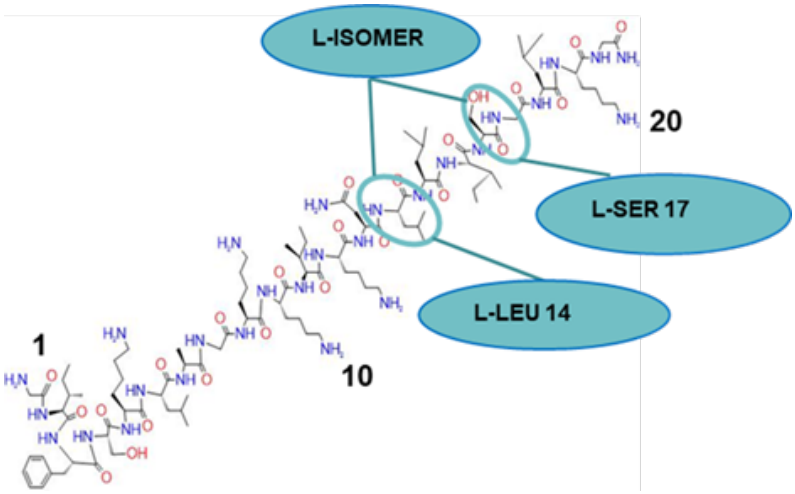

Fig. 13 Structure of Esc(1-21)

The main properties of Esc(1-21) are the following.

- **Net positive charge +6:** this is an important feature for the electrostatic interaction of the peptide with the negatively charged membranes of microbial cells. (Gellatly et al., 2013; Mangoni et al., 2015).

- **Potent antimicrobial activity (ranging from 1 µM to 25 µM):** particularly against Gram-negative bacteria such as *P. aeruginosa* (Luca et al., 2013).
- **Weaker antimicrobial activity against Gram-positive bacteria:** in comparison to the activity showed against Gram-negative bacteria (Kolar et al., 2015).

- **Lower cytotoxicity**: against human erythrocytes in comparison to Esc(1-18) (Islas-Rodriguez et al., 2009; Luca et al., 2013).

Esc(1-21) and other AMPs share common limitations that hinder their therapeutic potential. These limitations include low biostability, cytotoxicity at high concentrations, and challenges in achieving effective concentrations at the site of infection. Various biochemical approaches have been used to enhance the biological properties of Esc(1-21). The diastereomer of Esc(1-21), known as Esc(1-21)-1c, was synthesized with modifications to increase its bioavailability by substituting two L amino acids in the C-terminal region, l-Leu_{14} and l-Ser_{17}, with the corresponding enantiomers in D configuration (Casciaro et al., 2019). Experimental data revealed that the isomer containing d-amino acids (Fig. 14)

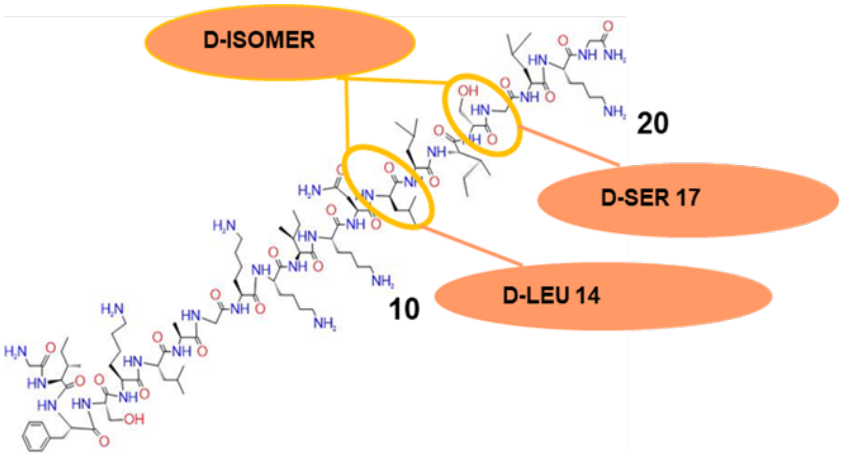

Fig. 14 Structure of Esc(1-21) -1c

The following properties compared to the original Esc(1-21).

- **Similar haemolytic activity** (< 10%)

- **Greater stability in serum**: the percentage of intact diastereomer in 10% serum amounts to about 46% compared to 22% of the "wild-type" peptide (Di Grazia et al., 2015)

- **Significant reduction of cytotoxicity towards mammalian cells:**
  The decrease of cytotoxicity was found towards different types of mammalian cells including erythrocytes (red blood cells), lymphocytes (white blood cells), macrophages (immune cells), and epithelial cells (cells lining body surfaces) with a 256 μM compared to 64 μM of Esc(1-21) (Rodriguez et al., 2009; Di Grazia et al., 2015; Baltimore et al., 1989). This lower toxicity is likely due to a minor helical content in comparison to Esc(1-21), as proved by through NMR studies using dodecylphosphocholine (DPC) micelles mimicking the zwitterionic composition of the outer leaflet of the cell membrane of mammalian cells (Loffredo et al., 2017) (Fig. 15).

- **Neutralization of LPS:** the diastereomer Esc(1-21)-1c exhibits reduced ability to neutralize the toxic effects of LPS , highlighting a diminished anti-endotoxic activity (Ghosh et al., 2016).

Both Esc(1-21) and Esc(1-21)-1c (namely Esc peptides) exert their antimicrobial activity primarily by disrupting the integrity of microbial cell membranes.

It was demonstrated that almost the total perturbation of model bacterial membrane was achieved by Esc(1-21) within 5 min (at concentrations ranging from 16 μM to 32 μM) or 15 min (in the concentration range from 2 μM to 8 μM). This effect was significantly weaker and slower compared to that of Esc(1-21)-1c (Loffredo et al., 2017).

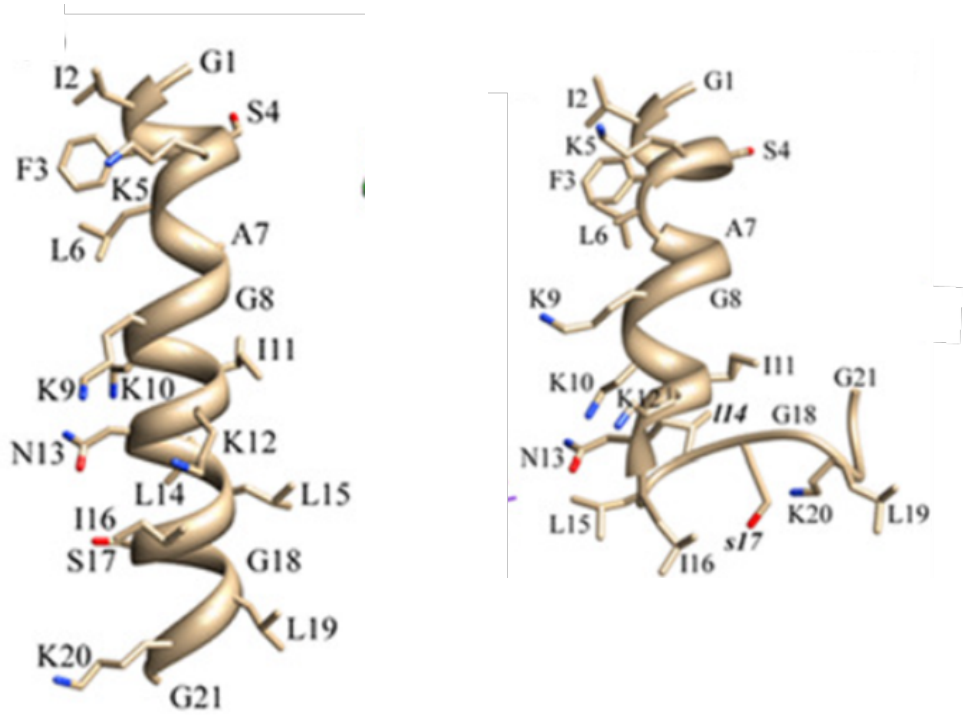

Fig. 15 Three-dimensional solution structures (NMR study) of: Esc(1-21)and (B) Esc(1-21)-1c in DPC micelles. (Loffredo et al., 2017)

As showed in Fig. 15 by solution NMR studies in dodecylphosphocholine (DPC) micelles, which simulate the neutral membrane of mammalian cells, an α-helical structure was preserved along the entire amino acid sequence of Esc(1-21), while a highly flexible C-terminal arm was present in Esc(1-21)-1c. The diastereomer, in DPC micelles, exhibits a partial α-helical conformation only at the N-terminal region between residues I2-N13. In fact, in comparison to Esc(1-21), Esc(1-21)-lc adopts a partial helical conformation only at the N-terminal region (G1-K12) while the C-terminal region (N13-G21) is unstructured and adopts a flexible conformation.

This was attributed to the presence of d-amino acids at 14^{th} and 17^{th} position, which broke the stereo chemical integrity of the sequence made of l-amino acids (Loffredo et al., 2017).

1.8.1 Antimicrobial activity against planktonic and biofilm forms of *P. aeruginosa*

In a previous work, (Di grazia et al., 2015) it was demonstrated that both Esc peptides at low concentrations (ranging from 1 and 4μM), have potent antimicrobial activity against various strains of *P. aeruginosa* Esc(1-21) exhibited comparable efficacy against different strains of *P. aeruginosa,* as indicated by the similar minimal inhibitory concentration (MIC), which is the lowest concentration of the peptide that inhibits microbial growth (Luca et al., 2013). Similarly, the diastereomer Esc(1-21)-1c showed comparable efficacy, achieving the same level of effectiveness especially against the biofilm form of microorganisms.

Subsequently, they were found to rapidly kill both the planktonic (free-floating) and biofilm forms of *P. aeruginosa* (Casciaro et al., 2020).

Esc(1-21) was able to induce significant damage to the cytoplasmic membrane of the planktonic and biofilms cells of *P. aeruginosa* PAO1 cells (Luca et al., 2013).

The diastereomer Esc(1-21)-1c was reported to be more efficient in eradicating *Pseudomonas* biofilm (Loffredo et al., 2017). Furthermore, Esc(1-21)-1c was found to have inhibitory effects on *P. aeruginosa* biofilm formation. This inhibition was attributed to several factors. The diastereomer reduced the swimming, swarming, and twitching motility of *P. aeruginosa*. By reducing these motility mechanisms, Esc(1-21)-1c would hinder the ability of *P. aeruginosa* to form biofilms, by interfering with the bacterial capability to achieve a surface for the establishment of a sessile community.

The same peptide was also able to provoke a substantial reduction in the level of mRNA encoding for rhamnosyl transferase subunits, i.e. RhlA and RhlB, both being key enzymes in the biosynthesis of rhamnolipids, that are bacterial surfactants which modulate *P. aeruginosa* swarming motility and biofilm formation/maintenance (Lin et al., 2018).

By using the rhodamine-labeled Esc(1-21)-1c it was observed that the peptide was mainly accumulated at the membrane level, but that it also penetrated into the bacterial cytosol within the first 5 minutes.

The proposed mechanism of action for these inhibitory effects may involve the interaction of the peptides with the bacterial alarmone guanosine tetraphosphate (ppGpp), which is a nucleotide with a distinctive role in the stress-induced biofilm development and maintenance (Xu et al., 2016).

Based on these findings, it would be interesting to expand our knowledge on the mechanism(s) of interaction of Esc peptides with bacterial membranes.

1.8.2 Synergistic effect between Esc(1-21)-1c and the antibiotic aztreonam against *P. aeruginosa*

Combination of antibiotics and AMPs can be a promising strategy to enhance their antimicrobial spectrum and to improve therapeutic outcomes.

By using a combination of agents with different mechanisms of action, it is possible to target multiple pathways or vulnerabilities in the microorganisms, thereby increasing the chances of successful treatment (Tabbene et al., 2015).

The observation that in contrast to conventional antibiotics (ciprofloxacin, tobramycin, colistin and aztreonam) Esc peptides do not induce resistance in *P. aeruginosa cells,* upon subsequent treatments, highlights their advantage for the development of new anti-infective drugs (Casciaro et al., 2018).

Previous work indicated that Esc(1-21)-1c combined with aztreonam showed a synergistic activity in inhibiting the growth of *P. aeruginosa*.

Synergism occurs when the effect of two combined agents is greater than the sum of their individual effects (Casciaro et al., 2018).

The mechanism of action of Esc peptide in combination with known antibiotics is not yet clear; it is therefore important to conduct further investigations to understand how such combinations work.

1.8.3 Wound healing activity of Esc peptides in bronchial epithelial cells

The airway epithelial surface plays a crucial role in the host defense against microbial pathogens that are inhaled into the respiratory tract.

It serves as the first line of defense and acts as a barrier to prevent the entry of pathogens into the underlying tissues.

In the context of cystic fibrosis, impaired epithelial cell migration and wound healing would contribute to lung damage and susceptibility to infections.

The ability of Esc peptides to stimulate migration of bronchial epithelial cells expressing a functional copy of CFTR (wt-CFBE) or expressing CFTR with F508 mutation (F508del-CFBE cells), at 10 μM for Esc(1-21) and 1 μM for its diastereomer, is a significant finding and suggests their potentiality for the development of new therapeutic agents able not only to eradicate infectious microorganisms but also to accelerate recovery of tissue integrity (Cappiello et al., 2016).

Previous studies indicated that CFBE cells expressing F508del-CFTR exhibit a slower cell migration speed compared to wild-type cells (Trinh et al., 2012). This observation is consistent with the impaired function of CFTR and its impact on processes involved in cell migration, highlighting the importance of CFTR function in the proper healing and repair of damaged airway epithelium.

Considering the role of CFTR in maintaining lung function and wound repair and considering the ability of Esc peptides to promote migration of bronchial epithelial cells expressing CFTR, it would be interesting to explore the effect of Esc peptides on the ions current controlled by CFTR.

2. Aims

The problem statement is the increase in bacterial strains resistant to conventional antibiotics is an alarming problem for human health and could cause future pandemics. Among such bacterial pathogens responsible for a large variety of severe infections there is *P. aeruginosa*. Therefore, there is an extreme need for new molecules with antimicrobial activity or that can act as adjuvants of antibiotics already in use. In this scenario, AMPs hold great promise for the near future. Recently, a derivative of the frog-skin AMP esculentin-1a, namely Esc(1-21), was found to display a fast and potent killing activity against both the planktonic and biofilm forms of *P. aeruginosa* with a membrane perturbing activity as a plausible mode of action. However, no studies have been carried out so far to explore the mechanism employed by this peptide to perturb bacterial membranes, in real time. Furthermore, a diastereomer of Esc(1-21), named Esc(1-21)-1c, containing two d amino acids, i.e. d-Leu14 and d-Ser17, revealed to be more resistant to proteases, less cytotoxic and with a higher antibiofilm efficacy than the all-l parental peptide. Esc(1-21)-1c was also discovered to display a synergistic effect in inhibiting the growth of *P. aeruginosa* when combined with the antibiotic aztreonam. However, studies dealing with the combinatorial effect of this peptide with a panel of antibiotics belonging to different classes, on the growth of *P. aeruginosa* cells, along with the underlying molecular mechanism are still missing. Note that *P. aeruginosa* is the main bacterial pathogen responsible for chronic lung infections leading to mortality in CF patients.

Even in the era of CFTR modulation therapies, management of pulmonary infections in CF remains highly challenging especially for individuals with advanced stages of lung disease.

Considering (i) the ability of Esc peptides to stimulate migration of bronchial epithelial cells, which is expected to restore the integrity of a damaged lung tissue and (ii) the role of CFTR in maintaining lung function and wound repair, it is reasonable to investigate the effect of Esc peptides on the ion currents controlled by this channel. Indeed, in contrast with clinically used CFTR modulators, Esc peptides would give particular benefit to CF patients by combining their capability to eradicate lung infections and to act as promoters of airway wound repair with their ability to ameliorate the activity of the channel with conductance defects.

Based on these premises, the aims of this work thesis were the following:

2.1 To study the interaction of Esc(1-21) on lipid bilayers mimicking bacterial membranes by atomic force microscopy (AFM) and molecular dynamics simulations (MD);

2.2 To investigate the ability of Esc(1-21)-1c to potentiate the effect of antibiotics in inhibiting the growth of *P. aeruginosa* cells and the plausible mode of action, by differential proteomic analysis;

2.3 To study the effect of Esc peptides on the activity of CFTR, by electrophysiology and computational methods.

3. Materials and Methods

3.1 Effect of Esc(1-21) on lipid bilayers mimicking bacterial membranes by atomic force microscopy and molecular dynamic simulation

3.1.1 Peptides synthesis

The synthetic peptides, Esc(1-21) and the diastereomer Esc(1-21)-1c, were purchased from Selleck Chemicals, located in Houston, TX, USA. The peptides were synthesized using a step-wise solid-phase synthesis approach employing the F-moc strategy. Following synthesis, they were purified using reverse-phase high-performance liquid chromatography (RP-HPLC) on a semipreparative C_{18}-bonded silica column (Kromasyl, 5 μm, 100 Å, 25 cm × 4.6 mm). A gradient of acetonitrile in 0.1% aqueous trifluoroacetic acid was utilized at a flow rate of 1.0 ml/min during the purification process (Luca et al., 2013). The molecular mass of the peptides was confirmed using MALDI-TOF Voyager DE (Applied Biosystems) (Islas-Rodriguez et al., 2009).

This technique allows for the accurate determination of the molecular mass of the peptides.

3.2 Atomic force microscopy

The vesicle deposition method was used to form the supported lipid bilayer (SLB) on solid surface (Fig. 16). Net negatively charged SLBs act as a simple mimic of the anionic bacterial membranes, on which the effects of the cationic AMP Esc(1-21) was investigated to form a pore disrupting in the bilayer of the membrane. The vesicle deposition method offers several advantages for creating SLBs.

It allows for the controlled formation of a lipid bilayer on a solid surface, enabling the study of various membrane-related phenomena in a controlled experimental setup. Additionally, the electrostatic interactions between the vesicles and the substrate facilitate the uniform distribution of lipids and the formation of a well-defined lipid bilayer.

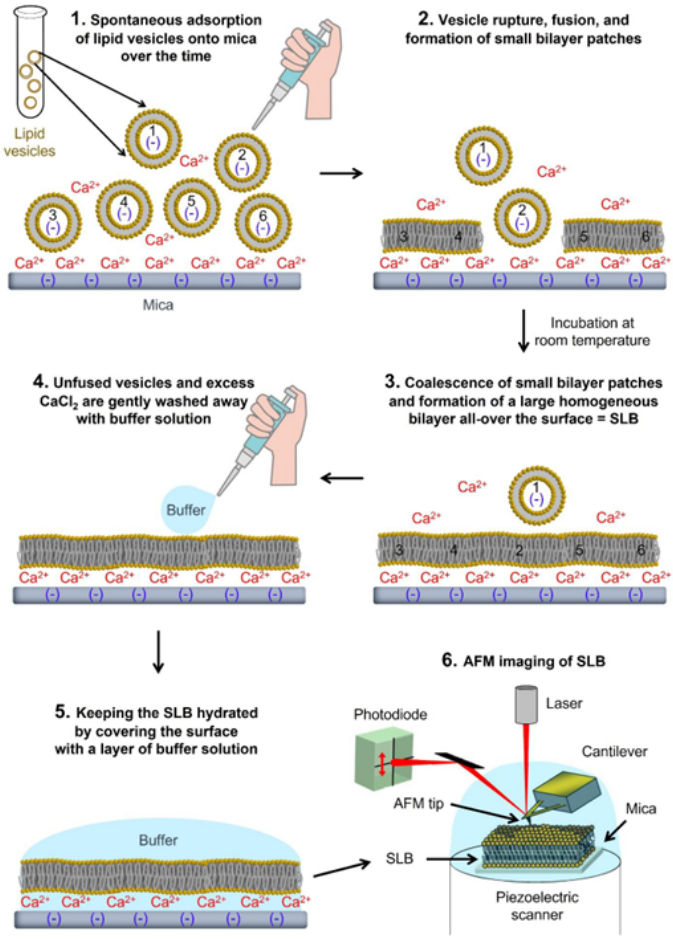

Fig. 16 Schematic flow diagram of vesicle deposition method for SLB formation, Taken from" AFM protocol to investigate the effects of peptides on supported lipid bilayer" (AFM protocol from Robert Vácha research group)

3.2.1 Small unilamellar vesicles (SUVs) preparation for AFM

Preparation of lipid vesicles

The preparation of Small Unilamellar vesicles (SUVs), mimicking the bacterial membrane, consists in two steps: the first one is the lipid film preparation and the second one the SUV preparation of 1-Palmitoyl-2-oleoyl-sn-glycero-3-phosphocholine (POPC) and anionic 1-Palmitoyl-2-oleoyl-sn-glycero-3-phospho-(1'-rac-glycerol) (POPG) lipids in a 1:1 molecular ratio. The lipid film preparation was obtained adding 15.2 μL POPC in $CHCl_3$ [25 mg/ml] and 15.4 μL POPG in $CHCl_3$ [25 mg/ml] and it was transferred into a clean test tube using a gas-tight Hamilton syringe. The chloroform was then evaporated in a gentle stream of air. The lipid film was further dried for 2 hours in the dessicator. The SUV preparation was obtained solubilizing dry lipid film in 0.5 mL of lipid film dissolution (LFD) buffer on vortex and the lipid solution concentration was 2mM. Every lipid sample underwent ten freeze-thaw cycles: the first step was to put ethanol in a polystyrene bowl and to add dry ice into the bath. The sample was frozen freeze by submerging the test tube to the ethanol bath for 1.5min; after the sample was thawed in 50°C water for 0.5 minutes and the last two steps were repeated to repeat 10 times. After this, the sample was sonicated (bath) for 30 minutes. The lipid suspension was extruded trough a polycarbonate membrane filter with 50 nm pore size for formation Small Unilamellar vesicles (SUV).

3.2.2 Preparation of buffer solutions for AFM experiment

The buffers (or solutions) for AFM experiment were prepared using LFD buffer (50 mM Tris-HCl and 50 mM KCl in Milli-Q water), SLB buffer (50 mM Tris-HCl and 300 mM KCl in Milli-Q water .with a pH 7.4) and $CaCl_2$ solution (100 mM $CaCl_2$ in 100 mL of Milli-Q water)

The preparation of supported lipid bilayers (SLBs) was obtained using 0.5 mM of lipids concentration in 200 μL SLB buffer. The volume of 10 μL of 100 mM $CaCl_2$ solution was added to reach a final concentration of 5 mM Ca^{2+}. Adhesive tapes were used to peel off the outer layers of mica for at least 5 times. After this 150 μL of the SUV-SLB-$CaCl_2$ suspension onto the mica were gently added to have a homogeneous solution on the entire surface.

The mica was covered with a lid and incubated at room temperature for one hour. During this incubation the SLB was formed by vesicle deposition method. After taking images of a good supported lipid bilayers (SLB), 20 μL of Esc(1-21) was added over the SLB to reach the final concentrations 10 and 50 μM.

3.2.3 AFM measurements

For the AFM measurements the following parameters were used:

AFM Instrument (Bruker Dimension Icon AFM- Santa Barbara, CA, USA) operated in Peak Force Quantitative Nanomechanical (QNM) Property Mapping hybrid mod; probe and parameters for initial confirmation and

characterization of SLB properties (Bruker ScanAsyst-Fluid+ silicon nitride probe).

This probe had a sharp tip with a 2 nm nominal end radius and a 0.7 N/m spring constant to purpose high-resolution imaging and force measurements; for an increased resolution of bilayer images and for capturing the biomolecular interactions, Bruker PeakForce-HIRS-F-B probe was used.

This probe had an ultrasharp tip with 1 nm nominal end radius and 0.12 N/m spring constant, ideal for high resolution imaging, but not good for force measurements because of the sharpness of the tip. The following parameters were used for AFM measurements of SLBs and the biomolecular interactions with peptide: scan rate (0.8 - 1 Hz); sample/line (256 or 512); feedback gain (9); peak force setpoint (100 - 200 pN); peak force amplitude (25 - 30 nm); peak force frequency (2 - 4 kHz9). The force measurements were performed using Bruker Nano Scope Analysis software. The captured images were processed using Gwyddion software (http://gwyddion.net/) for line-by-line background subtraction (i.e., flattening), plane fitting with polynomial functions, and cross-sectional measurements.

3.3 Computer simulation: MD study

Coarse-grained simulations were performed using Martini 2 forcefield. The membrane system comprising POPC: POPG in the ratio 1:1 were prepared using the CHARMM-GUI web server.

Peptides were prepared using MODELER version 9.11 (24) and then coarse-grained using the martinize.py script version 2.6 (https://github.com/cgmartini/martinize.py).

All the molecular dynamics simulations were performed with Gromacs package version 2021.4. The peptides were placed on the membrane and then solvated with 14189 MARTINI Water beads.

To mimic the physiological conditions, randomly selected water beads were replaced with ions to obtain 0.15 M NaCl concentration. The system was then energy minimized using the steepest descent algorithm with a maximal force tolerance of 100 kJ mol^{-1} nm^{-1}. A flat-bottom potential was employed using the pull code to avoid the peptides to diffuse from the membrane. The system was equilibrated for 100 ns with the v-rescale thermostat to maintain a temperature of 310 K.

Pressure was kept at 1 bar using Parinello-Rahman barostat with a coupling constant of 12 ps. Semi-isotropic pressure coupling was employed to independently scale the simulation box in the *xy* plane and on the *z-axis* with a compressibility of 3×10^{-4} bar^{-1}. The production dynamics were run for 24 microseconds with similar settings as equilibration. The trajectories were visualized using the visualization software VMD.

3.4 Effect of Esc(1-21)-1c on the susceptibility of *P. aeruginosa* cells to conventional antibiotics

3.4.1 Microorganisms

The bacterial strain used was the reference *P. aeruginosa* PAO1 (ATCC 15692) and a tetracycline-resistant clinical isolate named 24717(1), kindly provided by Prof. Giammarco Raponi from the strain collection of Policlinico Umberto I. The antibiotics were purchased from Sigma-Aldrich (Milan, Italy).

3.4.2 Checkerboard assay

To determine the combinatorial effect of Esc(1-21)-1c and antibiotics, the checkerboard titration method was employed. The procedure involved adding combinations of the two compounds in a serial two-fold dilution to the wells of a 96-well plate containing 1x 10^6 CFU/mL of *P. aeruginosa* PAO1 in a final volume of 100 µL of MH. The plates were incubated for 24 h at 37 °C at 125 rpm and the Fractional Inhibitory Concentration (FIC) index for combination of two compounds was calculated according to the formula:

$$\text{FIC index} = FIC_A + FIC_B = A / MIC_A + B / MIC_B$$

where A and B are the MICs of drug A and drug B in the combination, while MIC_A and MIC_B represent the MIC values of the compounds alone. The FIC indices were interpreted as follows:

- FIC ≤0.5, synergy;
- 0.5<FIC ≤ 1, additivity,
- 1 < FIC ≤ 2, no interaction,
- FIC >2, antagonism.

3.4.3 Differential proteomic analysis

P. aeruginosa PAO1 cells were grown in 3 mL of LB medium until an optical density (OD, λ= 590 nm) of 0.5 was reached and treated with 25 µM of Esc (1-21)-1c at 37 °C for 3 h under stirring. Untreated cells were used as control and the experiment was performed in duplicate. The pellets were recovered by centrifugation at 4°C for 10 min at 4,700 x g (5,000 rpm), resuspended in PBS 1X, 5% SDS and 1 mg/mL lysozyme, and subjected to mechanical lysis by sonication.

The samples were centrifuged at 4°C for 30 min at 21380 x g (15,000 rpm) to collect non lysed cells and cellular debris and the recovered supernatant was quantified by bicinchoninic acid (BCA) protein assay kit assay purchased from Thermo Scientific (Rockford,USA) 50 µg of each sample was digested by trypsin onto Solid phase protein extraction and digestion (S-trap) TM micro spin columns, following the standard protein digestion protocol of the manufacturer (Protifi, Huntington, NY) (Fig. 17)

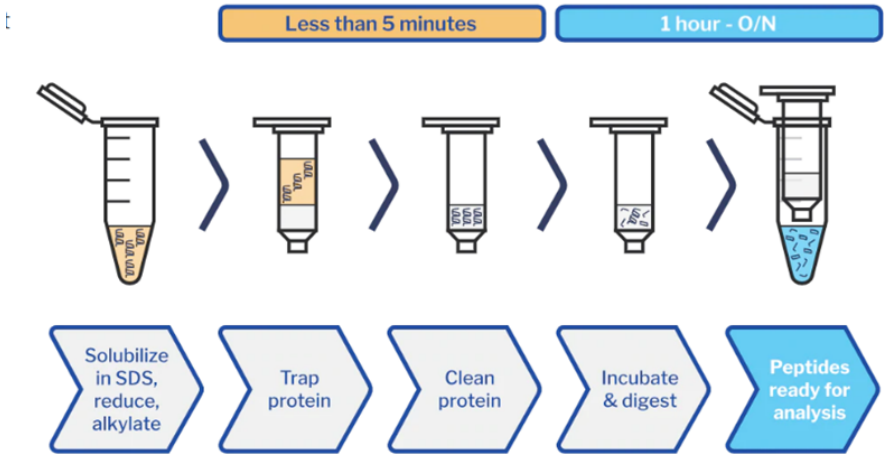

Fig. 17 S-Trap: steps of the standard protein digestion protocol

The resulting peptide mixtures were analyzed by liquid chromatography/tandem mass spectrometry (LC-MS/MS) using a LTQ Orbitrap XL coupled to a nanoLC system (ThermoFisher Scientific, Waltham, MA). All peptide mixtures were fractionated onto a C_{18} capillary reverse-phase column (200 mm lenght, 75 μm ID, 5 μm diameter of biosphere), using a non-linear 5% to 50% gradient for eluent B (0.2% formic acid in 95% acetonitrile) in A (0.2% formic acid and 2% acetonitrile in MilliQ water) over 260 minutes MS/MS analyses were performed using data-dependent acquisition (DDA) mode by fragmenting the 10 most intense ions in Collision induced dissociation (CID) modality All samples were run in duplicates.

Raw data obtained from nano LC-MS/MS were analyzed with MaxQuant (v.1.5.2.8) using UniProt P. aeruginosa as database for Andromeda search.

The selected parameters for protein identification were the following: minimum 2 peptides, at least 1 unique; variable modifications allowed were methionine oxidation and pyroglutamate formation on N-terminal glutamine; accuracy for the first search was set to 10 ppm, then lowered to 5 ppm in the main search; 0.01 FDR was used, with a reverse database for decoy; retention time alignment and second peptides search functions were allowed. The fold changes (FCs) were calculated according to LFQ values.

3.4.4 Gene Expression Analysis

RNA extraction has been performed as previously described (Letizia et. al.,2022) on *P. aeruginosa* strains treated or not with compound Esc(1-21)1c.

For each condition, three different pools of RNA were extracted in independent experiments (biological triplicates).

Strains were grown in 50 mL LB at 37°C with shaking (200 rpm) until reaching an optical density (OD 600) of 0.5. Subsequently, strains were incubated at 37°C with 25 µM Esc(1-21)1c dissolved in distilled sterile H_2O or with an equal amount of distilled sterile H_2O.

RNA was extracted from bacterial cultures after 3 h of treatment. For each sample, 1 mL of culture were collected and incubated for 5 min at room temperature (RT) after the addition of 2 mL RNA Protect Bacteria Reagent (Qiagen).

Bacterial suspensions were then centrifuged for 20 min at 4000 rpm, 20°C. The resulting pellets were suspended in 570 µL of TE buffer (10 mM Tris-HCl, 1 mM ethylenediaminetetraacetic acid; pH 8.0) and lysed by the addition of 1 mg/mL lysozyme and by sonication (2 cycles of 10 sec pulsed sonication for each sample).

RNA was extracted from lysed bacterial samples by using the RNeasy Minikit (Qiagen), including the on-column DNase I digestion step.

To ensure optimal DNA removal, eluted RNA was treated for 1 h at 37°C with TURBO DNase (0.2 U per mg of RNA; Ambion) and with SUPERase-In (0.4 U per mg of RNA; Ambion).

DNase I was removed with the RNeasy Column Purification kit (Qiagen).

The absence of contaminating DNA in the samples was verified via PCR analysis by using the oligonucleotides FWPpqsB and RVPpqsB. Purified RNA samples were quantified using the NanoDrop 2000 spectrophotometer (Thermo Fisher Scientific).

DNA synthesis was performed from 1 µg of purified RNA using the iScript Reverse Transcription Supermix for RT-qPCR kit (Bio-Rad Laboratories).

The resulting cDNA samples were quantified by using the NanoDrop 2000 spectrophotometer (Thermo-Fisher Scientific).

qRT-PCR analysis was performed on cDNA samples by using the iTaq Universal SYBR Green Supermix kit (Bio-Rad Laboratories), and the AriaMX thermocycler (Agilent).

The design of the gene-specific oligonucleotides employed in this analysis (**Table 3**), was performed using the Primer-BLAST software (www.ncbi.nlm.nih.gov/tools/primer-blast) to avoid nonspecific amplification of P. aeruginosa PAO1 DNA.

The 16S rRNA was used as the internal control to normalize the qRT-PCR data in every single run (Letizia et. al.; 2022) and to calculate the relative fold change (FC) in gene expression using the $2^{-\Delta\Delta Ct}$ method.

Means and standard deviation were obtained from three biological replicates.

Table 3. Oligonucleotides used in this study**.**

Name	Sequence (5'-3')
FW16S	GAGAGTTTGATCCTGGCTCAG
RV16S	CTACGGCTACCTTGTTACGA
FW*oprM*	TCAACCTGCCGATCTTCACC
RV*oprM*	GAGCTGGTAGTACTCGTCGC
FW*oprD*	AAGACCATGCTGAAGTGGGG
RV*oprD*	CCTGCGTAGGTGGCATAGAG
FW*oprI*	GCAGCCACTCCAAAGAAACC
RV*oprI*	TACTTGCGGCTGGCTTTTTC
FW*mexA*	CGAAGGTCTCCCTGAAGCTG
RV*mexA*	AGGATGGCCTTCTGCTTGAC
FW*mexB*	ACCTGAGCAAGTGGTACGTG
RV*mexB*	CTTGACGATCTCCTCGACCG
FW*secA*	TCAGCCTGGACGACAAGTTC
RV*secA*	TTGCCCTCGACCTCTTCAAC
FW*pilQ*	AGCATCATCGCCTATCAGCC
RV*pilQ*	TCCCGATATTGCCGTCCTTG
FW*PpqsB*	CCGCTCGAGCGACCAGGGCTATCGCA
RV*PpqsB*	CCGGAATTCCTTATGCATGAGCTTCTCC

3.4.5 Quantitative analysis by LC-MS/MS in MRM scan mode

Cell culture pellets, treated for 3 h in the presence of Esc(1-21)-1c, were resuspended in water and subjected to three cycles of freezing and sonication. Protein precipitation occurred in cold methanol (MeOH) for 30 minutes at -20°C.

Untreated cells were used as control. Following centrifugation, the supernatants were recovered, dried in SpeedVac and used for the metabolomic study, while the pellets were used for the proteomic analysis.

The metabolomic samples were resuspended in acidified H2O and desalted using Oasis HLB cartridges.

Metabolomic analyses were analysed by liquid chromatograph-mass spectrometry (LC-MS/MS) by injecting 1 µL of supernatant and using the AB-sciex 5500 QTRAP® system with a high-performance liquid chromatography (HPLC) system Exion LC™. The mobile phase was generated by mixing eluent A (0.1 % Formic Acid in water) and eluent B (0.1 % Formic Acid in acetonitrile) and the flow rate was 0.200 mL/minute. Chromatographic gradient was 5% B for 1 min, then from 5% to 90% B in 4 min, hold for 1 min, return to 5 % B in 2 min and hold for 2 minutes. Tandem mass spectrometry was performed using Turbo VTM ion source in positive ion mode, and the multiple reaction monitoring (MRM) mode was used for the selected analytes. The extracted mass chromatographic peaks of metabolite was integrated using Skyline software for data processing.

The in silico analysis carried out by means of this software, allowed to identify specific precursor ion-product ion transitions to select a unique peptide for each target protein.

The specific peptides used to monitor the three target proteins were the following:

MexB: FLMLAAQNPALQR;

MexA: IITEGLQFVQPGVEVK

OprM: ADQAQLQLTK

Protein extracts from bacterial cells treated with tetracycline alone or in combination with Esc(1-21)-1c, and proteins extracted from untreated cultures, as control, were digested with trypsin and analysed by LC-MS/MS in MRM scan mode monitoring the ion current associated to the mass transitions for the 3 selected peptides. The average peak areas were recorded for each peptide from MexA, MexB and OprM.

The content of tetracycline in bacterial cells was quantified using the following calibration curve (Fig. 18) where the calibrator was the tetracycline and calibration line was constructed with three technical replicates.

In this graph an error of 5% was set because, for each concentration point taken into consideration, the error did not exceed 5%.

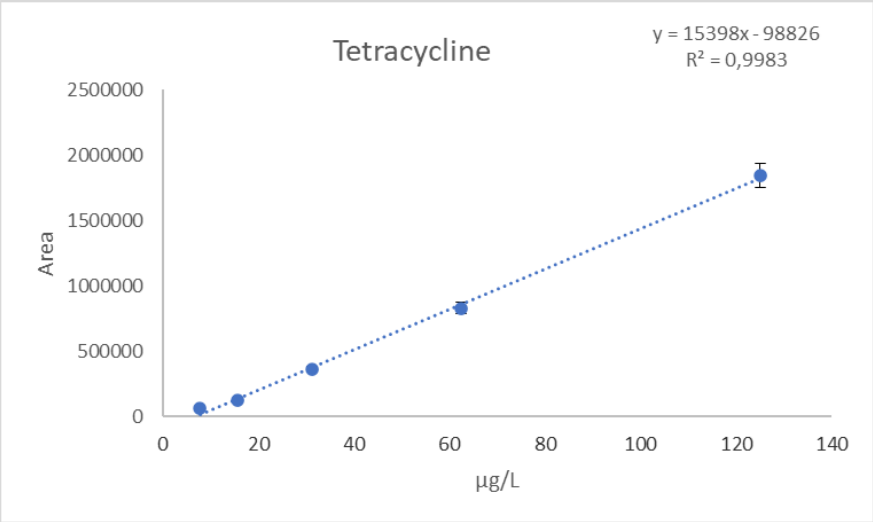

Fig. 18 The average of the calibration curves.

The protein pellets were solubilized in 6 M urea and 50 mM ammonium bicarbonate and subjected to protein hydrolysis by using an in-solution digestion protocol (Illiano et. al., 2021) followed by desalting step performed on custom-made chromatographic microcolumns.

Skyline software (3.7, 64-bit version MAcCoss Lab Software, University of Washington, United States) was used to select the best precursor ion –product ion transitions and instrumental parameters like collision energy (CE), dwell time and cone voltage (Di Somma et. al., 2022) selection of proteotypic peptides for each protein target was calculated by matching data from the Skyline software and those collected in online repositories, e.g. SRM Atlas.

Peptide mixtures were analysed by LC-MS/MS in MRM ion mode using a Xevo TQ-S (Waters, Milfors, MA, United States) equipped with an IonKey UPLC Microflow Source coupled to an UPLC Acquity System (Waters, Milfors, MA, United States).

The volume of 1 µL of peptide mixtures was injected and separated on a TS3 1.0 mm× 150 mm analytical RP column (Waters, Milford, MA, USA) at 45 °C with a flow rate of 3 µL/min using 0.1% HCOOH in water (LC-MS grade) as eluent A and 0.1% HCOOH in ACN as eluent B. Peptides were eluted (starting from 1 min after injection) with a linear gradient of eluent B in A from 7% to 95% in 55 minutes.

The column was re-equilibrated at initial conditions for 4 minutes. The MRM mass spectrometric analyses were performed in positive ion mode using an MRM detection window of 0.5-1.6 min per peptide.

The duty cycle was set to automatic and dwell times were minimal 5 ms. Cone voltage was set to 35V.

Last version of skyline software (20.2 - 64 bit version MacCossLab Software, University of Washington, USA) (Abbatiello et al., 2013) was used for the in silico selection of peptides with unique sequence for each selected protein. Peptides with zero missed cleavages were considered and the best two to five transitions per peptide were selected from the top ranked y-fragments.

3.5 Effect of Esc peptides on cells lines (FRT and CFBE) expressing F508del-CFTR by electrophysiology and computational studies

3.5.1 Cells

Two types of cell lines were used: Fischer rat thyroid (FRT) cells and bronchial epithelial (CFBE41o-) cells.

The specific cell lines used were F508del-FRT (expressing mutated CFTR), wt-FRT (expressing wild- type CFTR), F508del-CFBE41o- (expressing mutated CFTR), and wt-CFBE41o- (expressing wild-type CFTR) (Sondo et al., 2011). The FRT cells were cultured in Coon's modified Ham's F-12 medium (provided by Sigma-Aldrich, St. Louis, MO). On the other hand, CFBE41o- cells were cultured in minimal essential medium (MEM). Both culture media were supplemented with 10% fetal calf serum, 2 mM L-glutamine, 100 U/ml penicillin, and 100 µg/ml streptomycin.

Additionally, primary human bronchial epithelial cells derived from individuals with cystic fibrosis (CF) and non-CF individuals were obtained from the Italian Cystic Fibrosis Foundation (FFC) Cell Culture Service. These cells were cultured in proliferative serum-free medium, which consisted of a 1:1 mixture of RPMI 1640 and LHC basal medium (provided by Life Technologies, Monza, Italy). The culture medium for the primary human bronchial epithelial cells was supplemented with various hormones and supplements, 100 U/ml penicillin, and 100 µg/ml streptomycin.

3.5.2 Method for cell counting

After reaching 90-95% confluence in the flask, the cells needed to be detached and transferred to a new flask.

The first step was to discard the culture medium from the flask containing the confluent cells.

After this, it was performed two quick washes were performed and one 20-minute wash with a phosphate-buffered solution (CMF) that was free of magnesium and calcium. These cations were essential for intercellular adhesion junctions, and by removing them, the cells' connections with the support were compromised, facilitating detachment.

Trypsin-EDTA 1x solution was added to the flask. Trypsin is a proteolytic enzyme that degrades proteins present in the extracellular matrix, aiding in cell detachment.

The presence of EDTA in the solution chelated magnesium and calcium, further assisting in the detachment process.

The flask was incubated at 37°C and 5% CO2 for approximately 10 minutes. During this time, the cells became rounded and detached, as observed under a microscope.

To inactivate trypsin, the Coon's modified Ham's F-12 medium (for FRT cells) or MEM (for CFBE41o- cells) supplemented with 2mM L-Glutamine, 10% fetal bovine serum (FBS), and 1x penicillin-streptomycin (P/S) were added into flask. The cell suspension was transfered from the flask into a 50 mL Falcon tube: this tube was centrifuged at 1000 rpm for 5 minutes.

This step helped to pellet the cells, separating them from the supernatant. Carefully the supernatant was discard, ensuring not to disrupt the cell pellet which was resuspend in their respective growth medium, in a volume appropriate for the size of the new flask where the cells were transferred into at the end of the process.

The volume 10 µL of aliquot of cell resuspension was taken and placed it on a cell counting chamber (Fig. 19), such as a hemocytometer or a specialized counting slide.

This allowed for the determination of the cell density and helped in calculating the number of cells to be transferred to the new flask.

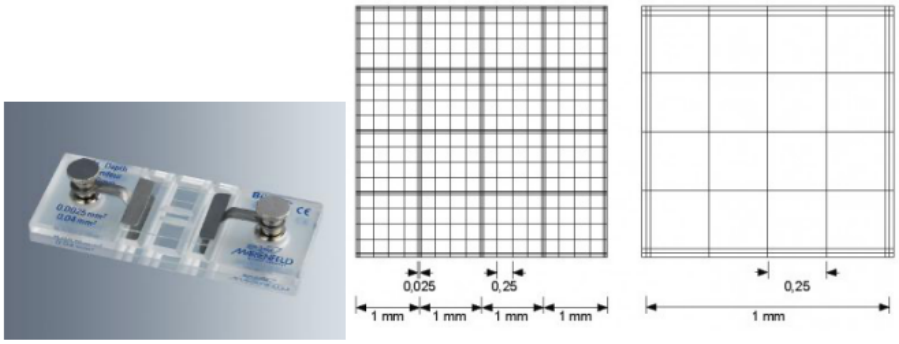

Fig. 19 Representation of a Bürker chamber and its reticular structure on the specimen slide.

3.5.3 Cytotoxicity assay: wt-CFBE, ΔF508 cells

The effect of Esc(1-21) and its diastereomer, Esc(1-21)-1c, on the viability of wt-CFBE and ΔF508 cells was assessed using the colorimetric MTT assay.

The MTT assay is based on the intracellular reduction of the yellow tetrazolium salt (MTT) to a purple formazan compound by mitochondrial dehydrogenases (Fig. 20A) (Grieco et al., 2013b).

The intensity of the purple color formed is directly proportional to the number of metabolically active cells (Fig. 20B).

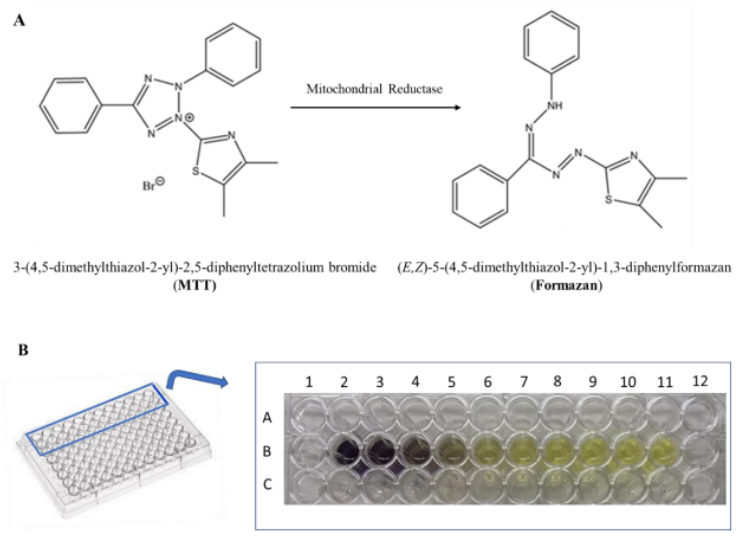

Fig. 20 Reduction of the yellow tetrazolium salt (MTT) to purple insoluble formaz, by metabolically-active cells (A). The intensity of the purple dye is proportional to the number of viable cells. The transparent yellow color in the B11 well corresponds to MTT solution without cells (B).

Approximately 4×10^4 cells were suspended in the corresponding culture medium. The culture medium was supplemented with glutamine and contained 2% fetal bovine serum (FBS), but no antibiotics were added. The cells were then plated in each well of a 96-well microtiter plate.

After plating, the cells were allowed to incubate overnight at 37 °C in a 5% CO2 atmosphere to promote cell attachment and growth.

Following the overnight incubation, the medium was removed from each well with 100 µl of fresh serum-free MEMg, DMEMg or Hank's buffer (136 mM NaCl; 4.2 mM Na_2HPO_4; 4.4 mM KH_2PO_4; 5.4 mM KCl; 4.1 mM $NaHCO_3$, pH 7.2, supplemented with 20 mM d-glucose) with or without the peptide at different concentrations.

After incubation for 2 hours or 24 hours at 37 °C in a 5% CO2 atmosphere, the medium in each well was removed and replaced with 100 µl of Hank's buffer containing 0.5 mg/ml of MTT (tetrazolium salt). The plate was then incubated at 37 °C and 5% CO2 for an additional 4 hours. During this time, viable cells metabolically reduced the MTT to formazan crystals. Absorption of each well was measured using a microplate reader (Infinite M200; Tecan, Salzburg, Austria) at 570 nm. The percentage of metabolically active cells compared to control samples (cells not treated with peptide) was calculated according to the formula:

(*absorbance sample – absorbance blank) / (absorbance control – absorbance blank) × 100*

where the blank is given by samples without cells and not treated with the peptide.

3.5.4 The transepithelial electrical resistance (TEER) to evaluate lung epithelial integrity and CFTR activation

To evaluate the lung epithelia integrity, lung epithelial cells (FRT and CFBE41o cells) were seeded onto permeable supports in 24-well Millicell plates with a pore size of 24 (PSHT01QR1). These permeable supports allow for the formation of a polarized monolayer of cells, simulating the epithelial barrier found in the lung. They were incubated for 24 h in their standard culture medium in the presence of peptides, at different concentration.

DMSO (0.1% v/v final concentration), that was used to solubilize each compound, was included as control (Srinivasan et al., 2015).

After the 24-hour incubation period, the medium in each well was replaced with a saline solution. The composition of the saline solution was made of the following compounds: 130 mM NaCl, 2.7 mM KCl, 1.5 mM KH_2PO_4, 1 mM $CaCl_2$, 0.5 mM $MgCl_2$, 10 mM glucose, 10 mM Na- Hepes with a value of pH 7.4. Samples were incubated for 10 min at 37 °C and TEER was measured in basal conditions without CFTR activation, with the epithelial voltmeter (MILLICELL ERS-2, Millipore Burlington, MA) (Fig. 21). To evaluate CFTR activation, the same saline solution described previously was used. For cells expressing the F508del mutation, they were incubated with 1 μM VX-809 to promote the rescue of the mutant CFTR protein.

After measurement of basal TEER, 20 µM FSK+10 µM GEN as positive control, or FSK+peptides at the desired concentration were added on the epithelium apical side.

Finally, 30 µM PPQ102 was added on the epithelium apical side to block CFTR, so to measure the own activity of CFTR. TEER measurement was performed at 37 °C after 10 min from the addition of each compound.

From the values of TEER measured before and after CFTR inhibition, we calculated the CFTR-dependent TEER for each condition. All values of TEER were converted to transepithelial conductance (TEEC) using the formula TEEC=1/TEER (Sondo et al., 2018).

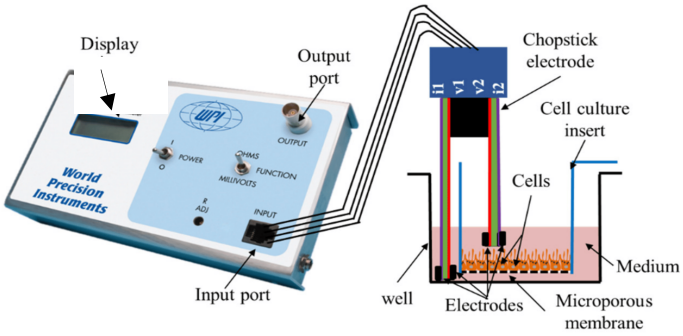

Fig. 21 The modified representation of the measurement of TEER using epithelial voltmeter. (Raut et al. 2021)

3.5.5 Patch-clamp experiments (Inside-out configuration)

Patch clamp ("area blocking") is an electrophysiological technique (inside-out configuration) used to measure the currents passing through ion channels in a small piece of the cell membrane excised from the cell (Fig. 22).

It works by attaching a piece of cell membrane to the glass tube, exposing its cytosolic surface.

This gives access to the surface through the electrolyte solution bath.

This method is used when changes are being made at the intracellular surface of the ion channels.

Inside-out membrane currents were recorded in FRT cells stably expressing F508del CFTR after incubation with 1 μM of the corrector VX-809 for 24 h to increase mutated CFTR membrane expression.

For inside-out patch-clamp experiments, the pipette solution contained (in mM): 150 N-methyl-D-glucamine chloride (NMDG-Cl), 3 $CaCl_2$, 2 $MgCl_2$, 10 Na-Hepes (pH 7.3). The bath solution for these experiments contained (in mM): 150 NMDG-Cl, 2 $MgCl_2$, 10 EGTA, 10 Na-Hepes, 1 ATP, which was supplemented with 125 nM catalytic subunit of PKA (Promega, Sunnyvale, CA) and peptides at 10 μM. Pipette electrical resistance for inside-out experiments was 3–5 MΩ.

The protocol to correlate current intensity and voltage for stimulation consisted of 500-ms voltage steps from -100 to+100 mV or from -80 to+120 mV in 20 mV increments, starting from a holding potential of -60 mV.

The time-dependence of CFTR activation and inactivation was monitored by application of steps of 50 ms pulses to−100,−50, 0, 50 and 100 mV every 5 s from a holding potential of−60 mV. The interval between steps was 4 s.

Membrane currents were filtered at 1 kHz and digitized at 5 kHz by a low–pass 4–pole Bessel filter.

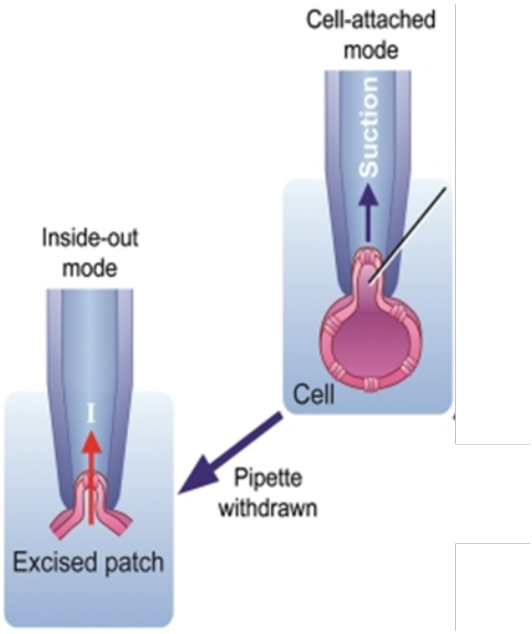

Fig. 22 Image modified of inside-out mode of the patch-clamp technique (Kirichok et al., 2011)

3.5.6 Computational studies

The initial rough structure of the F508del form of NBDs was generated by homology modelling with Prime (Schrodinger, LLC, New York) (Jacobson et al., 2004).

The resulting F508del NBDs structure was included in a rectangular box of explicit TIP3P type water molecules buffering 10 Å from the protein surface.

The system was then relaxed through energy minimization and MD simulations with Amber18 (Salomon-Ferrer et al., 2013; Case et al., 2018).

The representative structure of the F508del NBDs was extrapolated from MD trajectories by cluster analysis with the CPPTRAJ software (Roe et al., 2013). A Nuclear Magnetic Resonance (NMR) reference structure of Esc peptides was retrieved from the Protein Databank (www.rcsb.org/pdb) under the PDB-ID 5XDJ (Loffredo et al., 2017).

The recognition and binding of peptides was simulated using the MD procedure described above, by placing each peptide and the F508del NBDs in the simulation box at a distance higher than 40 Å and in a random reciprocal orientation.

Three independent MD replicas of 500 ns were run for each system. The electrostatic surface potential was calculated by the Adaptive Poisson-Boltzmann Solver (APBS) (Baker et al., 2001).

4. Results

4.1 Effect of Esc(1-21) on lipid bilayers mimicking bacterial membranes

Previous studies highlighted the ability of Esc(1-21) to perturb the membrane of *P. aeruginosa* cells by causing the leakage of large cytosolic components, i.e. the β-galactosidase (Luca et al., 2013) within 15 min, in a dose-dependent manner. To get insight into the type of membrane damage and to explore the ability of Esc (1-21) to form pores and/or membrane defects, AFM and MD simulations represent ideal tools to investigate these aspects in real time.

4.1.1 Formation of transient membrane e defects/pores highlighted by AFM

SLB composed of a mixture of zwitterionic POPC and anionic POP lipids in a 1:1 molecular ratio was selected as simple model membrane of the net negatively charged bacterial lipid POPG (Zasloff et al., 2002). A well-organized and stable SLB has a flat, smooth, and homogeneous surface without or with some intact vesicles appearing like white spots in AFM measurements (Fig. 23 A- 24 A- 25 A- 26 A). To ensure that there is a lipid bilayer and not a lipid free surface of mica, the force-distance curve needs to be measured. This curve captures a force profile of the probe being pushed towards the surface. If there is a peak/spike in the monotonously increasing curve, this peak indicates a bilayer rupture event and the force required to pierce the bilayer, a so called “breakthrough force”.

The aim of this study was to evaluate the induced effects by Esc(1-21) on the SLB. The effects were evaluated by capturing the SLB surface images before and after the peptide treatment. After adding Esc(1-21) peptide to the SLB no pores formation was observed at the final peptide concentrations of 1μM corresponding to peptide to lipid ratios (P:L) of 1:500, (mol/mol).

The intactness of the bilayer indicated that the peptide did not induce significant structural changes or membrane perturbations (Fig. 23).

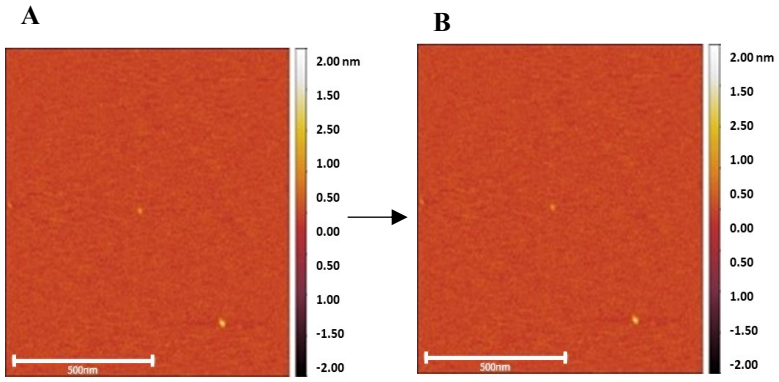

Position 1: same area of image A

Fig. 23 AFM topographic images of: A) supported lipid bilayers composed of POPC:POPG (1:1 mol/mol) lipids. B) membrane after 10-15 minutes incubation with 1μM concentration of Esc(1-21) peptide, showing the intactness of the bilayer; position 1 represents the same area of image A taken after peptide addition.

However, at the high peptide concentration of 10 μM, the images revealed dark spots of different sizes ranging from 20 nm to 50 nm in diameter after 10-15 min from peptide addition (P:L ratio 1:50) (Fig. 24).

Observing the Fig. 24 C one of these dark spots was closed within few minutes because of the presence of white spot at the position of previous defect. The obtained dark spots had depth around 2 nm, which is roughly half of the bilayer thickness (4 nm). These results indicated the peptide's ability to induce membrane defects in the lipid membrane.

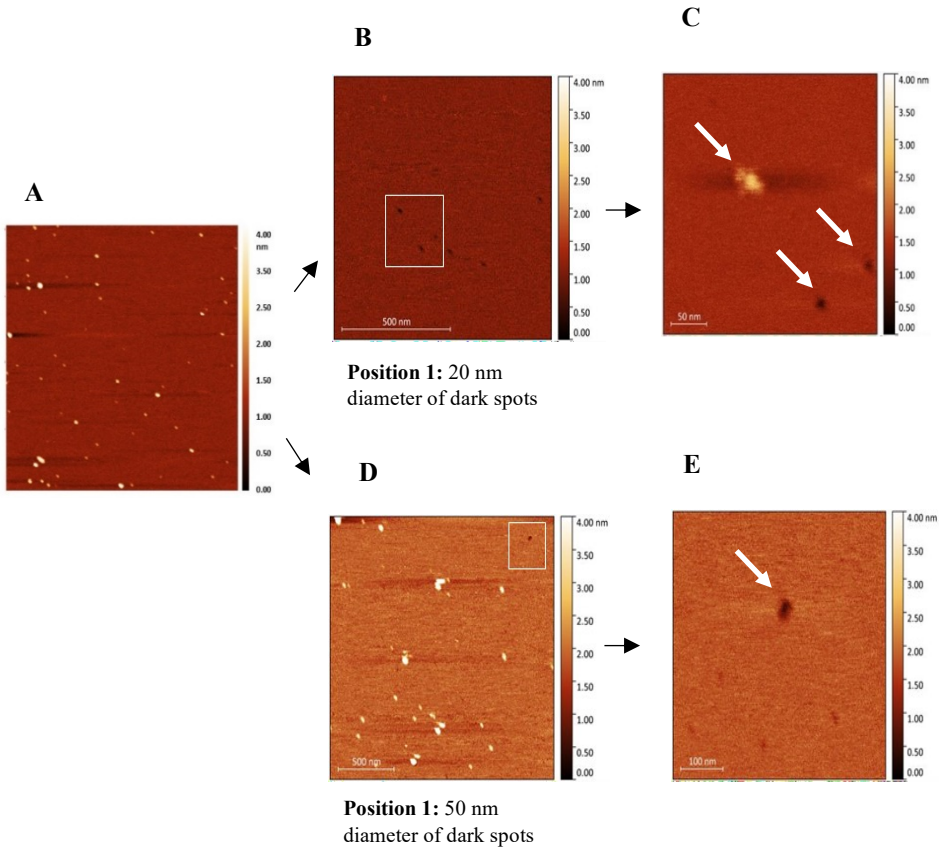

Fig 24 AFM topographic images of: A) supported lipid bilayer composed of POPC:POPG (1:1 mol/mol) lipids. B-D) membrane after 10-15 minutes incubation with 10 μM concentration of Esc (1-21) peptide, showing dark spots, as highlighted by the white square. C-E) the zoom of white rectangles of image B-D: dark spots with a diameter of 20-50 nm and 2 nm depth; one white spot that protruding structure formed over the SLB (white arrows). Position 1 represents the same area of the image A taken after peptide addition.

Moreover, when using again 10μM of peptide, another time the closure of the dark spots was observed within few minutes (Fig. 25).

This time dependent change suggested temporary lifetime of defects and resulted in the presence of white spots at the position of previous defects. These white spots suggest a protruding structure out of SLB.

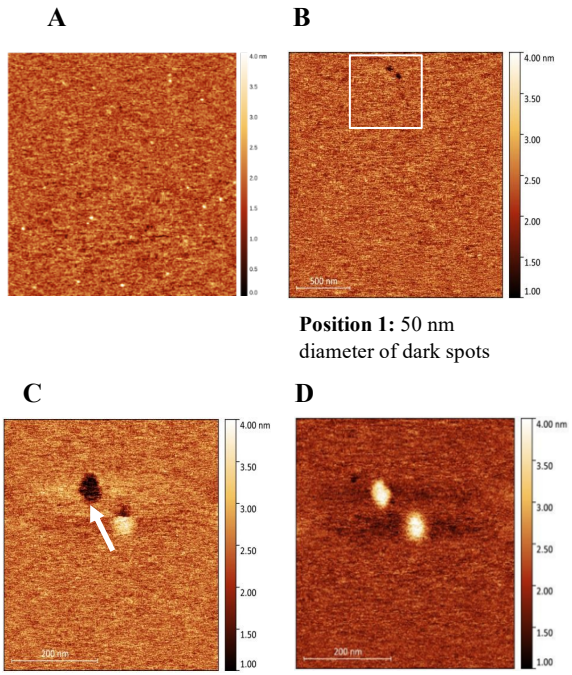

Fig. 25 AFM topographic images of: A) the supported lipid bilayer composed of POPC:POPG (1:1 mol/mol) lipids (the length of image is 50 nm). B) membrane after 10-15 minutes. incubation with 10 μM of Esc (1-21) peptide showing membrane dark spots highlighted white square. The dark spots diameter was approximately 50 nm and 2 nm depth. C)the zoom of white rectangle of the image B: where darks are disappearing in 5 minutes. It is evident from a white spot (highlighted with white arrow) that protruding structure formed over the SLB. D) the closure of dark spots covered by white spots. Position 1 represents the same area of image A taken after peptide addition.

When we used the higher peptide concentration of 50 µM (P:L ratio is 1:10 (mol/mol), membrane pores with different size (30-40 nm of diameter) and depth around 3-4 nm were observed (Fig. 26).

The formation of membrane pores demonstrated a concentration-dependent peptide effects on the lipid bilayer including full local disruption.

The variability in pore size and depth may be attributed to factors including differences in local peptide concentration and the inherent heterogeneity of the lipid bilayer itself.

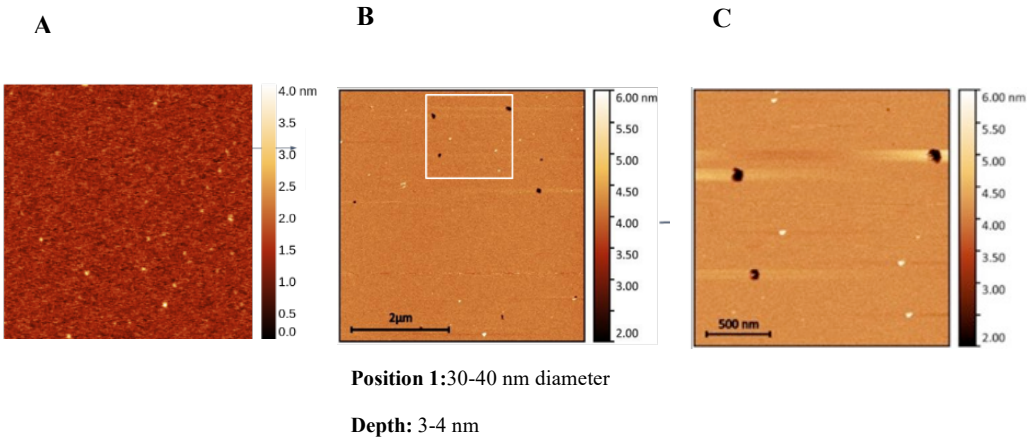

Fig. 26 AFM topographic images of A) the supported lipid bilayer composed of POPC:POPG (1:1 mol/mol) lipids (scale bar is indicated), B) membrane after 10-15 minutes incubation with 50 µM concentration of Esc(1-21) peptide, showing membrane pore formation (white square), and C) the zoom of the white rectangle of the image B: pores with a diameter of 30-40 nm and depth 3-4 nm. Position 1represents the same area of image A taken after peptide addition.

It is interesting to note that the observed pores in this study do not resemble the classic barrel-stave pore described in the literature, (Deb et al. 2022) due to differences in shape, size, and depth.

This latter phenomenon indicates the formation “transient pores” suggesting a toroidal pore or a different mechanism of action. These experimental observations were complemented with molecular dynamics (MD) simulations.

4.1.2 Dynamics of membrane pores, highlighted by Molecular Dynamic (MD) simulation

With the aim to model the conditions of AFM experiments, we setup the simulation using an asymmetric system made of POPC: POPG 1:1, with peptides adsorbed on only one leaflet at high concentration.

Using an asymmetric system with Esc(1-21) (P:L ratio ranging from 1:50 and 1:10 mol/mol) and a running of simulation of 20 μs , the formation of small pores that slowly close, was observed (Fig. 27).

These pores appeared after the interaction between the polar heads of phospholipids and the peptides present over the bacterial membrane surface (Fig. 27A) showing the pores opening (Fig. 27 B i-ii) and their closure (Fig. 27 B iii-iv), also they were able to translocate from one leaflet to the other (Fig. 28 C).

The size of the pores would depend on the peptide concentration, which was chosen in a way to maximize the surface area covered by peptides on the membrane and to emulate AFM experiments.

This high tension of the peptides resulted in the transient pores and water channels (Fig. 28 D).

It is crucial, in those generating pores, to consider important factors such as the number of peptides interacting with the membrane, their initial structure (monomers or small oligomers), the specific conformation that they adopt during the interaction, and whether any refolding occurs during pore formation.

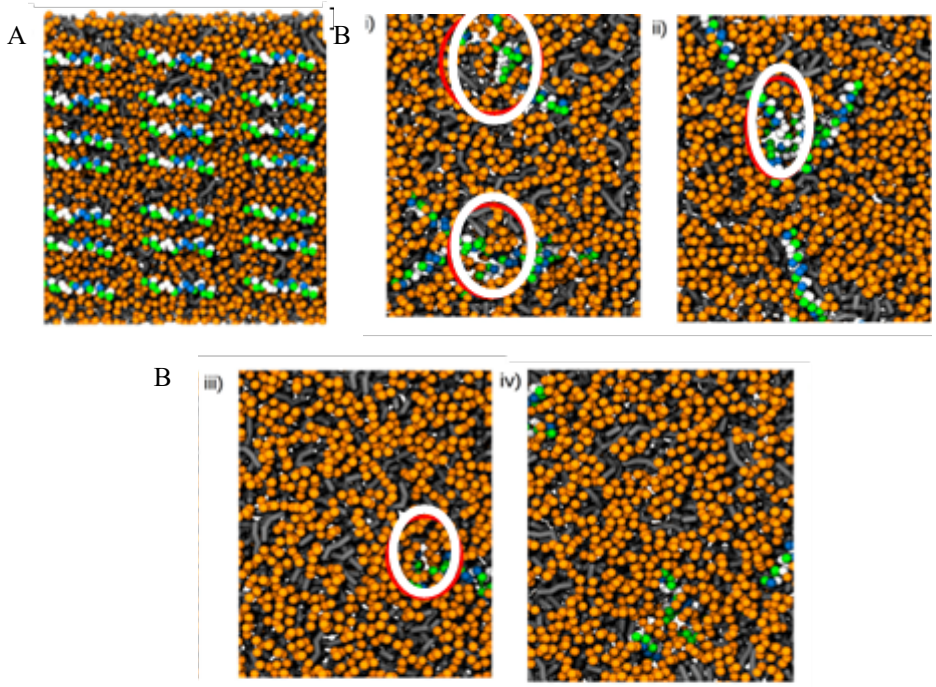

Fig. 27 Molecular Dynamic (MD) Simulation. A) Top view of initial structure of the asymmetric system made of POPC: POPG 1:1 with peptide (white and green color) covering the phospholipid membrane (orange polar heads and black tails). (B) The simulation snapshots from the start to the finish depicting small transient pores (highlighted with white circles) and their closure.

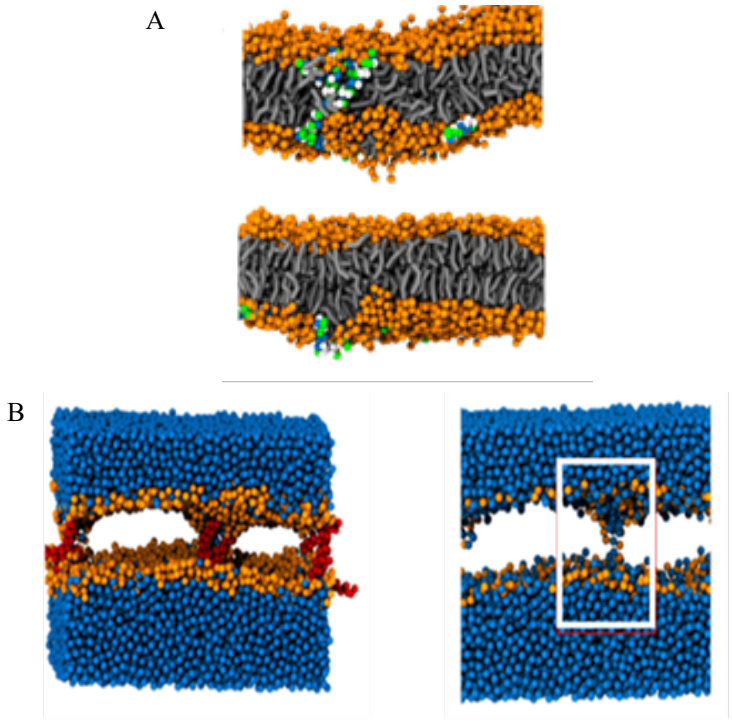

Fig. 28 Molecular Dynamic Simulation (A) The side view of the simulation showing the peptide translocation from one leaflet to the other. (B) The side view of pore formation in the presence of water molecules (blue) with the peptide (red) (left panel) and the representation of the passage of water through the pore highlighted with white rectangle (right panel)

The formation of these transient pores is likely a result of the peptide interaction with the lipid molecules in the upper leaflet, leading to increased leaflet tension and local disruptions of the bilayer structure.

Overall, the observation of transient pore formation indicates that Esc(1-21) has the potential to perturb the membrane integrity temporarily.

4.2 Effect of Esc(1-21)-1c on the susceptibility of *P. aeruginosa* cells to conventional antibiotics

The increase in bacterial strains resistant to conventional antibiotics is a pressing problem for human health and is expected to cause future pandemics. Among such bacterial pathogens responsible for a large variety of severe infections there is *P. aeruginosa*. Therefore, there is an extreme need for new molecules with antimicrobial activity or that can act as adjuvants of antibiotics already in use. In this scenario, the Esc(1-21)-1c AMP, endowed with antipseudomonal activity without being cytotoxic to human cells, was combined with a panel of antibiotics belonging to different classes and studied for its ability to potentiate the effect of antibiotics in inhibiting the growth of *P. aeruginosa* cells. Afterwards, a proteomic approach was used to investigate the underlying mechanism of action.

Differential proteomics is indeed an attractive method for identifying differentially expressed proteins and the corresponding protein networks involved in specific mechanisms.

4.2.1 Combination of Esc(1-21)-1c with antibiotics to evaluate the synergistic effect by the checkerboard assay

The combinatorial effect of the peptide Esc(1-21)-1c with different antibiotics belonging to various classes was assessed by the checkerboard assay on *P. aeruginosa* PAO1.

The fractional inhibitory concentration index (FICI) was determined to evaluate the interaction between the peptide and antibiotics.

According to the results reported in **Table 4**, no synergistic or additive effect was observed when Esc(1-21)-1c was combined with tobramycin (FIC = 2). However, when Esc(1-21)-1c was combined with other antibiotics, the bacterial growth inhibition was greater than that achieved by the same concentrations of the compounds used individually.

Specifically:

(i) an additive effect ($0.5 < FIC \leq 1$) was observed when Esc(1-21)-1c (at its ½ MIC) was combined with ceftazidime;

(ii) a synergistic effect ($FIC \leq 0.5$) was found when the peptide was combined with erythromycin (at its ¼ MIC), tetracycline (at its ¼ MIC), and chloramphenicol (at its 1/8 MIC).

Tab.4: Effect of Esc(1-21)-1c and various antibiotics on *P. aeruginosa* PAO1, either used individually or in combination.

Molecules	**MIC alone µg/mL[µM]**	**MIC in combination µg/mL[µM]**	**FIC**
Esc(1-21)-1c	6.8	6.8	2
Tobramycin	1	1	
Esc(1-21)-1c	6.8	3.4	0.625
Ceftazidime	8	1	
Esc(1-21)-1c	6.8	1.7	0.375
Erythromycin	256	32	
Esc(1-21)-1c	6.8	0.85	0.25
Chloramphenicol	32	4	
Esc(1-21)-1c	6.8	1.7	0.375
Tetracycline	8	1	

These results indicate that the combination of sub-inhibitory concentrations of Esc(1-21)-1c with ceftazidime, erythromycin, tetracycline, or chloramphenicol has a more potent inhibitory effect on the growth of *P. aeruginosa* compared to the compounds when used individually at the same concentrations.

The percentage of growth of *P. aeruginosa* PAO1 treated with ceftazidime, erythromycin, chloramphenicol, and tetracycline in combination with the peptide (at its best concentration giving a synergistic/additive effect, as indicated in **Table 4**) are reported in Fig. 29 (panels A-D, respectively). Bacterial cells were clearly able to grow in the presence of either the antibiotic or the peptide alone whereas no growth was observed when *P. aeruginosa* was treated with each single antibiotic in combination with Esc(1-21)-1c.

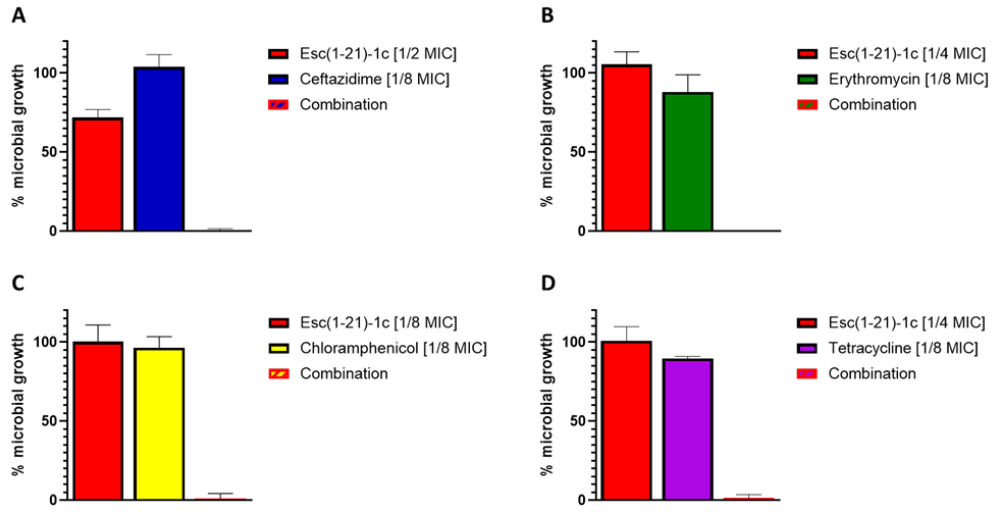

Fig. 29 Percentage of P. aeruginosa PAO1 growth with the respect to the control after 16 h in the presence of either the antibiotic or Esc(1-21)-1c alone or in combination. Panel A: ceftazidime; Panel B: erythromycin; Panel C: chloramphenicol; Panel D: Tetracycline.

The data are the mean ± standard deviation (SD) of three independent experiments.

4.2.2 Effect of Esc(1-21)-1c on the bacterial proteome by Differential Proteomic analysis

To identify differentially expressed proteins in response to Esc (1-21)-1c treatment, a differential proteomics approach was designed. These experiments were done in collaboration with the Professor Angela Duilio's research group (Dept. of Chemical Science- University Federico II- Naples).

Specifically, a label-free procedure was employed, comparing the proteomic patterns of *P. aeruginosa* PAO1 before and after treatment with 25 μM Esc (1-21)-1c (a peptide concentration that does not affect bacterial growth) for three hours.

This comparison enabled the identification of proteins that exhibit significant changes in the expression levels in response to the treatment.

Note that a significantly higher number of bacterial cells was necessary for this experiment compared to the checkerboard assay.

After treatment with Esc(1-21)-1c, the cells were lysed, and the entire protein content was purified by solid-phase extraction, digested with trypsin, and analysed by LC-MS/MS procedures.

The results showed a total of 108 identified proteins, 57 up- and 51 down-regulated indicating an increase or decrease in their expression levels compared to the untreated cells.

Bioinformatic analysis was performed using the software STRING and the up- and down-regulated proteins were grouped according to the interactions they are engaged (Fig. 30).

A B

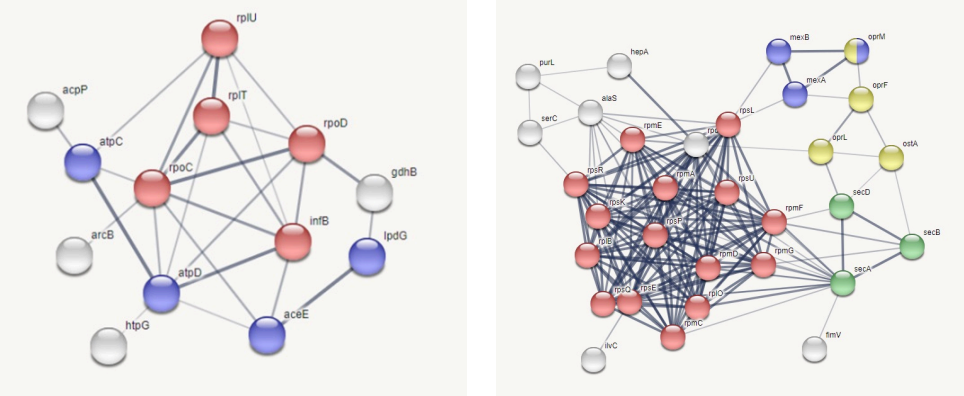

Fig. 30 STRING analysis of up-regulated proteins(A) and down-regulated proteins (B). Protein clusters were formed based on the major biological processes in which proteins are involved

Among the down-regulated and up-regulated proteins, there were some of particular interest reported in **Table 5**, along with SwissProt code, protein name, gene, and FC.

Table.5: Summary of the detected regulation of proteins that are involved in the influx/efflux of antibiotic molecules

SwissProt code	Protein name	Gene	Effect	FC
P32722	Porin D	*oprD*	+	1.45
P52477	Multidrug resistance protein MexA	*mexA*	-	0.78
Q9HU56	Protein-export protein SecB	*secB*	-	0.72
Q9LCT3	Protein translocase subunit SecA	*secA*	-	0.56
P13794	Outer membrane porin F	*oprF*	-	0.40
Q51487	Outer membrane protein OprM	*oprM*	-	0.53
P52002	Multidrug resistance protein MexB	*mexB*	-	0.29
P11221	Outer membrane lipoprotein I	*oprI*	-	0.22

+, up-regulated; -, down-regulated

Among the downregulated proteins emerged the membrane proteins MexA, MexB and OprM. All together they form a well-known tripartite efflux pump that plays a central role in multidrug resistance of this bacterium (Fig. 31) (Ma et al., 2021). Indeed, MexAB-OprM efflux pump is known to actively expel various drug compounds, including β-lactams, chloramphenicol, macrolides, quinolones, and tetracyclines. Moreover, SecA, SecB, OprF and OprI proteins involved in the secretion of proteins, antibiotics and metabolites were also down-regulated, possibly decreasing the capability of *P. aeruginosa* to extrude antimicrobial drugs. The down regulation of these proteins due to Esc(1-21)-1c treatment might then significantly contribute to the decrease of the intrinsic antibiotic resistance of *P. aeruginosa*. Conversely, the differential proteomic investigation indicated an increasing level of OprD, the major porin of *P. aeruginosa* involved in the uptake of antibiotics.

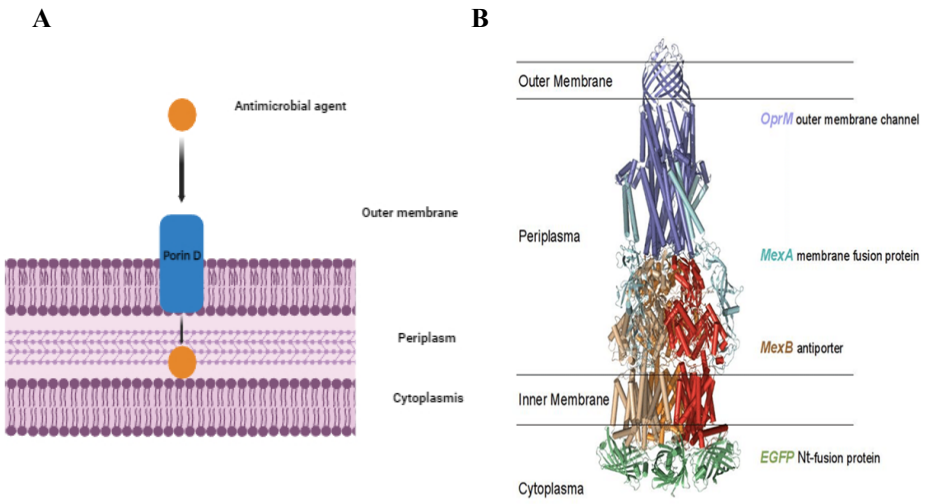

Fig. 31 Schematic illustration of bacterial porin and drug efflux pumps: A) OprD; B) MexA, MexB, OprM proteins (Ding et al., 2014)

4.2.3 Evaluation of Esc(1-21)-1c on the production of efflux pumps by transcriptional analysis

To know whether the effect of Esc (1-21)-1c was exerted by modulating gene transcription or by other mechanisms at post-transcriptional level, transcriptional analysis of the genes encoding the main proteins identified from the differential proteomic experiment was performed. *P. aeruginosa* PAO1 cells were treated with 25 μM Esc (1-21)-1c for 3 hours and the mRNA level of selected genes was evaluated by means of RT-qPCR analysis compared to untreated samples. These experiments were conducted in collaboration with Professor Giordano Rampioni (Department of Science, Roma Tre University, Italy).

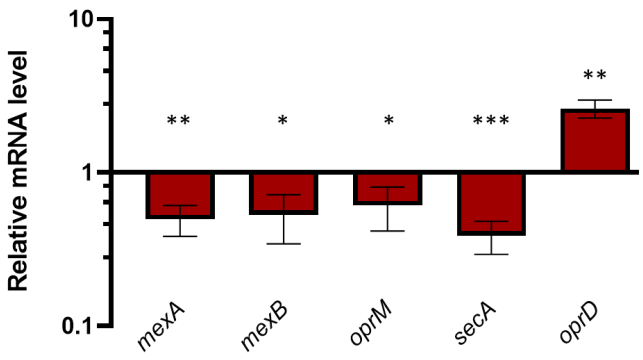

*Fig. 32. RT-qPCR measurements of specific mRNAs in P. aeruginosa PAO1 cultures treated with 25 μM Esc(1-21)-1c relative to untreated P. aeruginosa PAO1 cultures. The average of three independent experiments is reported with SD. *, P < 0.05; **, P < 0.01; ***, P < 0.001; ns, not statistically significant.*

As reported in Fig. 32, AMP treatment led to a significant downregulation of the expression of mexA, mexB and oprM genes belonging to the mexAB-oprM operon and of the secA gene.

In comparison, the expression of oprD gene was upregulated in the Esc(1-21)1c-treated cultures relative to the untreated controls. These data are in agreement with the proteomic results supporting the notion that the ability of *P. aeruginosa* to release antibiotics from bacterial cells and to limit their uptake was altered by Esc(1-21)-1c treatment.

4.2.4 Quantitative analyses of tetracycline within *P. aeruginosa* cells

The decreased expression of the MexAB-OprM efflux pump upon peptide treatment might explain the ability of the peptide to potentiate the effect of several antibiotics, including tetracycline, by retaining their intracellular content (Fig. 33).

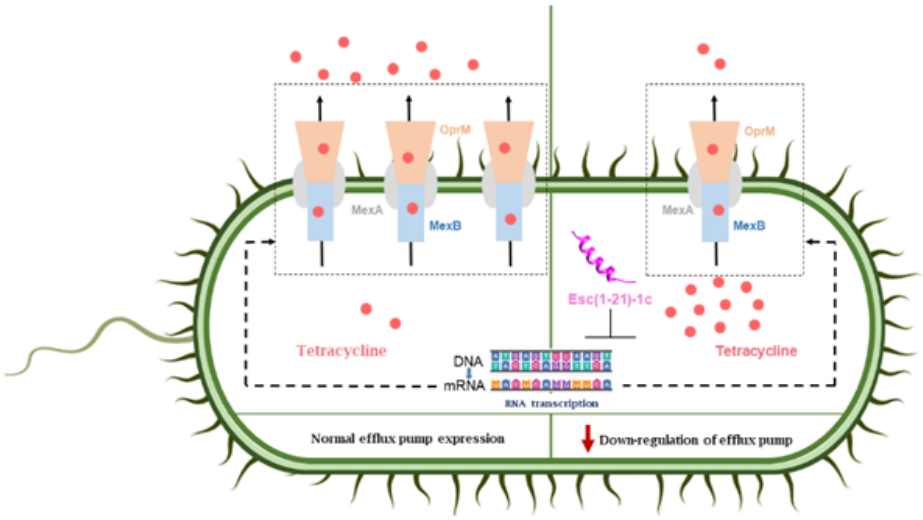

Fig.33 Schematic representation of the effect of peptide treatment on the expression of the MexAB-OprM efflux pump and the consequent accumulation of antibiotics inside the bacterial cell (right side) with respect the normal condition (left side).

To date, tetracycline is still used in clinical practice, and this confirms its effectiveness as antibiotic (LaPlante et al.,2022). Therefore, the quantitative analysis of tetracycline incorporated by *P. aeruginosa* cells in the presence and in the absence of Esc(1-21)-1c was carried out.

Initially, standard solutions of tetracycline at different concentrations were analysed by LC-MS/MS in MRM conditions to establish the optimal instrument settings and to define the best parent ion-fragment ions mass transitions.

The metabolites extracted from *P. aeruginosa* cells treated with tetracycline alone or in combination with Esc(1-21)-1c for 3 hours, were analysed by tandem mass spectrometry procedure based on MRM scan mode to evaluate the amount of tetracycline present in bacterial cells.

Fig. 34 shows the quantitative analysis of tetracycline extracted from the sample.

The amount of tetracycline within *P. aeruginosa* cells treated with the combination of peptide plus antibiotic increased twice compared to the level found in samples treated with tetracycline alone, supporting the hypothesis that the administration of Esc(1-21)-1c in combination with certain antibiotics increases their uptake and/or decreases their efflux.

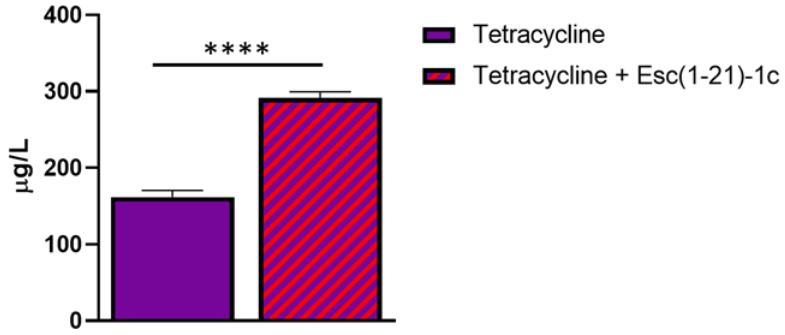

*Fig. 34 Relative amounts of tetracycline detected within P. aeruginosa cells in samples treated with the antibiotic alone (violet bar) and with a combination of antibiotic plus Esc(1-21)-1c (violet + red bar). Data represents the mean ± SD; the level of statistical significance among groups is indicated as follows: ****, p<0.0001.*

Relative quantification of proteins from *P. aeruginosa*

As reported in the paragraphs above, proteomic and transcriptional analyses proved the down-regulation of the MexA, MexB and OprM proteins and of the corresponding genes.

To validate these data, quantitative analysis of these proteins in bacterial cells following incubation with tetracycline alone or in combination with Esc(1-21)-1c, was performed by MRM tandem mass spectrometry.

Quantitative evaluation of the MRM/MS data highlighted a significant reduction in the amount of the selected proteins within *Pseudomonas* cells treated with tetracycline plus Esc(1-21)-1c compared to both tetracycline-treated and control samples (Fig. 35), supporting the transcriptional and

proteomic data on the downregulation of *mexAB-oprM* genes and the decreased expression of the corresponding proteins.

On the contrary, tetracycline alone did not affect the level of the analysed proteins.

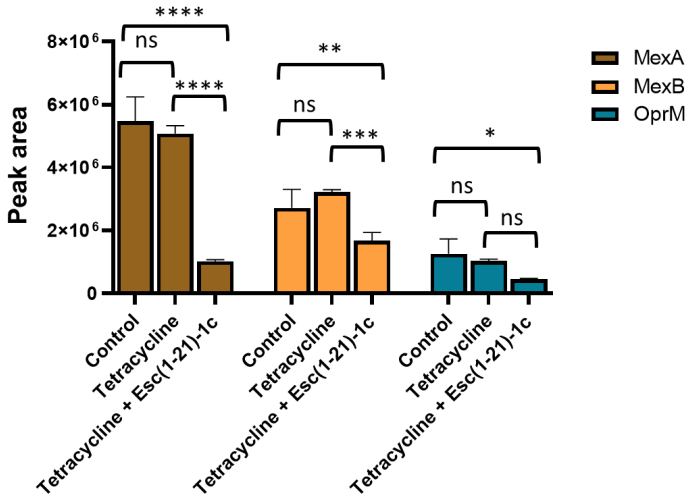

*Fig.35 Quantitative measurements of MexA (brown bars), MexB (orange bars) and OprM (cyan bars) by LC-MS/MS in MRM mode in P. aeruginosa cells treated with either the antibiotic alone or a combination of antibiotic plus Esc(1-21)-1c. Data represents the mean ± SD; the level of statistical significance among groups is indicated as follows: *, p<0.05; ** p<0.01; *** p<0.001, p<0.0001.*

4.3 Effect of Esc peptides on cell lines (FRT and CFBE) expressing F508del-CFTR by electrophysiology and computational studies

Considering either (i) the role of the airways epithelium and CFTR in maintaining lung functions and wound repair (Cappiello et.al.; 2016) or (ii) the wound healing properties of Esc peptides on bronchial epithelial cells, the potential ability of Esc peptides to affect the ion currents controlled by CFTR using Fisher rat thyroid cells (FRT) and Human bronchial epithelia cells (CFBE) ,was investigated along with the underlying molecular mechanism, by means of electrophysiology techniques and computational studies. Unfortunately, even in the era of CFTR modulation therapies, management of pulmonary infections in CF remains highly challenging especially in patients with advanced stages of lung disease.

Currently, CF research community is trying to identify small molecules that can assist the delivery of the mutated channel to the plasma membrane (namely correctors) and/or that increase the ions permeation through the defective channel (namely potentiators). However, now there no compound able to restore the complete functionality of mutated CFTR.

Having a compound endowed not only with an antibacterial and wound healing properties but also with the capability to restore the function of defective CFTR would be extremely advantageous for the development of new therapies to treat lung pathology in CF.

So no studies on the effects of AMPs on CFTR have been reported.

4.3.1 Permeability of FRT and CFBE epithelial cells by transepithelial resistance measurements

The epithelial barrier integrity, that is vital for respiratory functions especially in CF lung, can be assessed by measuring the transepithelial electrical resistance (TEER) across a proper cellular monolayer mimicking the airways epithelium. Indeed, TEER measurements provide an indication of the tightness of intercellular junctions and the overall integrity of the epithelial barrier (Srinivasan et al., 2015). The impact of the peptide treatment at different concentrations on polarized epithelia formed by Fischer rat thyroid (FRT) cells expressing mutated or wild-type CFTR (F508del-FRT and wt-FRT, respectively) was initially studied. FRT cells have been widely utilized as a model system to study CFTR protein (Gottschalk et al., 2016). These cells form a cellular monolayer that is stabilized by intercellular junctions, including tight junctions, adherents junctions, and desmosomes, which play important roles in regulating the diffusion of water and solutes across the cell layer, allowing for the establishment of selectively permeable barriers (Kraus et al., 2006). When FRT cells expressing mutated or wild-type CFTR were treated for 24h with different concentrations of peptides, minor changes in TEER, reported as transepithelial electrical conductance (G), were observed compared to the control samples treated with the vehicle dimethyl sulfoxide (DMSO) highlighted by the solid black line in the figure (Fig. 36).

Similar results were obtained for the bronchial epithelial cell line CFBE41o- expressing either F508del- or wt-CFTR (F508del-CFBE41o- or wtCFBE41o- and further support the finding that the peptides did not significantly affect the epithelial integrity up to a concentration of 80 μM (Fig. 36).

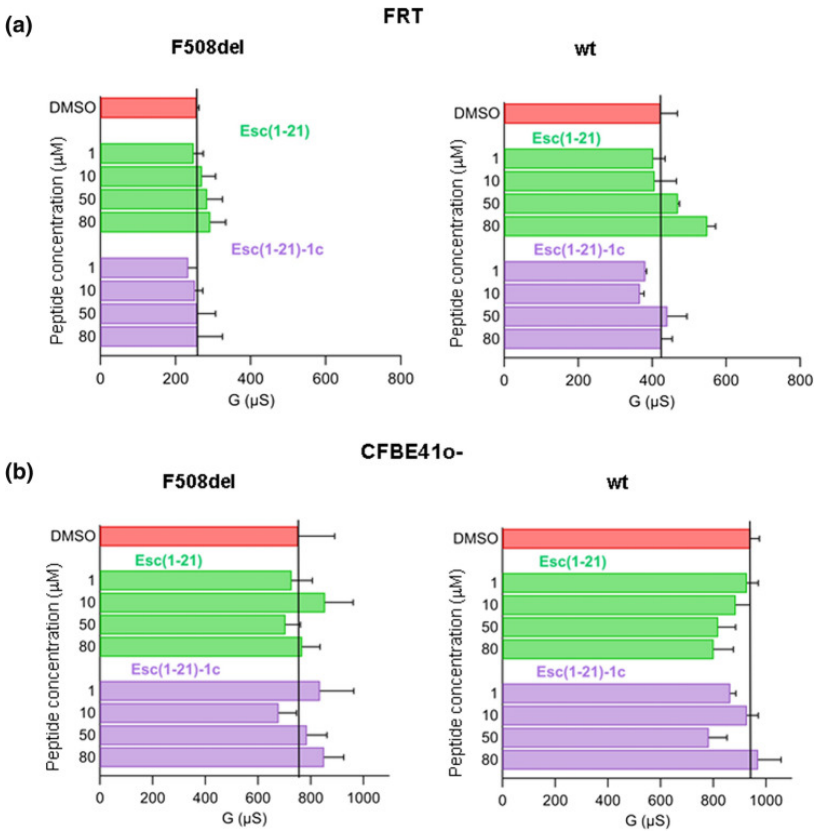

Fig. 36 Effect of peptides on the epithelial integrity by the TEER assay on FRT (a) and CFBE41o-cells (b) expressing either F508del-CFTR (left panels) or wt-CFTR (right panels). Data are expressed as mean±SEM from at least six independent experiments, each in triplicate.

These different G values between these two cell lines can depend on their intrinsic characteristics in the differentiation process of the epithelium (Srinivasan et al., 2015; Kreft et al., 2015).

4.3.2 Potentiator effect of Esc peptides on CFTR activity

The effect of Esc peptides on the activity of CFTR was investigated by measuring the CFTR-mediated transepithelial electrical conductance (TEEC), referred to as delta conductance (ΔG), in epithelia formed by FRT and CFBE41o-cells which overexpress F508del-CFTR.

To be active, the CFTR channel needs to be phosphorylated at multiple sites of the R domain by cAMP-dependent protein kinases, i.e. pKA, and to bind 2 ATP at the two NBD domains.

In vitro, the complete activation of CFTR with gating defects can be achieved upon addition of two compounds: forskolin (FSK) which increases the intracellular level of cAMP and genistein (GEN), a CFTR potentiator which increases the ions permeation by stabilizing the NBD dimerization upon direct interaction with the phosphorylated channel.

The epithelia were preincubated for 24 h with the corrector lumacaftor to assist the delivery of the mutated channel to the membrane and then treated, for 10 min, with the combination FSK+Esc peptide (at various concentrations ranging from 1 to 80 μM) or FSK+ GEN (as our positive control).

ΔG was calculated as the difference between the TEEC obtained after 10 min treatment of the corrected epithelium with FSK alone or in combination with either GEN or Esc peptides and the conductance measured after the addition of the CFTR inhibitor PPQ102.

The results shown in Fig. 37a (left panel) indicate that when the epithelium was exposed to each Esc peptide at a concentration of 10 μM, there was significant increase of ΔG compared to the values obtained for samples treated with FSK alone.

This increase in conductance was approximately 1.5-fold higher than the FSK-treated samples. Similar data were achieved for F508del-CFBE41o- (Fig. 37b left panel).

Based on these findings, the concentration of 10 μM for the Esc peptides was selected for further experiments.

Furthermore, the enhancement of CFTR-mediated conductance was slightly more pronounced for the Esc(1-21)-1c isomer, whose activity was comparable to that of the potentiator GEN when used at the same concentration of 10 μM (always in combination with FSK).

These results indicate that the Esc peptides, especially the Esc(1-21)-1c isomer, have the ability to potentiate CFTR function and to enhance the ion permeability of the epithelial monolayer.

The dose-response behaviour of Esc peptides, characterized by a bell-shaped curve with a stimulatory effect at lower concentrations and an inhibitory effect at higher dosages, aligns with previous findings in CFTR studies with known potentiators (Illek et al., 1996) and suggests a CFTR potentiator effect of Esc peptides as that displayed by GEN on the mutated channel after rescue to the membrane.

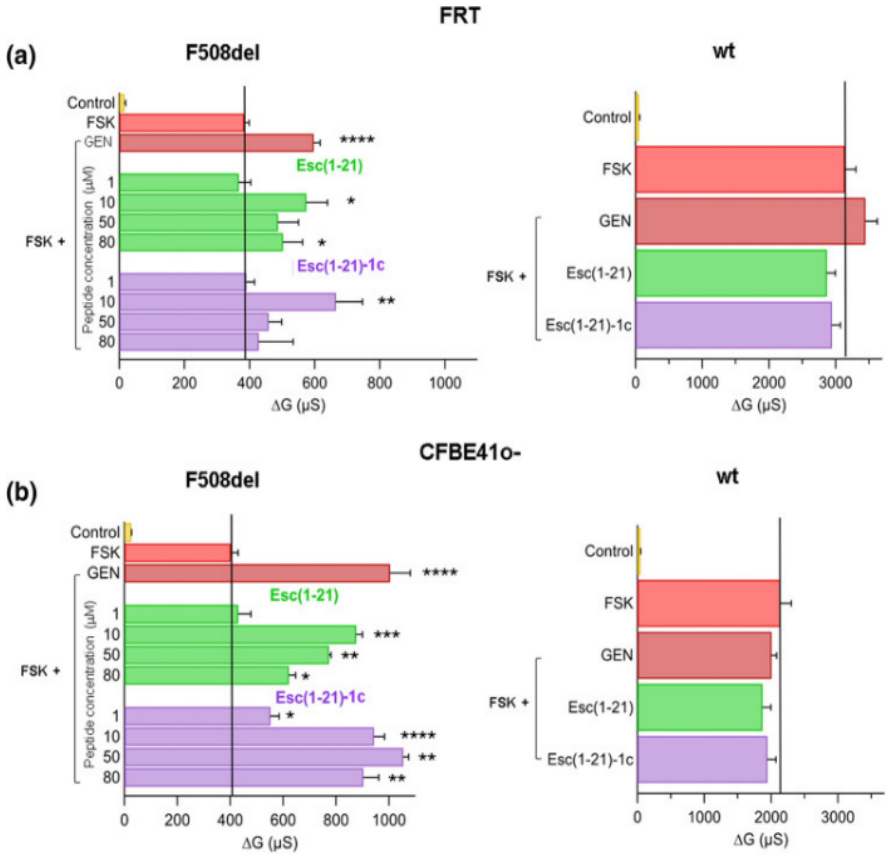

*Fig. 37 Potentiator effect of Esc peptides on CFTR activity. A and B, left panels F508del-FRT and F508del-CFBE41o- epithelia. A and B right panels FRT and CFBE41o- expressing wt-CFTR respectively. The level of statistical significance of samples versus FSK is indicated as follows: *, p<0.05; **p<0.01; ***p<0.001; ****p<0.0001. Comparison between data was done by Student's t test.*

The same experiments were also conducted in FRT and CFBE41o- cells expressing wild-type CFTR. The lack of an increase of ΔG, after treatment of the epithelium with FSK plus Esc peptides compared to FSK-treated samples, could be related to the fact that channel phosphorylation by FSK alone is sufficient to induce the complete activation of CFTR.

To explore whether the potentiator effect of Esc peptides relied on their primary structure, and mostly on the presence of d-Ser^{17} and its potential phosphorylation by intracellular kinases, the evaluation of different peptide analogues with variations in their amino acids sequence, specifically at position 17, was carried out. The synthesized analogues included peptides with different d/l amino acids at position 17, such as alanine, glycine, threonine, and phenylalanine. Additionally, an analogue with d-phosphoSer at position 17 was included for comparison.

Figure. 38 illustrates the difference in ΔG measured in F508del-FRT cells after 10-minute stimulation of CFTR with FSK alone or in combination with 10 μM of each peptide analog. By comparing the effects of the different peptide analogues, it is possible to assess the impact of specific amino acid substitutions on the potentiator activity of CFTR. This analysis helped to determine whether the presence of Ser 17 and/or its phosphorylation were crucial for the potentiator effect of the Esc peptides.

The results indicated that, among the tested peptide isoforms, only the peptide [d-Leu14, d-phosphoSer17]Esc significantly improved the function of F508del-CFTR (Fig. 38).

This peptide exhibited a stronger effect compared to the other Esc peptides, or the potentiator GEN. The observed enhancement in CFTR function was approximately twofold higher than that induced by FSK alone. Furthermore, shorter fragments of Esc peptides were analysed for their ability to potentiate CFTR activity. Specifically, the 1-14 and 9-21 fragments of Esc(1-21) were evaluated in TEER experiments. However, no significant variation in CFTR-mediated conductance was observed with these shorter peptide fragments suggesting that a full-length Esc peptide is necessary to restore the function of F508del-CFTR.

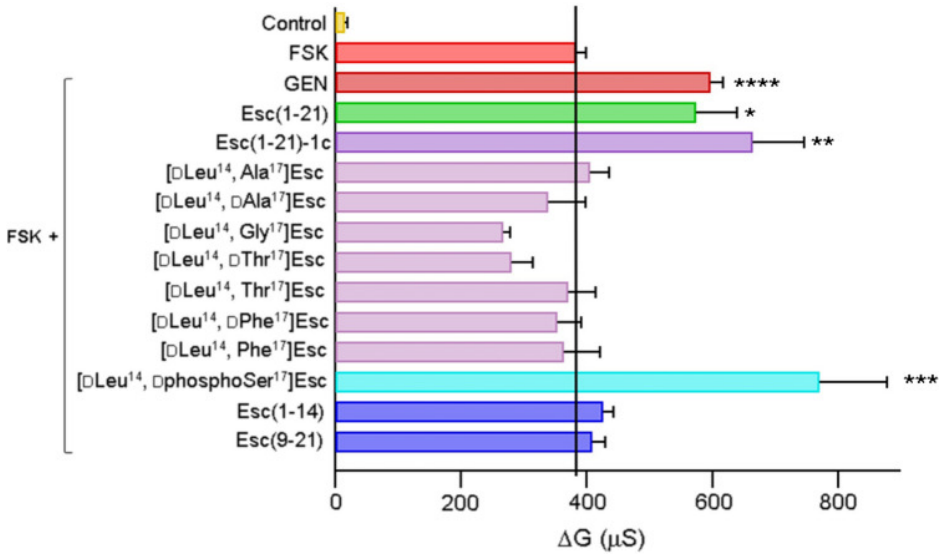

*Fig.38 Effect of different analogues of Esc peptides on the CFTR dependent transepithelial conductance in corrector-rescued F508delFRT cells. The level of statistical significance of samples versus FSK is indicated as follows: *p<0.05; **p<0.01; ***p<0.001; ****p<0.0001. Comparison between data was done by Student's t test.*

4.3.3 Esc peptides modulate F508del-CFTR-mediated chloride current (patch-clamp experiments)

To gain a deeper understanding of the mechanism of CFTR activation by Esc peptides, patch-clamp experiments were conducted on VX809-rescued F508del-FRT cells. These experiments were conducted in collaboration with Dr, Loretta Ferrera, at Institute Giannina Gaslini (IRCCS- Genoa-Italy). The patch-clamp technique allows a direct measurement of ion channel activity. More precisely, CFTR activation by Esc peptides was studied under cell-free conditions by the inside-out patch-clamp configuration using large pipette tips to obtain membrane patches containing multiple CFTR channels.

The [d-Leu14, dphosphoSer 17]Esc peptide was also included for comparison.

In the patch-clamp experiments on VX809-rescued F508del-FRT cells, the phosphorylation of the channel was achieved by phosphorylating CFTR upon addition of ATP and the catalytic subunit of PKA. The results showed a clear increase of CFTR-mediated current in response to the administration of the peptides in the presence of ATP and the catalytic subunit of PKA. Specifically, the [d-Leu14, dphosphoSer 17]Esc peptide demonstrated the highest activity (Fig. 39).

In this case, currents activated by the peptides were rapidly blocked by the selective channel blocker CFTRInh-172 (Fig. 39), supporting the conclusion that activation of CFTR implies direct binding of the peptides likely to the cytosolic side of the ion channel.

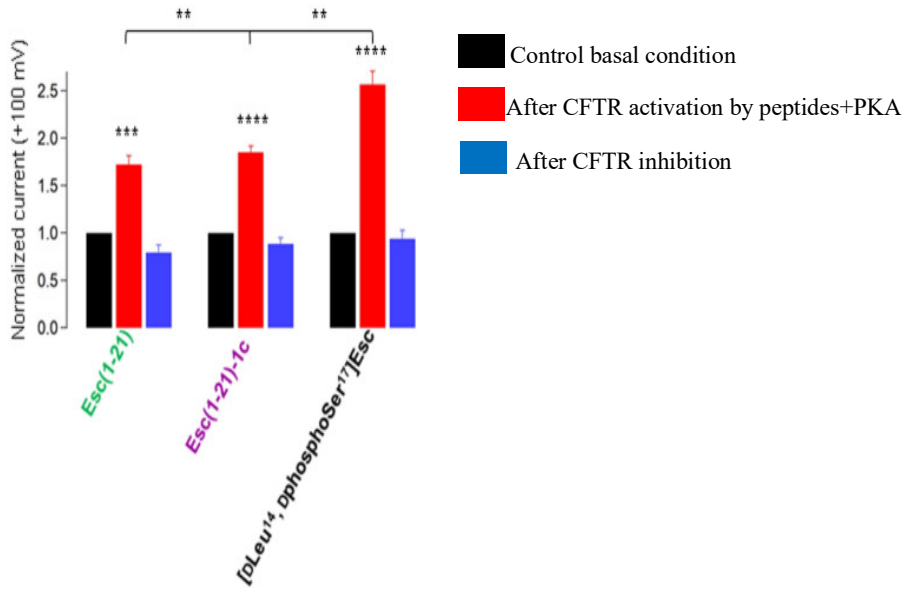

*Fig. 39 Analysis of membrane currents at 100 mV, in F508del-FRT cells from inside-out patch-clamp. The level of statistical significance of samples versus the control basal condition, as well as the statistical significance among samples after CFTR activation are indicated as follows: **p<0.01; ***p<0.001; ****p<0.0001. Comparison between data was done using Student's t test.*

4.3.4 Esc peptides interaction with F508del-CFTR by simulation studies

Molecular dynamics (MD) simulations were carried out to investigate the potential interaction between the NBDs of F508del CFTR and the peptides Esc(1–21) and [d-Leu14, d-phosphoSer 17]Esc. The study was conducted in collaboration with Prof. Mattia Mori (Department of Biotechnology, Chemistry and Pharmacy- University of Siena-Italy).

MD simulations were initiated by randomly placing each peptide and the NBDs heterodimer in a reciprocal orientation within the simulation box.

They were initially positioned at a distance greater than 40 Å from each other to allow for unbiased exploration of potential binding modes. By employing this blind approach, the simulations aimed to capture the recognition and binding events between the F508del NBDs and each peptide without any predefined conformational or positional bases. The results revealed that Esc(1-21) and [d-Leu 14, d-phosphoSer 17]Esc interact with different binding sites on the NBDs of F508del CFTR, likely due to the differences in the chemical composition, physicochemical properties, and phosphorylation state of the two peptides. Specifically, Esc(1–21) consistently recognized a binding site located on the lateral edge of NBD1, in close proximity to its N-terminal tail and near the binding interface with NBD2 (Fig. 40). This interaction is facilitated by the electrostatic complementarity between the positive charges of the peptide and the negative charges on the NBD surface. Differently, the [d-Leu 14, d-phosphoSer 17]Esc peptide bound near the cytoplasmic side of the NBDs, bridging NBD1 with NBD2 (Fig .40). This binding mode suggests a preference for hydrophobic interactions between the peptide and the NBD surface.

The distinct binding sites suggest that Esc(1–21) and [d-Leu14, d-phospho Ser17]Esc interact with different regions of the NBDs, potentially leading to different modes of action and effects on CFTR function (Fig. 40).

In the case of Esc(1–21), the simulations indicated that it primarily interacts with NBD1.

It forms a network of hydrogen bond interactions with the backbone of residues Phe 409, Glu 621, and Glu 1329 and hydrophobic interactions (Fig. 40).

The [d-Leu14, d-phosphoSer 17]Esc binds with a similar polarity establishing H-bond interactions with Glu 632 and Arg 1386, while the nonpolar edge of the peptide establishes an extended network of hydrophobic interactions with the NBD1/NBD2 interface (Fig. 40)

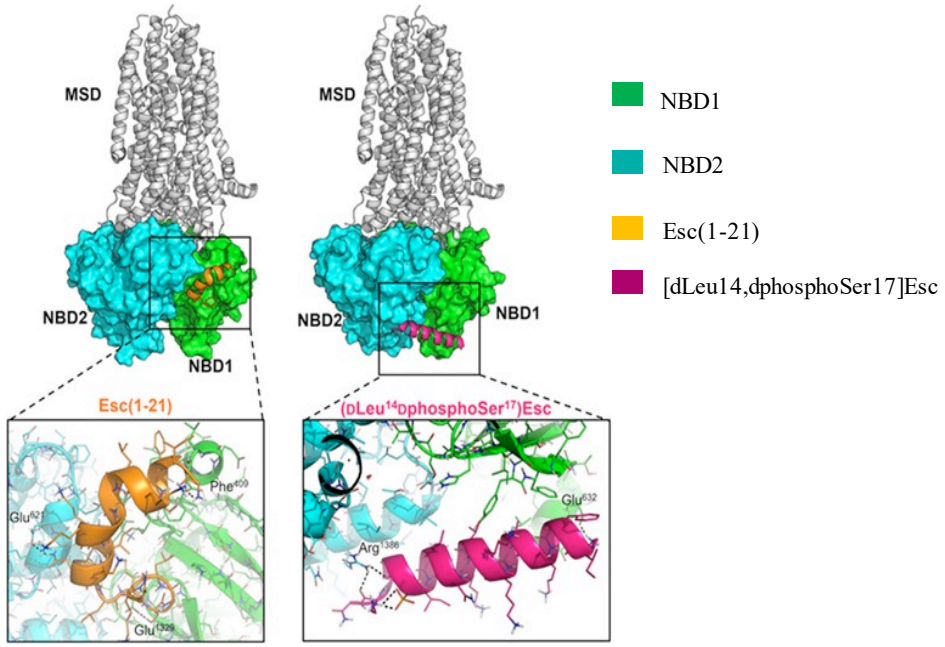

Fig. 40 Structural insights into intermolecular recognition and binding of peptides to F508del NBDs by MD simulations. Left: Esc(1–21)/NBDs; right: [dLeu14, dphosphoSer17]Esc/NBDs.

The identification of different binding sites for Esc(1–21) and [dLeu14, dphosphoSer17]Esc peptides, along with their distinct theoretical affinity, suggests their potential role in gating the chloride channel pore.

5. Discussion and Conclusions

Interaction of Esc(1-21) with lipid bilayers mimicking bacterial membranes

The antimicrobial activity of membrane-active AMPs, such as Esc peptides, is influenced by various factors encompassing the concentration of the peptide, their self-assembly and oligomerization state, the phospholipid composition and the fluidity of the target membrane; all these factors collectively contribute to determine the efficiency of AMPs in perturbing the phospholipid bilayer and in exerting their antimicrobial activity.

AFM is a versatile, high-resolution imaging technique that enables the direct and real-time (from minutes to hours) monitoring of the dynamics of biological membranes, and their interactions with biomolecules and drugs at nanometer resolution (Ando et al., 2014; Hammond et al., 2021). The AFM experiments, conducted in collaboration with Prof. Robert Vacha's research group, have shed light on the membrane perturbation mechanism of Esc(1-21). This appears to be related to the peptide ability to form transient membrane defects (that are temporary openings or disruptions), likely in the form of non-canonical transmembrane barrel-stave pores. It was observed that Esc(1-21) interacts with the anionic model membrane, causing the formation of pores with varying sizes and depths, depending on the peptide concentration. In bacterial cells these pores would allow the passage of ions, small molecules, or even enzymes, in line with previous studies showing the extracellular release of beta-galactosidase upon treatment of *P. aeruginosa* cells with Esc(1-21) at a concentration ranging from 8 to 64 μM (Luca et. al.; 2013).

The transient nature of these pores means that they do not have permanent structural features. Over time, these pores tend to close, likely due to the dynamic nature of the lipid bilayer and the self-repair mechanisms of the membrane. The ability of Esc(1-21) to form transient pores is not a common property of membrane-active AMPs and understanding their formation and closure should provide insights into the dynamic interactions between AMPs and bacterial membranes; a crucial aspect for the design and development of future membrane-active compounds. However, AFM has limitations in resolving the molecular-scale details of the membrane and the precise structure of the transient pores. Additionally, factors such as the tip-sample interaction and imaging conditions can influence the observed features. The use of molecular dynamics (MD) simulations to investigate the interaction of Esc(1-21) peptide with the bacterial membrane is a valuable complement to the experimental data. Molecular dynamics (MD) simulations are powerful computational tools used to investigate the behaviour of biomolecules, including peptides. This computational technique was used to investigate the dynamics and molecular interactions for a broad range of molecules including organic, inorganic, and biomolecular complexes. With the current state-of-art technologies, it is now possible to study the structural dynamics of biological macromolecules for longer timescales.

By running MD simulations of Esc(1-21) on the bilayer membrane, it is possible to obtain information about various aspects, such as the peptide's conformation, its interaction with the lipid molecules, and the formation of transient pores or other perturbations in the membrane.

MD simulations allow to simulate the behaviour and interactions of atoms and molecules over time, providing insights into the dynamics and structural changes occurring at the atomic level. On the other hand, MD simulations are limited by the accuracy of the force fields and assumptions made in the simulation setup. The choice of force fields, water models, and simulation parameters can also affect the outcome of the simulations. In this case, the MD simulations provided further support to the experimental observations of the interaction of Esc(1-21) with anionic membranes mimicking the bacterial membranes. The simulations revealed that Esc(1-21) peptide perturbs the lipid bilayer by creating small-sized pores. When an asymmetric system with high peptide concentration on one of the leaflets was used and simulated for 20 μs, Esc(1-21) peptide molecules aggregated, thinned the membrane, and formed small transient pores through which they could translocate from one leaflet to the other. The size of the pores would possibly depend on the peptide concentration. These simulations showed an immediate formation of small pores (running of simulation is 20 μs) while they slowly closed as reported in Fig 18, in agreement with the transient pores observed in the AFM.

Overall, the MD simulations, along with the experimental data, confirm the ability of Esc(1-21) peptide to perturb the bacterial membrane by creating membrane defects that transiently permeabilize the phospholipid bilayer. However, the exact mechanisms through which the peptide induces pore formation and membrane perturbation requires further investigation. Future studies can be built upon these findings to explore additional aspects, such as the influence of different lipid compositions, or the role of specific peptide-membrane interactions.

It is crucial to have comparable in vitro and in vivo conditions and to consider important factors such as the number of peptides interacting with the membrane, their initial structure (monomers or small oligomers), the specific conformation that they adopt during the interaction and pore formation.

Overall, by considering the results from AFM and MD, we gained deeper insights into the membrane-perturbing property of Esc(1-21); a relevant aspect for optimizing the design and development of AMPs with enhanced antimicrobial properties.

Ability of Esc(1-21)-1c to potentiate the effect of antibiotics in inhibiting the growth of P. aeruginosa

The emergence and spread of superbugs, which are microbes resistant to multiple classes of antimicrobial agents, has increased significantly over the years. These superbugs pose a major threat because they limit the treatment options available to healthcare providers. In the Gram-negative *bacterium P. aeruginosa*, one of the mechanisms associated to MDR is the extrusion of antibiotics from bacterial cells, generally mediated by efflux pumps of the Resistance-Nodulation-Division (RND) family (Nikaido et al., 1998b). These consist of a tripartite complex formed by a transmembrane protein in the cytoplasmic membrane, a periplasmic protein and a porin associated to the outer membrane (Lorusso et al., 2022) and actively remove antibiotics from the bacterial cell, reducing their concentration and efficacy. On the other hand, outer membrane proteins play a crucial role in controlling the entry of various substances, including antibiotics.

Increased production of these proteins can potentially enhance the effectiveness of traditional antibiotics by limiting the ability of bacteria to resist or evade their action.

Currently, alternative therapies that are under clinical trial to tackle the global problem of increasing MDR microbial strains, including *P. aeruginosa*, rely on the usage of traditional antibiotics in combination with compounds that are able to potentiate their effect. Among these compounds, AMPs hold great promise (Maisetta et al., 2009; Gupta et al., 2015). The present study has demonstrated that combination of the AMP Esc(1-21)-1c with erythromycin, chloramphenicol, or tetracycline provides a synergistic effect in inhibiting the growth of *P. aeruginosa* PAO1, while an indifferent effect was obtained when the peptide was tested in the presence of tobramycin. By conducting differential proteomic experiments an alteration of the drugs uptake/efflux mechanisms in *P. aeruginosa* cells was discovered, following incubation with Esc(1-21)-1c at its sub-MIC. In particular, the expression level of the components of the MexAB-OprM efflux pump was decreased while the expression of OprD protein, involved in the outer membrane permeability (Li et al., 2012), significantly raised. These data were also supported by transcriptional analysis of the corresponding genes and by direct measurements of the amount of the specific proteins, by LC-MS/MS procedures in the MRM scan mode.

Impairment in the efflux activity of the MexAB-OprM pump, and augmented uptake activity *via* the OprD porin would enhance drug content in intact cells, making bacteria more susceptible to the antibiotic.

This was confirmed by the direct measurement of tetracycline levels within *P. aeruginosa* cells exposed to Esc(1-21)-1c at its sub-MIC, which indicated a significant higher tetracycline level in peptide-treated samples compared to amount found in bacterial cells treated only with tetracycline. Furthermore, this study did not indicate any synergistic effect when Esc(1-21)-1c was combined with tobramycin.

This is reasonable, considering that resistance to aminoglycosides in *P. aeruginosa* is mainly provided by the activity of the modifying enzyme aminoglycoside nucleotidyl transferase rather than by active efflux (Pang et al., 2019). Finally, the down-regulation of SecA, SecB, OprF and OprI proteins support the hypothesis that the presence of Esc(1-21)-1c can interfere with the ability of *P. aeruginosa* to export antibiotics, generating a series of negative effects for the survival of the bacterium. Further investigations are needed to define the specific role of Esc(1-21)-1c in affecting the expression of the efflux pump components, although a negative transcriptional control can be supposed based on transcriptional analysis. The MexAB-OprM pump is regulated by both local and global regulators (Aguilar-Rodea et al., 2022). The reduced expression of the pump may be due to the interaction of the peptide with some molecules involved in the regulatory mechanisms of the MexAB-OprM efflux system (Aguilar-Rodea et al., 2022). Nowadays, the development of efflux pump inhibitors (EPIs) constitutes an important area of drug discovery and great perspectives can be foreseen for their use to inhibit or limit the emergence of multidrug resistance bacteria (Van Bambeke et al., 2003; Stavri et al., 2007).

Remarkably, it was demonstrated a novel function of Esc(1-21)-1c and AMPs in general, that is the capability to significantly reduce the production of MexAB-OprM efflux pump in *P. aeruginosa* and to increase the synthesis of OprD. This opens the avenues for the development of novel AMP/antibiotics formulations and may accelerate the traditional process of drug development by potentiating "old" antibiotics already known to be safe and effective in humans.

Effect of Esc peptides on the activity of CFTR

In this thesis work, an unprecedented property of AMPs has been discovered, which is the capability to act as modulators of CFTR with conductance defects. This is a relevant property for the development of new multifunctional drugs for treatment of lung pathology in CF patients. Indeed, the principal issue in CF patients is the reduced permeation of chloride and bicarbonate ions across defective CFTR in the apical membrane of epithelial cells, with abnormal lung secretions and loss of respiratory function, which is still fatal in early adulthood (O'Sullivan et al., 2009; Ratjen et al., 2015). In contrast to the clinically used CFTR modulators, Esc peptides would give particular benefit especially to CF sufferers with *P. aeruginosa* lung infection, by combining their antibacterial activity with a potentiating effect of CFTR. The finding of a rapid raise of ion conductance when each Esc peptide was added to corrector-rescued F508del-CFTR expressing epithelium in the presence of FSK and the return of such conductance to the initial value (measured before CFTR activation), upon administration of the selective CFTR inhibitor, clearly proved that the conductance increase stimulated by Esc peptides is mediated by the activated CFTR.

Such findings suggested the capability of Esc peptides to augment the ion permeability of the rescued-F508del-CFTR by presumably modifying the channel open-closed probability, like for GEN.

This was then supported by patch-clamp experiments showing the peptides' ability to increase the ion current through F508del-CFTR. Furthermore, electrophysiological experiments and computational studies have underscored how the potentiator effect of Esc(1–21) and its diastereomer is (i) a highly specific process relying on their primary structure and particularly on the presence of Ser 17; and (ii) the result of a direct interaction of the peptides with CFTR, as proposed for other CFTR activators, including GEN (Weinreich et al., 1997; French et al., 1997; Wang et al., 1998).

Computational studies suggested that a direct interaction between peptides and NBDs of F508del CFTR does occur, although in different sites depending on the phosphorylation state of the peptide at Ser 17. One hypothesis is that Esc peptides can interact directly with CFTR from the cytosolic site, upon entrance into epithelial cells.

Once in the cytoplasm, the diastereomer Esc(1–21)-1c in particular could be phosphorylated at the level of d-Ser 17, thus switching to the more efficient form to improve CFTR pore opening. However, it cannot be excluded the potential interaction of Esc peptides with the extracellular domain of CFTR Furthermore, it was demonstrated that the two Esc peptides do not alter the airway epithelial barrier permeability or the paracellular ions transport.

This was indicated by the high level of transepithelial electrical resistance (low conductance) upon 24-h treatment of CFBE41o- and FRT epithelia with Esc(1–21) or its diastereomer Esc(1–21)-1c, meaning that cell junctions remain well tightened.

Many studies have disclosed that chemically modifed ATP analogs and small organic molecules like isofavones have good potentiator effect by enhancing CFTR channel gating. However, the expected unspecific binding of ATP analogs to other proteins involved in physiological functions limits their development to the clinic. Despite the current ivacaftor/lumacaftor combination therapy (Orkambi and more recently Trikafta from Vertex Pharmaceuticals) designed for CF patients with the genetic F508del mutation in homozygosity have a good efficacy (Almughem et al., 2020), treatment of lung pathology in CF would benefit from antimicrobial compounds with a repairing action of the lung epithelium in addition to a potentiation of CFTR activity.

All these activities are covered by Esc peptides and are of remarkable relevance, due to the occurrence of chronic infections in CF lungs and to the impaired re-epithelialization of airway wounds in CF patients (Trinh et al., 2012). Overall, these findings concur to emphasize Esc peptides as attractive novel agents for treatment of CF lung pathology, likely upon inhalation.

This work has provided the first evidence that AMPs, namely the Esc peptides, can affect the activity of F508del-CFTR likely upon direct interaction with NBD domains.

This feature has not been explored previously with any other AMP and highlights the potential of these peptides as pharmaceuticals for treatment of CF pulmonary disease by working not only as antibacterial agents, but also as promoters of airway epithelium wound repair and potentiators of mutated CFTR channel.

In summary, this thesis work has demonstrated (i) the capability of the membrane-active AMP Esc(1-21) to form membrane pores in bacterial-mimicking membranes; (ii) the ability of the diastereomer Esc(1-21)-1c (at its sub-MIC doses) to act as an adjuvant agent of traditional antibiotic by potentiating their effect in inhibiting the growth of *P. aeruginosa* cells, by decreasing the production of the mexAB-oprM efflux pump and (iii) the efficacy of Esc peptides in rescuing the function of CFTR with conductance defects, by likely interacting with the channel, at the same concentrations displaying an antibacterial and wound healing activities.

The existence of multiple features and mode(s) of action of AMPs will presumably offer the possibility of a new up-and-coming pharmacological approach to overcome AMR and to address serious microbial infections, such as those associated to *P. aeruginosa* in the lungs, especially of CF patients.

6. References

- **Abbatiello S.E, Mani D.R , Schilling B. et al.,** 'Design, Implementation and Multisite Evaluation of a System Suitability Protocol for the Quantitative Assessment of Instrument Performance in Liquid Chromatography-Multiple Reaction Monitoring-MS (LC-MRM-MS)', Molecular & Cellular Proteomics: MCP 12, no. 9 (2013): 2623–39, https://doi.org/10.1074/mcp.M112.027078.

- **Afacan N.J., Yeung T.Y., Pena O.M. and Hancock R.E.W.,** 'Therapeutic Potential of Host Defense Peptides in Antibiotic-Resistant Infections', *Current Pharmaceutical Design* 18, no. 6 (2012): 807–19, https://doi.org/10.2174/138161212799277617.

- **Ageitos J.M. Sánchez-Pérez A., Calo-Mata P. and Villa T.G.,** 'Antimicrobial Peptides (AMPs): Ancient Compounds That Represent Novel Weapons in the Fight against Bacteria', Biochemical Pharmacology 133(2017):117–38, https://doi.org/10.1016/j.bcp.2016.09.018.

- **Akram F., Memoona I. and Haq I.ul.,** 'Emergent Crisis of Antibiotic Resistance: A Silent Pandemic Threat to 21st Century', *Microbial Pathogenesis* 174 (2023): 105923, https://doi.org/10.1016/j.micpath.2022.105923.

- **Alba A., López-Abarrategui C. and Otero-Gonzálezst A.J.,** 'Defense Peptides: An Alternative as Antiinfective and

Immunomodulatory Therapeutics', *Biopolymers* 98, no. 4 (2012): 251–67, https://doi.org/10.1002/bip.22076.

- **Almughem F.A., Aldossary A.M., Tawfik E.A. et al.,** 'Cystic Fibrosis: Overview of the Current Development Trends and Innovative Therapeutic Strategies', *Pharmaceutics* 12, no. 7 (2020): 616, https://doi.org/10.3390/pharmaceutics12070616.

- **Ando T., Uchihashi T. and Scheuring S.,** 'Filming Biomolecular Processes by High-Speed Atomic Force Microscopy', *Chemical Reviews* 114, no. 6 (2014): 3120–88, https://doi.org/10.1021/cr4003837.

- **Baker N.A., Sept D., Simpson J., Holst M.J. and McCammonet J.A.,** 'Electrostatics of Nanosystems: Application to Microtubules and the Ribosome', *Proceedings of the National Academy of Sciences of the United States of America* 98, no. 18 (2001): 10037–41, https://doi.org/10.1073/pnas.181342398.

- **Bals R.,** '[Antimicrobial peptides and pe ptide antibiotics]', *Medizinische Klinik (Munich, Germany: 1983)* 95, no. 9 (15 September 2000): 496–502, https://doi.org/10.1007/pl00002139.

- **Baltimore R.S., Christie C.D.C. and Smith G.J.W.,** 'Immunohistopathologic Localization of Pseudomonas Aeruginosa in Lungs from Patients with Cystic Fibrosis. Implications for the Pathogenesis of Progressive Lung Deterioration', *The American*

Review of Respiratory Disease 140, no. 6 (1989): 1650–61, https://doi.org/10.1164/ajrccm/140.6.1650.

- **Boman H.G.,** 'Peptide Antibiotics and Their Role in Innate Immunity', *Annual Review of Immunology* 13 (1995): 61–92, https://doi.org/10.1146/annurev.iy.13.040195.000425.

- **Brogden K.M.,** 'Antimicrobial Peptides: Pore Formers or Metabolic Inhibitors in Bacteria?', *Nature Reviews. Microbiology* 3, no. 3 (March 2005): 238–50, https://doi.org/10.1038/nrmicro1098.

- **Camus L., Vandenesch F. and Moreau1 K.,** 'From Genotype to Phenotype: Adaptations of Pseudomonas Aeruginosa to the Cystic Fibrosis Environment', *Microbial Genomics* 7, no. 3 (2021): mgen000513, https://doi.org/10.1099/mgen.0.000513.

- **Cappiello F., Di Grazia A., Segev-Zarko L. et. al.,** 'Esculentin-1a-Derived Peptides Promote Clearance of Pseudomonas Aeruginosa Internalized in Bronchial Cells of Cystic Fibrosis Patients and Lung Cell Migration: Biochemical Properties and a Plausible Mode of Action', *Antimicrobial Agents and Chemotherapy* 60, no. 12 (2016): 7252–62, https://doi.org/10.1128/AAC.00904-16.

- **Casciaro B., Cappiello F., Loffredo M.R., Ghirga F. and Mangoni M.L.,** 'The Potential of Frog Skin Peptides for Anti-Infective Therapies: The Case of Esculentin-1a(1-21)NH2', *Current Medicinal*

Chemistry 27, no. 9 (2020): 1405–19, https://doi.org/10.2174/0929867326666190722095408.

- **Casciaro B., Cappiello F., Verrusio W., Cacciafesta M. and Mangoni M.L.,** 'Antimicrobial Peptides and Their Multiple Effects at Sub-Inhibitory Concentrations', *Current Topics in Medicinal Chemistry* 20, no. 14 (2020): 1264–73, https://doi.org/10.2174/1568026620666200427090912.

- **Casciaro B., Loffredo M.R., Luca V., Verrusio W., Cacciafesta M. and Mangoni M.L.,** 'Esculentin-1a Derived Antipseudomonal Peptides: Limited Induction of Resistance and Synergy with Aztreonam', *Protein and Peptide Letters* 25, no. 12 (2018): 1155–62, https://doi.org/10.2174/0929866525666181101104649.

- **Case D.A.,** AMBER 2018 University of California, San Francisco. https://ambermd.org/doc12/Amber18.pdf

- **Chen L.F., Chopra T. and Kaye K.S.,** 'Pathogens Resistant to Antibacterial Agents', *The Medical Clinics of North America* 95, no. 4 (2011): 647–76, vii, https://doi.org/10.1016/j.mcna.2011.03.005.

- **Cheng S.H., Gregory R.J., Marshall J. et al.,** 'Defective Intracellular Transport and Processing of CFTR Is the Molecular Basis of Most Cystic Fibrosis', *Cell* 63, no. 4 (1990): 827–34, https://doi.org/10.1016/0092-8674(90)90148-8.

- **Chileveru H.R., Lim S.A., Chairatana P. et al.,** 'Visualizing Attack of Escherichia Coli by the Antimicrobial Peptide Human Defensin 5', Biochemistry 54, no. 9 (2015): 1767–77, https://doi.org/10.1021/bi501483q.

- **Cho N.J., Frank C.W., Kasemo B. and Höök F.,** 'Quartz Crystal Microbalance with Dissipation Monitoring of Supported Lipid Bilayers on Various Substrates', *Nature Protocols* 5, no. 6 (2010): 1096–1106, https://doi.org/10.1038/nprot.2010.65.

- **Conlon J.M.**, 'Reflections on a Systematic Nomenclature for Antimicrobial Peptides from the Skins of Frogs of the Family Ranidae', Peptides 29, no. 10 (October 2008): 1815–19, https://doi.org/10.1016/j.peptides.2008.05.029.

- **Conlon J.M., Kolodziejek J., Nowotny N. et. al.,** 'Antimicrobial Peptides from Ranid Frogs: Taxonomic and Phylogenetic Markers and a Potential Source of New Therapeutic Agents', *Biochimica Et Biophysica Acta* 1696, no. 1 (2004): 1–14, https://doi.org/10.1016/j.bbapap.2003.09.004.

- **Dalemans W., Barbryt P., Champignyt G. et al.,** 'Altered Chloride Ion Channel Kinetics Associated with the Delta F508 Cystic Fibrosis Mutation', *Nature* 354, no. 6354 (1991): 526–28, https://doi.org/10.1038/354526a0.

- **Davies J.C., Moskowitz S.M., Brown C. et al.,** 'VX-659-Tezacaftor-Ivacaftor in Patients with Cystic Fibrosis and One or Two Phe508del Alleles', *The New England Journal of Medicine* 379, no. 17 (2018): 1599–1611,https://doi.org/10.1056/NEJMoa1807119.

- **Davidson D.J.,** 'The Cationic Antimicrobial Peptide LL-37 Modulates Dendritic Cell Differentiation and Dendritic Cell-Induced T Cell Polarization', *Journal of Immunology (Baltimore, Md.: 1950)* 172, no. 2 (2004): 1146–56, https://doi.org/10.4049/jimmunol.172.2.1146.

- **Denning G.M., Anderson M.P., Amaraet J.F. et al.,** 'Processing of Mutant Cystic Fibrosis Transmembrane Conductance Regulator Is Temperature-Sensitive', *Nature* 358, no. 6389 (1992): 761–64, https://doi.org/10.1038/358761a0.

- **Di Grazia A., Cappiello F., Cohen H. et al.,** 'D-Amino Acids Incorporation in the Frog Skin-Derived Peptide Esculentin-1a(1-21)NH2 Is Beneficial for Its Multiple Functions', *Amino Acids* 47, no. 12 (2015): 2505–19, https://doi.org/10.1007/s00726-015-2041-y.

- **Di Somma A., Cané C., Moretta A. et al.,** 'The Antimicrobial Peptide Magainin-2 Interacts with BamA Impairing Folding of E. Coli Membrane Proteins', *Frontiers in Chemistry* 10 (2022): 1013788, https://doi.org/10.3389/fchem.2022.1013788.

- **Ding F., Lee K.J., Vahedi-Faridi A. et al.,** 'Design and Study of the Efflux Function of the EGFP Fused MexAB-OprM Membrane

Transporter in Pseudomonas Aeruginosa Using Fluorescence Spectroscopy', *The Analyst* 139, no. 12 (2014): 3088–96, https://doi.org/10.1039/c4an00108g.

- **Ehrenstein G. and Lecar H.,** 'Electrically Gated Ionic Channels in Lipid Bilayers', *Quarterly Reviews of Biophysics* 10, no. 1 (1977): 1–34, https://doi.org/10.1017/s0033583500000123.
  3 (1975): 754–60, https://doi.org/10.1152/ajplegacy.1975.229.3.754.

- **El-Mowafi S.A., Sineva E., Alumasa J. N. et al.,** 'Identification of Inhibitors of a Bacterial Sigma Factor Using a New High-Throughput Screening Assay', *Antimicrobial Agents and Chemotherapy* 59, no. 1 (2015): 193–205, https://doi.org/10.1128/AAC.03979-14.

- **Elborn J.S., Ramsey B.W., Boyle M.P. et al.,** 'Efficacy and Safety of Lumacaftor/Ivacaftor Combination Therapy in Patients with Cystic Fibrosis Homozygous for Phe508del CFTR by Pulmonary Function Subgroup: A Pooled Analysis', *The Lancet. Respiratory Medicine* 4, no. 8 (2016): 617–26, https://doi.org/10.1016/S2213-2600(16)30121-7.

- **Ensinck M.M. and Carlon M.S.,** 'One Size Does Not Fit All: The Past, Present and Future of Cystic Fibrosis Causal Therapies', *Cells* 11, no. 12 (2022): 1868, https://doi.org/10.3390/cells11121868.

- **Ferrera L., Cappiello F., Loffredo M.R., Puglisi E. et al.,** 'Esc Peptides as Novel Potentiators of Defective Cystic Fibrosis

Transmembrane Conductance Regulator: An Unprecedented Property of Antimicrobial Peptides', *Cellular and Molecular Life Sciences: CMLS* 79, no. 1 (2021): 67, https://doi.org/10.1007/s00018-021-04030-2.

- **Fjell C.D., Hiss J.A., Hancock1 R.E.W. and Schneider G.,** 'Designing Antimicrobial Peptides: Form Follows Function', *Nature Reviews. Drug Discovery* 11, no. 1 (2011): 37–51, https://doi.org/10.1038/nrd3591.

- **Flemming H.C., Wingender J., Szewzyk U. et al.,** 'Biofilms: An Emergent Form of Bacterial Life', *Nature Reviews. Microbiology* 14, no. 9 (2016): 563–75, https://doi.org/10.1038/nrmicro.2016.94.

- **Florin T., Maracci C., Graf M. et al.,** 'An Antimicrobial Peptide That Inhibits Translation by Trapping Release Factors on the Ribosome', *Nature Structural & Molecular Biology* 24, no. 9 (2017): 752–57, https://doi.org/10.1038/nsmb.3439.

- **Founou R.C., Founou L.L., Essacket S.Y. et. al.,** 'Clinical and Economic Impact of Antibiotic Resistance in Developing Countries: A Systematic Review and Meta-Analysis', *PloS One* 12, no. 12 (2017): e0189621, https://doi.org/10.1371/journal.pone.0189621.

- **Friedrich C.L., Rozek A., Patrzykat A. and Hancock R.E.W.,** 'Structure and Mechanism of Action of an Indolicidin Peptide Derivative with Improved Activity against Gram-Positive Bacteria',

The Journal of Biological Chemistry 276, no. 26 (2001): 24015–22, https://doi.org/10.1074/jbc.M009691200.

- **Gadsby D.C., Vergani P. and Csanády L.,** 'The ABC Protein Turned Chloride Channel Whose Failure Causes Cystic Fibrosis', *Nature* 440, no. 7083 (2006): 477–83, https://doi.org/10.1038/nature04712.

- **Gamberi T., Cavalieri D., Magherini F. et al.,** 'An Integrated Analysis of the Effects of Esculentin 1-21 on Saccharomyces Cerevisiae', *Biochimica Et Biophysica Acta* 1774, no. 6 (2007): 688–700, https://doi.org/10.1016/j.bbapap.2007.04.006.

- **Ganz T.,** 'Defensins: Antimicrobial Peptides of Innate Immunity', *Nature Reviews. Immunology* 3, no. 9 (September 2003): 710–20, https://doi.org/10.1038/nri1180.

- **Gaspar D., Salomé Veiga A. and Castanhoet Miguel A. R. B.,** 'From Antimicrobial to Anticancer Peptides. A Review', *Frontiers in Microbiology* 4 (2013): 294, https://doi.org/10.3389/fmicb.2013.00294.

- **Gellatly S.L., Hancock R.E.W. et al.,** 'Pseudomonas Aeruginosa: New Insights into Pathogenesis and Host Defenses', *Pathogens and Disease* 67, no. 3 (2013): 159–73, https://doi.org/10.1111/2049-632X.12033.

- **Ghosh A., Bera S., Shai Y., Mangoni M.L. and Bhunia A.,** 'NMR Structure and Binding of Esculentin-1a (1-21)NH2 and Its Diastereomer to Lipopolysaccharide: Correlation with Biological Functions', *Biochimica Et Biophysica Acta* 1858, no. 4 (2016): 800–812, https://doi.org/10.1016/j.bbamem.2015.12.027.

- **Gottschalk L.B., Vecchio-Pagan B., Sharmaet N. et. al.,** 'Creation and Characterization of an Airway Epithelial Cell Line for Stable Expression of CFTR Variants', *Journal of Cystic Fibrosis: Official Journal of the European Cystic Fibrosis Society* 15, no. 3 (2016): 285–94, https://doi.org/10.1016/j.jcf.2015.11.010.

- **Grage S.L., Afonin S., Kara S. et al.,** 'Membrane Thinning and Thickening Induced by Membrane-Active Amphipathic Peptides', *Frontiers in Cell and Developmental Biology* 4 (2016): 65, https://doi.org/10.3389/fcell.2016.00065.

- **Grieco P., Carotenuto A., Auriemma L. et al.,** 'Novel α-MSH Peptide Analogues with Broad Spectrum Antimicrobial Activity', *PloS One* 8, no. 4 (2013): e61614, https://doi.org/10.1371/journal.pone.0061614.

- **Habboush Y. and Guzman N.,** 'Antibiotic Resistance', in *StatPearls* (Treasure Island (FL): StatPearls Publishing, 2023), http://www.ncbi.nlm.nih.gov/books/NBK513277/.

- **Hammond K., Ryadnov M.G. and Hoogenboomet B.W.,** 'Atomic Force Microscopy to Elucidate How Peptides Disrupt Membranes', *Biochimica Et Biophysica Acta. Biomembranes* 1863, no. 1 (2021): 183447, https://doi.org/10.1016/j.bbamem.2020.183447.

- **Hamosh A., Trapnell B.C., Zeitlin P.L. et al.,** 'Severe Deficiency of Cystic Fibrosis Transmembrane Conductance Regulator Messenger RNA Carrying Nonsense Mutations R553X and W1316X in Respiratory Epithelial Cells of Patients with Cystic Fibrosis', *The Journal of Clinical Investigation* 88, no. 6 (1991): 1880–85, https://doi.org/10.1172/JCI115510.

- **Hancock R.E.W. and Sahl H-G.,** 'Antimicrobial and Host-Defense Peptides as New Anti-Infective Therapeutic Strategies', *Nature Biotechnology* 24, no. 12 (2006): 1551–57, https://doi.org/10.1038/nbt1267.

- **Hancock R.E.W.,** 'Peptide Antibiotics', *Lancet (London, England)* 349, no. 9049 (1997): 418–22, https://doi.org/10.1016/S0140-6736(97)80051-7.

- **Ho Y.H., Shah P., Chen Y-W and Chene C-S.,** 'Systematic Analysis of Intracellular-Targeting Antimicrobial Peptides, Bactenecin 7, Hybrid of Pleurocidin and Dermaseptin, Proline-Arginine-Rich Peptide, and Lactoferricin B, by Using Escherichia Coli Proteome Microarrays', Molecular & Cellular Proteomics: MCP 15, no. 6 (2016): 1837–47, https://doi.org/10.1074/mcp.M115.054999.

- **Huan Y., Kong Q., Mou H. and YietH.,** 'Antimicrobial Peptides: Classification, Design, Application and Research Progress in Multiple Fields', *Frontiers in Microbiology* 11 (2020): 582779, https://doi.org/10.3389/fmicb.2020.582779.

- **Illiano A., Pinto G., Gaglione R. et al.,** 'Inflammation Protein Quantification by Multiple Reaction Monitoring Mass Spectrometry in Lipopolysaccharide-Stimulated THP-1 Cells', *Rapid Communications in Mass Spectrometry: RCM* 35, no. 20 (2021): e9166, https://doi.org/10.1002/rcm.9166.

- **Islas-Rodrìguez A.E., Marcellini L., Orioni B. et al.,** 'Esculentin 1-21: A Linear Antimicrobial Peptide from Frog Skin with Inhibitory Effect on Bovine Mastitis-Causing Bacteria', *Journal of Peptide Science: An Official Publication of the European Peptide Society* 15, no. 9 (2009): 607–14, https://doi.org/10.1002/psc.1148.

- **Jacquot J., Puchelle E., Hinnrasky J. et al.,** 'Localization of the Cystic Fibrosis Transmembrane Conductance Regulator in Airway Secretory Glands', *The European Respiratory Journal* 6, no. 2 (1993): 169–76.

- **Keating D., Moskowitz S.M., Brown C. et al.,** 'VX-445-Tezacaftor-Ivacaftor in Patients with Cystic Fibrosis and One or Two Phe508del Alleles', *The New England Journal of Medicine* 379, no. 17 (2018): 1612–20, https://doi.org/10.1056/NEJMoa1807120.

- **Kirichok Y. and Lishko P.V.,** 'Rediscovering Sperm Ion Channels with the Patch-Clamp Technique', Molecular Human Reproduction 17, no. 8 (2011): 478–99, https://doi.org/10.1093/molehr/gar044.

- **Klein T., Eckhard U., Dufour A. et al.,** 'Proteolytic Cleavage—Mechanisms, Function, and "Omic" Approaches for a Near-Ubiquitous Posttranslational Modification', *Chemical Reviews* 118, no. 3 (2018): 1137–68, https://doi.org/10.1021/acs.chemrev.7b00120.

- **Klockgether J. and Tümmleret B.,** 'Recent Advances in Understanding Pseudomonas Aeruginosa as a Pathogen', *F1000Research* 6 (2017): 1261, https://doi.org/10.12688/f1000research.10506.1.

- **Kolar S.S.N., Luca V., Baidouri H. et al.,** 'Esculentin-1a(1-21)NH2: A Frog Skin-Derived Peptide for Microbial Keratitis', *Cellular and Molecular Life Sciences: CMLS* 72, no. 3 (2015): 617–27, https://doi.org/10.1007/s00018-014-1694-0.

- **Kraus D. and Peschel A.,** 'Molecular Mechanisms of Bacterial Resistance to Antimicrobial Peptides', *Current Topics in Microbiology and Immunology* 306 (2006): 231–50, https://doi.org/10.1007/3-540-29916-5_9.

- **Kreft M.E., Jerman U.D., Lasič E. et al.,** 'The Characterization of the Human Cell Line Calu-3 under Different Culture Conditions and

Its Use as an Optimized in Vitro Model to Investigate Bronchial Epithelial Function', *European Journal of Pharmaceutical Sciences: Official Journal of the European Federation for Pharmaceutical Sciences* 69 (2015): 1–9, https://doi.org/10.1016/j.ejps.2014.12.017.

- **Ladram and Nicolas P.,** 'Antimicrobial Peptides from Frog Skin: Biodiversity and Therapeutic Promises', *Frontiers in Bioscience (Landmark Edition)* 21, no. 7 (2016): 1341–71, https://doi.org/10.2741/4461.

- **La Plante K.L., Dhand A., Wright K. and Lauterio M.,** 'Re-Establishing the Utility of Tetracycline-Class Antibiotics for Current Challenges with Antibiotic Resistance', *Annals of Medicine* 54, no. 1 (2022): 1686–1700, https://doi.org/10.1080/07853890.2022.2085881.

- **Lai Y. and Gallo R.L.,** 'AMPed up Immunity: How Antimicrobial Peptides Have Multiple Roles in Immune Defense', *Trends in Immunology* 30, no. 3 (2009): 131–41, https://doi.org/10.1016/j.it.2008.12.003.

- **Lei J., Sun L., Huang S. et al.,** 'The Antimicrobial Peptides and Their Potential Clinical Applications', *American Journal of Translational Research* 11, no. 7 (2019): 3919–31.

- **Letizia M., Mellini M., Fortuna A. et al.,** 'PqsE Expands and Differentially Modulates the RhlR Quorum Sensing Regulon in

Pseudomonas Aeruginosa', *Microbiology Spectrum* 10, no. 3 (2022): e0096122, https://doi.org/10.1128/spectrum.00961-22.

- **Lin J., Deslouches B., Montelaro R.C., Di Y.P. et al.,** 'Prevention of ESKAPE Pathogen Biofilm Formation by Antimicrobial Peptides WLBU2 and LL37', *International Journal of Antimicrobial Agents* 52, no. 5 (2018): 667–72, https://doi.org/10.1016/j.ijantimicag.2018.04.019.

- **Lobanovska M. and Pilla G.,** 'Penicillin's Discovery and Antibiotic Resistance: Lessons for the Future?', *The Yale Journal of Biology and Medicine* 90, no. 1 (2017): 135–45.

- **Loffredo M.R., GhoshA., Harmouche N. et al.,** 'Membrane Perturbing Activities and Structural Properties of the Frog-Skin Derived Peptide Esculentin-1a(1-21)NH2 and Its Diastereomer Esc(1-21)-1c: Correlation with Their Antipseudomonal and Cytotoxic Activity', *Biochimica Et Biophysica Acta. Biomembranes* 1859, no. 12 (2017): 2327–39, https://doi.org/10.1016/j.bbamem.2017.09.009.

- **Lopes B.S., Hanafiah A., Nachimuthuet R. et. al.,** 'The Role of Antimicrobial Peptides as Antimicrobial and Antibiofilm Agents in Tackling the Silent Pandemic of Antimicrobial Resistance', *Molecules (Basel, Switzerland)* 27, no. 9 (2022): 2995, https://doi.org/10.3390/molecules27092995.

- **Luca V., Stringaro A., Colone M. et al.,** 'Esculentin(1-21), an Amphibian Skin Membrane-Active Peptide with Potent Activity on Both Planktonic and Biofilm Cells of the Bacterial Pathogen Pseudomonas Aeruginosa', *Cellular and Molecular Life Sciences: CMLS* 70, no. 15 (2013): 2773–86, https://doi.org/10.1007/s00018-013-1291-7.

- **Ludtke S.J., He K., Heller W.T. et al.,** 'Membrane Pores Induced by Magainin', *Biochemistry* 35, no. 43 (1996): 13723–28, https://doi.org/10.1021/bi9620621.

- **Ma B., Niu C., Zhou Y. et al.,** 'The Disulfide Bond of the Peptide Thanatin Is Dispensible for Its Antimicrobial Activity In Vivo and In Vitro', *Antimicrobial Agents and Chemotherapy* 60, no. 7 (2016): 4283–89, https://doi.org/10.1128/AAC.00041-16.

- **Ma B., Lustig M., Salem M. et al.,** 'MexAB-OprM Efflux Pump Interaction with the Peptidoglycan of Escherichia Coli and Pseudomonas Aeruginosa', *International Journal of Molecular Sciences* 22, no. 10 (2021): 5328, https://doi.org/10.3390/ijms22105328.

- **Madani F., Lindberg S., Langel U. et al.,** 'Mechanisms of Cellular Uptake of Cell-Penetrating Peptides', *Journal of Biophysics (Hindawi Publishing Corporation: Online)* (2011): 414729, https://doi.org/10.1155/2011/414729.

- **Mahlapuu M., Björn C., Ekblomet J. et al.,** 'Antimicrobial Peptides as Therapeutic Agents: Opportunities and Challenges', *Critical Reviews in Biotechnology* 40, no. 7 (2020): 978–92, https://doi.org/10.1080/07388551.2020.1796576.

- **Mangoni M.L., Fiocco D., Mignogna G. et al.,** 'Functional Characterisation of the 1-18 Fragment of Esculentin-1b, an Antimicrobial Peptide from Rana Esculenta', *Peptides* 24, no. 11 (2003): 1771–77, https://doi.org/10.1016/j.peptides.2003.07.029.

- **Mangoni M.L.,** 'Host-Defense Peptides: From Biology to Therapeutic Strategies', *Cellular and Molecular Life Sciences: CMLS* 68, no. 13 (2011): 2157–59, https://doi.org/10.1007/s00018-011-0709-3.

- **Mangoni M.L., Luca V. and McDermott A.M.,** 'Fighting Microbial Infections: A Lesson from Amphibian Skin-Derived Esculentin-1 Peptides', *Peptides* 71 (2015): 286–95, https://doi.org/10.1016/j.peptides.2015.04.018.

- **Mangoni M. L., Papo N., Saugar J.M. et. al.,** 'Effect of Natural L- to D-Amino Acid Conversion on the Organization, Membrane Binding, and Biological Function of the Antimicrobial Peptides Bombinins H', *Biochemistry* 45, no. 13 (2006): 4266–76, https://doi.org/10.1021/bi052150y.

- **Matsuzaki K., Murase O. and Miyajimaet K.,** 'Kinetics of Pore Formation by an Antimicrobial Peptide, Magainin 2, in Phospholipid Bilayers', *Biochemistry* 34, no. 39 (1995): 12553–59, https://doi.org/10.1021/bi00039a009.

- **Mingeot-Leclercq M.P., Deleu M., Brasseur R. and Dufrêne Y.F.,** 'Atomic Force Microscopy of Supported Lipid Bilayers', *Nature Protocols* 3, no. 10 (2008): 1654–59, https://doi.org/10.1038/nprot.2008.149.

- **Mojsoska B. and Jenssen H.,** 'Peptides and Peptidomimetics for Antimicrobial Drug Design', *Pharmaceuticals (Basel, Switzerland)* 8, no. 3 (2015): 366–415, https://doi.org/10.3390/ph8030366.

- **Mookherjee N. and Hancock R. E. W.**, 'Cationic Host Defence Peptides: Innate Immune Regulatory Peptides as a Novel Approach for Treating Infections', *Cellular and Molecular Life Sciences: CMLS* 64, no. 7–8 (2007): 922–33, https://doi.org/10.1007/s00018-007-6475-6.

- **Moran O. and Galietta L. J.V.,** 'Binding Site of Activators of the Cystic Fibrosis Transmembrane Conductance Regulator in the Nucleotide Binding Domains', *Cellular and Molecular Life Sciences: CMLS* 62, no. 4 (2005): 446–60, https://doi.org/10.1007/s00018-004-4422-3.

- **Morandat S., Azouzi S., Beauvais E. et al.,** 'Atomic Force Microscopy of Model Lipid Membranes', *Analytical and Bioanalytical*

Chemistry 405, no. 5 (2013): 1445–61, https://doi.org/10.1007/s00216-012-6383-y.

- **Morita Y., Tomida J. and Kawamura Y.,** 'Responses of Pseudomonas Aeruginosa to Antimicrobials', *Frontiers in Microbiology* 4 (2014), https://doi.org/10.3389/fmicb.2013.00422.

- **Morikawa N., Hagiwara K. and Nakajima T.,** 'Brevinin-1 and -2, Unique Antimicrobial Peptides from the Skin of the Frog, Rana Brevipoda Porsa', *Biochemical and Biophysical Research Communications* 189, no. 1 (1992): 184–90, https://doi.org/10.1016/0006-291x(92)91542-x.

- **Mulani M.S., Kamble E.E., Kumkar S.N. et al.,** 'Emerging Strategies to Combat ESKAPE Pathogens in the Era of Antimicrobial Resistance: A Review', *Frontiers in Microbiology* 10 (2019): 539, https://doi.org/10.3389/fmicb.2019.00539.

- **Nguyen L.T., Haney E.F. and Vogel H.J.,** 'The Expanding Scope of Antimicrobial Peptide Structures and Their Modes of Action', *Trends in Biotechnology* 29, no. 9 (2011): 464–72, https://doi.org/10.1016/j.tibtech.2011.05.001.

- **Nicolas P. and El Amriet C.,** 'The Dermaseptin Superfamily: A Gene-Based Combinatorial Library of Antimicrobial Peptides',

Biochimica Et Biophysica Acta 1788, no. 8 (2009): 1537–50, https://doi.org/10.1016/j.bbamem.2008.09.006.

- **Nordström R. and Malmsten M.,** 'Delivery Systems for Antimicrobial Peptides', *Advances in Colloid and Interface Science* 242 (2017): 17–34, https://doi.org/10.1016/j.cis.2017.01.005.

- **Odolczyk N., Fritsch J., Norez C. et al.,** 'Discovery of Novel Potent ΔF508-CFTR Correctors That Target the Nucleotide Binding Domain', *EMBO Molecular Medicine* 5, no. 10 (2013): 1484–1501, https://doi.org/10.1002/emmm.201302699.

- **Parchebafi A., Tamanaee1 F., Ehteram H. et al.,** 'The Dual Interaction of Antimicrobial Peptides on Bacteria and Cancer Cells; Mechanism of Action and Therapeutic Strategies of Nanostructures', *Microbial Cell Factories* 21, no. 1 (2022): 118, https://doi.org/10.1186/s12934-022-01848-8.

- **Patrzykat A., Friedrich C.L., Zhang L. et al.,** 'Sublethal Concentrations of Pleurocidin-Derived Antimicrobial Peptides Inhibit Macromolecular Synthesis in Escherichia Coli', *Antimicrobial Agents and Chemotherapy* 46, no. 3 (2002): 605–14, https://doi.org/10.1128/AAC.46.3.605-614.2002.

- **Pauter K., Friedrich C.L., Zhang L. et al.,** 'Determination and Identification of Antibiotic Drugs and Bacterial Strains in Biological

Samples', *Molecules (Basel, Switzerland)* 25, no. 11 (2020): 2556, https://doi.org/10.3390/molecules25112556.

- **Pedemonte N., Sonawane N.D., Taddei A. et al.,** 'Phenylglycine and Sulfonamide Correctors of Defective Delta F508 and G551D Cystic Fibrosis Transmembrane Conductance Regulator Chloride-Channel Gating', *Molecular Pharmacology* 67, no. 5 (2005a): 1797–1807, https://doi.org/10.1124/mol.105.010959.

- **Pedemonte N. Tulli D., Caci E. et al.,** 'Antihypertensive 1,4-Dihydropyridines as Correctors of the Cystic Fibrosis Transmembrane Conductance Regulator Channel Gating Defect Caused by Cystic Fibrosis Mutations', *Molecular Pharmacology* 68, no. 6 (2005b): 1736–46, https://doi.org/10.1124/mol.105.015149.

- **Pedemonte N., Lukacs G.L., Du K. et al.,** 'Small-Molecule Correctors of Defective DeltaF508-CFTR Cellular Processing Identified by High-Throughput Screening', *The Journal of Clinical Investigation* 115, no. 9 (2005c): 2564–71, https://doi.org/10.1172/JCI24898.

- **Pedemonte N., Boido D., Moran O. et al.,** 'Structure-Activity Relationship of 1,4-Dihydropyridines as Potentiators of the Cystic Fibrosis Transmembrane Conductance Regulator Chloride Channel', *Molecular Pharmacology* 72, no. 1 (2007): 197–207, https://doi.org/10.1124/mol.107.034702.

- **Pike L.J, Han X. and Grosset R.W.,** 'Epidermal Growth Factor Receptors Are Localized to Lipid Rafts That Contain a Balance of Inner and Outer Leaflet Lipids: A Shotgun Lipidomics Study', *The Journal of Biological Chemistry* 280, no. 29 (2005): 26796–804, https://doi.org/10.1074/jbc.M503805200.

- **Ponti D., Mignogna G., Mangoni M.L. et al.,** 'Expression and Activity of Cyclic and Linear Analogues of Esculentin-1, an Anti-Microbial Peptide from Amphibian Skin', *European Journal of Biochemistry* 263, no. 3 (1999): 921–27, https://doi.org/10.1046/j.1432-1327.1999.00597.x.

- **Pouny Y., Rapaport D., Mor A. et al.,** 'Interaction of Antimicrobial Dermaseptin and Its Fluorescently Labeled Analogues with Phospholipid Membranes', *Biochemistry* 31, no. 49 (1992): 12416–23, https://doi.org/10.1021/bi00164a017.

- **Powers J.S.P. and Hancock R.E.W. et al.,** 'The Relationship between Peptide Structure and Antibacterial Activity', *Peptides* 24, no. 11 (2003): 1681–91, https://doi.org/10.1016/j.peptides.2003.08.023.

- **Ramsey B., Davies J., McElvaney N. G. et al.,** 'A CFTR Potentiator in Patients with Cystic Fibrosis and the G551D Mutation', *The New England Journal of Medicine* 365, no. 18 (2011): 1663–72, https://doi.org/10.1056/NEJMoa1105185.

- **Raut B., Chen L.J., Hori T. and Kajiet H.,** 'An Open-Source Add-On EVOM® Device for Real-Time Transepithelial/Endothelial Electrical Resistance Measurements in Multiple Transwell Samples', *Micromachines* 12, no. 3 (2021): 282, https://doi.org/10.3390/mi12030282.

- **Rinaldi A.C., Mangoni M.L., Rufo A. et al.,** 'Temporin L: Antimicrobial, Haemolytic and Cytotoxic Activities, and Effects on Membrane Permeabilization in Lipid Vesicles', *The Biochemical Journal* 368, no. Pt 1 (2002): 91–100, https://doi.org/10.1042/BJ20020806.

- **Rodrigo-Troyano A. and Sibila O.,** 'The Respiratory Threat Posed by Multidrug Resistant Gram-Negative Bacteria', *Respirology (Carlton, Vic.)* 22, no. 7 (2017): 1288–99, https://doi.org/10.1111/resp.13115.

- **Roe D.R. and Cheathamet T.E.,** 'PTRAJ and CPPTRAJ: Software for Processing and Analysis of Molecular Dynamics Trajectory Data', *Journal of Chemical Theory and Computation* 9, no. 7 (2013): 3084–95, https://doi.org/10.1021/ct400341p.

- **Ruekit S., Srijan A., Serichantalergs O. et. al.,** 'Molecular Characterization of Multidrug-Resistant ESKAPEE Pathogens from Clinical Samples in Chonburi, Thailand (2017-2018)', *BMC Infectious Diseases* 22, no. 1 (2022): 695, https://doi.org/10.1186/s12879-022-07678-8.

- **Ruiz-Garbajosa P. and Cantòn R.,** 'Epidemiology of Antibiotic Resistance in Pseudomonas Aeruginosa. Implications for Empiric and Definitive Therapy', *Revista Espanola De Quimioterapia: Publicacion Oficial De La Sociedad Espanola De Quimioterapia* 30 Suppl 1 (2017): 8–12.

- **Salomón R.A. and Farias R. N.,** 'Microcin 25, a Novel Antimicrobial Peptide Produced by Escherichia Coli', Journal of Bacteriology 174, no. 22 (1992): 7428–35, https://doi.org/10.1128/jb.174.22.7428-7435.1992.

- **Salomon-Ferrer R., Case D.A. and Walker R.C.,** 'An Overview of the Amber Biomolecular Simulation Package', *WIREs Computational Molecular Science* 3, no. 2 (2013): 198–210, https://doi.org/10.1002/wcms.1121.

- **Santajit S. and Indrawattana N.,** 'Mechanisms of Antimicrobial Resistance in ESKAPE Pathogens', *BioMed Research International* 2016 (2016): 2475067, https://doi.org/10.1155/2016/2475067.

- **Sarkar T., Chetia M. and Chatterjeeet S.** 'Antimicrobial Peptides and Proteins: From Nature's Reservoir to the Laboratory and Beyond', *Frontiers in Chemistry* 9 (2021): 691532, https://doi.org/10.3389/fchem.2021.691532.

- **Sato S., Ward C.L., Krose M.E. et al.,** 'Glycerol Reverses the Misfolding Phenotype of the Most Common Cystic Fibrosis Mutation', *The Journal of Biological Chemistry* 271, no. 2 (1996): 635–38, https://doi.org/10.1074/jbc.271.2.635.

- **Schmieder R. and Edwards R.,** 'Insights into Antibiotic Resistance through Metagenomic Approaches', *Future Microbiology* 7, no. 1 (2012): 73–89, https://doi.org/10.2217/fmb.11.135.

- **Sengupta D., Leontiadou H., Mark A.E. and Marrinket S.J.,** 'Toroidal Pores Formed by Antimicrobial Peptides Show Significant Disorder', *Biochimica Et Biophysica Acta* 1778, no. 10 (2008): 2308–17, https://doi.org/10.1016/j.bbamem.2008.06.007.

- **Shai Y.,** 'Mechanism of the Binding, Insertion and Destabilization of Phospholipid Bilayer Membranes by Alpha-Helical Antimicrobial and Cell Non-Selective Membrane-Lytic Peptides', *Biochimica Et Biophysica Acta* 1462, no. 1–2 (1999): 55–70, https://doi.org/10.1016/s0005-2736(99)00200-x.

- **Shai Y.,** 'Mode of Action of Membrane Active Antimicrobial Peptides', *Biopolymers* 66, no. 4 (2002): 236–48, https://doi.org/10.1002/bip.10260.

- **Simmaco M., Mangoni M.L., Boman A., Barra D. and Boman H.G.,** 'Experimental Infections of Rana Esculenta with Aeromonas Hydrophila: A Molecular Mechanism for the Control of the Normal

Flora', *Scandinavian Journal of Immunology* 48, no. 4 (1998): 357–63, https://doi.org/10.1046/j.1365-3083.1998.00407.x.

- **Simmaco M., Mignogna G., Barra D. and Bossa F.,** 'Antimicrobial Peptides from Skin Secretions of Rana Esculenta. Molecular Cloning of cDNAs Encoding Esculentin and Brevinins and Isolation of New Active Peptides', *The Journal of Biological Chemistry* 269, no. 16 (1994): 11956–61.

- **Smith W.D., Bardin E., Cameron L. et al.,** 'Current and Future Therapies for Pseudomonas Aeruginosa Infection in Patients with Cystic Fibrosis', *FEMS Microbiology Letters* 364, no. 14 (2017), https://doi.org/10.1093/femsle/fnx121.

- **Taylor K., Barran P.E. and Dorinet J.R.,** 'Structure-Activity Relationships in Beta-Defensin Peptides', *Biopolymers* 90, no. 1 (2008): 1–7, https://doi.org/10.1002/bip.20900.

- **Sondo E., Tomati V., Caci E. et. al.,** 'Rescue of the Mutant CFTR Chloride Channel by Pharmacological Correctors and Low Temperature Analyzed by Gene Expression Profiling', *American Journal of Physiology. Cell Physiology* 301, no. 4 (2011): C872-885, https://doi.org/10.1152/ajpcell.00507.2010.

- **Sondo E., Falchi F., Caci E. et al.,** 'Pharmacological Inhibition of the Ubiquitin Ligase RNF5 Rescues F508del-CFTR in Cystic Fibrosis

Airway Epithelia', *Cell Chemical Biology* 25, no. 7 (2018): 891-905.e8, https://doi.org/10.1016/j.chembiol.2018.04.010.

- **Srinivasan A., Kolli A.R., Esch M.B. et al.,** 'TEER Measurement Techniques for in Vitro Barrier Model Systems', *Journal of Laboratory Automation* 20, no. 2 (2015): 107–26, https://doi.org/10.1177/2211068214561025.

- **Takahashi D., Shukla S.K., Prakash O. and Zhang G.,** 'Structural Determinants of Host Defense Peptides for Antimicrobial Activity and Target Cell Selectivity', *Biochimie* 92, no. 9 (2010): 1236–41, https://doi.org/10.1016/j.biochi.2010.02.023.

- **Trinh N.T.N., Bardou O., Prive´A. et al.,** 'Improvement of Defective Cystic Fibrosis Airway Epithelial Wound Repair after CFTR Rescue', *The European Respiratory Journal* 40, no. 6 (2012): 1390–1400, https://doi.org/10.1183/09031936.00221711.

- **Turner J., Cho Y., Dinh N.N. et al.,** 'Activities of LL-37, a Cathelin-Associated Antimicrobial Peptide of Human Neutrophils', *Antimicrobial Agents and Chemotherapy* 42, no. 9 (1998): 2206–14, https://doi.org/10.1128/AAC.42.9.2206.

- **van Eijk E., Wittekoek B., Kuijper E.J. and Smitset W.K.,** 'DNA Replication Proteins as Potential Targets for Antimicrobials in Drug-Resistant Bacterial Pathogens', *The Journal of Antimicrobial*

Chemotherapy 72, no. 5 (2017): 1275–84, https://doi.org/10.1093/jac/dkw548.

- **Vanzolini T., Bruschi M., Rinaldi A.C. et al.,** 'Multitalented Synthetic Antimicrobial Peptides and Their Antibacterial, Antifungal and Antiviral Mechanisms', *International Journal of Molecular Sciences* 23, no. 1 (2022): 545, https://doi.org/10.3390/ijms23010545.

- **Vergani P., Lockless S.W., Nairn A. C. and Gadsbyet D.C.,** 'CFTR Channel Opening by ATP-Driven Tight Dimerization of Its Nucleotide-Binding Domains', *Nature* 433, no. 7028 (2005): 876–80, https://doi.org/10.1038/nature03313.

- **Verkman A.S.,** 'Drug Discovery in Academia', *American Journal of Physiology. Cell Physiology* 286, no. 3 (March 2004): C465-474, https://doi.org/10.1152/ajpcell.00397.2003.

- **Wall S.,** 'Prevention of Antibiotic Resistance - an Epidemiological Scoping Review to Identify Research Categories and Knowledge Gaps', *Global Health Action* 12, no. 1 (13 December 2019): 1756191, https://doi.org/10.1080/16549716.2020.1756191.

- **Wang G., Li X. and Wang Z.,** 'APD3: The Antimicrobial Peptide Database as a Tool for Research and Education', *Nucleic Acids Research* 44, no. D1 (2016a): D1087-1093, https://doi.org/10.1093/nar/gkv1278.

- **Wang G., Zhang Y., Lee W-H. et. al.,** 'Novel Peptides from Skins of Amphibians Showed Broad-Spectrum Antimicrobial Activities', *Chemical Biology & Drug Design* 87, no. 3 (2016): 419–24, https://doi.org/10.1111/cbdd.12672.

- **Wang G.,** 'Post-Translational Modifications of Natural Antimicrobial Peptides and Strategies for Peptide Engineering', *Current Biotechnology* 1, no. 1 (February 2012): 72–79, https://doi.org/10.2174/2211550111201010072.

- **Wu W. K.K., Wong C.C.M., LI Z.J. et al.,** 'Cathelicidins in Inflammation and Tissue Repair: Potential Therapeutic Applications for Gastrointestinal Disorders', *Acta Pharmacologica Sinica* 31, no. 9 (2010): 1118–22, https://doi.org/10.1038/aps.2010.117.

- **Wu D.C., Chan W.W, Metelitsa A.I. et al.,** 'Pseudomonas Skin Infection: Clinical Features, Epidemiology, and Management', *American Journal of Clinical Dermatology* 12, no. 3 (2011): 157–69, https://doi.org/10.2165/11539770-000000000-00000.

- **Xu X., Yu H., Zhanget D. et. al.,** 'Role of ppGpp in Pseudomonas Aeruginosa Acute Pulmonary Infection and Virulence Regulation', *Microbiological Research* 192 (2016): 84–95, https://doi.org/10.1016/j.micres.2016.06.005.

- **Yeaman M.R. and Yount N.Y.,** 'Mechanisms of Antimicrobial Peptide Action and Resistance', *Pharmacological Reviews* 55, no. 1 (2003): 27–55, https://doi.org/10.1124/pr.55.1.2.

- **Zanetti M., Gennaro R., Skerlavaj B. et. al.,** 'Cathelicidin Peptides as Candidates for a Novel Class of Antimicrobials', *Current Pharmaceutical Design* 8, no. 9 (2002): 779–93, https://doi.org/10.2174/1381612023395457.

- **Zasloff M.,** 'Magainins, a Class of Antimicrobial Peptides from Xenopus Skin: Isolation, Characterization of Two Active Forms, and Partial cDNA Sequence of a Precursor', *Proceedings of the National Academy of Sciences of the United States of America* 84, no. 15 (1987): 5449–53, https://doi.org/10.1073/pnas.84.15.5449.

- **Zasloff M.,** 'Antimicrobial Peptides of Multicellular Organisms', *Nature* 415, no. 6870 (2002): 389–95, https://doi.org/10.1038/415389a.

- **Zhang Q.Y., Yan1 Z.B., Menget Y.M. et. al.**, 'Antimicrobial Peptides: Mechanism of Action, Activity and Clinical Potential', *Military Medical Research* 8, no. 1 (2021): 48, https://doi.org/10.1186/s40779-021-00343-2.

7. Acknowledgments

I would like to express my sincere thanks to my tutor Prof. Maria Luisa Mangoni for her support, encouragement during my PhD and the writing of this thesis. I thank my lab group, my colleagues, master's students for thesis and all the collaborators involved in this thesis work:

Researcher Loretta Ferrera (Gaslini Hospital-Genoa) for electrophysiological experiments for Esc (1-21), Esc(1-21)-1c and [d-Leu14, dphosphoSer 17]Esc;

Prof. Mattia Mori (Dep. of Biochemical Sciences-University of Pisa- Italy) fro molecular dynamic simulation of Esc (1-21) and dphosphoSer 17]Esc;

Group of research of Dep. of Chemistry (University Federico II- Naples) for proteomic study of Esc(1-21)-1c;

Group of research of University Roma Tre (Rome) for transcriptional analysis.

Last but not the least, I would like to thank my family and all my friends for supporting and believing in me during this hard but exciting period.